ADDIS ABABA UNIVERSITY

ADDIS ABABA INSTITUTE OF TECHNOLOGY

SCHOOL OF MECHANICAL AND INDUSTRIAL ENGINEERING

Research Thesis

on

The influence of non-uniform train speed distribution in curves and straight line on rail corrugation of Tram railway vehicle.

By

Natinael Mitiku

Id: GSR/3445/07

Advisor

***Mr. Habtmu* Tekubet(Msc.)**

Date: July. 2017

Acknowledgment

I would like to thank my Lord Jesus Christ for his love and courage and next I like to thanks my Advisor Mr. Habtamu Tekubet for his constrictive comment, help and criticism and then, and the Addis Ababa university Addis Ababa institute of technology library and railway institute library and administration for their support during my work and AALRT quality depot for information and data and finally like to thank my friend and family.

ADDIS ABABA INSTITUTE OF TECHNOLOGY

SCHOOL OF GRADUATE STUDIES

POSTGRADUATE PROGRAM IN RAILWAY ENGINEERING

ADDIS ABABA UNIVERSITY

The influence of non-uniform train speed distribution in curves and straight line on rail corrugation of Tram railway vehicle.

By: **Natinael Mitiku**

Approved by Board of Examiners

Dr. Daniel Tilahun	_____	_____
Railway center head	Signature	Date
Mr. Habtamu Tekubet	_____	_____
Advisor	Signature	Date
_____	_____	_____
Internal examiner	Signature	Date
_____	_____	_____
External examiner	Signature	Date

DECLARATION

I hereby declare that the work which is being presented in this thesis entitled "*The influence of non-uniform train speed distribution in curves and straight line on rail corrugation of Tram railway vehicle*." is original work of my own, has not been presented for a degree of any other university

Natinael Mitiku	_____ signature	_____ Date
Mr Habtamu Tekubet (Advisor)	_____ signature	_____ Date

Contents

List of figures

Tables

Abstract

The rail corrugation is a frequently occurring railhead wear pattern which is arise mostly in curve and in tangent(straight) track. Rail corrugation is caused by railway track dynamics and it is a significant problem in railway engineering, that manifests as periodic wear pattern on the contact surface of rails and lead to undesirable noise and vibration. This project investigates the effect of speed in the straight and curved line of tram railway vehicle. The project has been organized and analyzed by numerical approach and software analyzation. Simulation procedure developed in a project is used and further analyzed for both curved and straight track and it includes the following three steps: step one studying literature and finding research gaps, step two Simulation of dynamic vehicle-track interaction in curves and straight tracks with commercial software MATLAB and MATLAB /SIMULINK and the rail wheel structural flexibility is accounted for using the finite element method by ABAQUS , then the result observed in straight line that the traction and breaking are severe, the straight line will assuming that the wheel is acting like a linearized contact spring and is exciting the first pinned–pinned rail mode. For speed 20km/h,40km/h and 60km/h the corrugation growth is $2.5\times10^{-7}m$, $6\times10^{-9}m$ and$1\times10^{-9}m$ respectively and this results concluded at this speed the corrugation growth will decrease because of the friction between wheel and rail is lower while speed increase ,In the curve In low(inner) rail corrugation growth 30km/h per pass is about $1.21\times10^{-9}km$ and in high(outer) rail $1.1\times10^{-9}km$ this would cause, because of the traction ratio is greater at the high rail than on the low rail for almost all circumstances. Because of it, mostly expect that plastic flow would occur more readily on the high rail. but, when a bogie curves with cant excess, the traction ratio on the low rail wheel increases significantly because the trailing wheelset moves in towards the low rail, also in the severe traction wheel run from 0-5rpm suddenly cause material removal and leave deformity on the rail of strain about2.24×10^{-2} for time of sever breaking the wheel stopped from 5rpm to 0rpm and start to skid and result in 3.35×10^{-2} strain moved. Finally conclude that in both curved and straight line the speed will one of the parameter will be means of corrugation by affecting wheel rail interaction.

Chapter 1

1. Introduction

1.1. Background

Rail corrugation is the short-wave lengths irregularity in the rail and developed at different levels during the rail transit operating it will increase not only increases the wheel-rail noise and vibration, but also accelerates the fatigue failure of track and vehicle components which make a serious threat to operation safety. Since the late 70, most global researchers were doing in this area [1-3]. This researcher seeks to generation and development mechanism of rail corrugation, they take a great deal of theoretical and experimental research. But, because different factor affecting the interaction between vehicle and track [4-5], for instance dynamic characteristics of the bogie system and rail system, speed of the vehicle, load, material properties and scroll wheel-rail contact conditions, the running condition of the vehicle and the wheel rail surface irregularity roughness, but those scholars are not come agreement yet on the rail corrugation generation and development mechanism and means of control [6,7].

Figure 1-1. Corrugation in different rails [6,7]

According to the generally accepted model illustrated in Figure 2 below, the development of corrugation is explained by wear generated at wavelengths determined by the complex characteristics of the dynamic vehicle track interaction (wavelength-fixing mechanism). In literature, the comparison of corrugation growth on different types of track networks, the largest roughness levels were found on the low rail of metro curves [8].

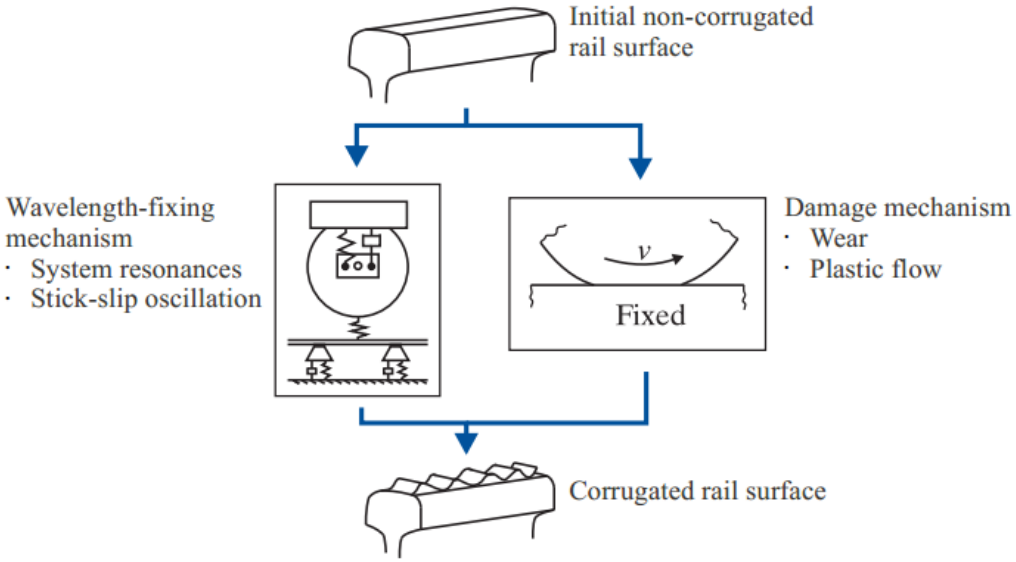

Figure 1-1. Illustration of development of rail corrugation as explained by a combination of wavelength fixing and damage mechanisms [8].

Railway traffic is the environmentally most friendly mode of transport. In fact, its most significant environmental impact is noise. Tram cars train are operated mostly in cities and are built in densely populated routs, the solving of noise issues is particularly important. Rail corrugation induces pronounced dynamic loading that leads to increased generation of noise and vibration, and in severe cases to damage of vehicle and track components. Complaints regarding high noise levels regularly reach Stockholm Public Transport Public Transport (SL) from passengers and from people living close to their track network [9].

Irregularities rails give rise the noise and ground-borne vibration also more general dynamic loading, variable speed of the vehicle also the stability of the train which increases damage of components of both vehicle and track. Both wheels and rails are prone to develop quasi-sinusoidal irregularities but this paper particularly deal with the irregularity in the rail, which are known as corrugation which have wavelength is less than about a meter. Longer wavelength irregularities are usually known waves this is not said to be corrugation but it also caused in the rail and the wheel. The effects of irregularities are substantially the same whether they occur on wheels or rails, the mechanism but which most types of irregularities occur differs in significant respects. Consequently, while this article is relevant in several respects to irregularities on both wheels and rails, it concentrates on rail corrugation.

Excellent references on wheel irregularities are the review paper by Nielsen and Johansson [10] and the proceedings of a workshop held at the Technical University of Berlin in 1997 [11] In this paper, by study the uniformity in train pass speeds over a site enhances corrugation growth rate and that broadening the probabilistic pass speed distribution may be a possible method of mitigating corrugation growth in Addis Ababa light rail transit.

To manage the corrugation problem with rail corrugation, infrastructure managers are forced to run regular and expensive rail grinding programs. It is not potential of preventing corrugation to reappear and obviously does not offer a satisfying long-term solution to the problem. Accurate prediction models, however, are important tools in the search for effective treatments of corrugation growth. In particular, by simulating the prevailing wavelength-fixing mechanisms at a specific location, directed mitigation measures can be taken. Ultimately, if incorporated in the design-phase of vehicles and track, prediction models can contribute to create a vehicle track system that does not promote corrugation growth.

1.2. Statement of the problem

Rail corrugation is a dynamic wheel-rail contact phenomenon that manifests as a periodic wear pattern on rail heads [12]. rail corrugation is a significant problem in railway operation in various country and it is not a new concept, is now attracting considerable global attention as a viable process to provide noiseless and smooth drive of the rail ways vehicles for longest time. Despite these undesirable periodic wear pattern on the contact surface of rails. It is a significant problem in railways worldwide that grows over many train passages, causing unwanted vibrations, excessive noise and other associated problems.

These profile variations will lead to the dynamic and fatigue load in the car body and cause part failure problems. Unfortunately, in train passing speed has been shown to accelerate corrugation growth while widening the probabilistic speed distribution can be shown to mitigate the phenomena.

In tram car the speed of light train will vary in different sites because of the cornering and dynamic force caused by the periodic variation of wheel-rail interaction along the track. This periodic

dynamic force makes the creep force on wheel-rail interface complex and increases rail wearing [13].

The paper study vehicle speed changes and effect of curving in the corrugation of the railway track by curved and straight line of tram car using the MATLAB and ABAQUS also numerical investigation to calculation the corrugation growth due to wear.

1.3. Objective

The aim of this project is to study the effect of non-uniform speed of the tram railway vehicle on rail corrugation growth through numerical analyses and analytical study with the final goal to identify the effect of speed on growth rate of corrugation that would be happen.

1.3.1. Specific objective.

To achieve the above objectives: -

I. Identify the effect of speed in the growth rate of railhead corrugation of both straight and curved track.

II. Develop Mathematical modeling of the tram car with non- uniform speed and the numerical analysis to identify rate of growth.

III. Simulation of dynamic vehicle–track interaction in deferent speed with the MATLAB 2013b.

IV. Calculation of accumulated damage (i.e. corrugation growth due to wear) in MATLAB.

1.4 Limitation

This project is focused on only the effect of the non-uniform speed distribution and its effect in the wear-rail corrugation using numerical and ABAQUS investigation and observing the result using the MATLAB in the light Addis Ababa train. Analyzing and investigating different factor including the vehicle design, material property of the rail and other operational parameters will not be included.

1.5 Literature review.

Literature review surveys scientific articles, books, journals, conferences that could be heled and other sources relevant to this project, area of research, or theory, providing a description, summary, and critical evaluation of each work from general to specific and finally identify and discussed on the research gaps.

1.5.1. Railhead corrugation.

Rail corrugation periodic irregularities of various wavelengths mostly develop on the railhead and on the wheel tread in the straight and curved tracks.

Railhead corrugation to be appear on every kind of railway track line, from heavy haul tracks to lightweight city line. The growth rate of corrugation on the railhead is explained by the dynamics of the train-track system and linked to resonance effects in the combined rail-wheel and wheelset system. It is assumed to be so, because the irregularities that develop are periodic of a certain wavelength, mostly the irregularity growth are in the range of 30 to 300 mm. Such periodic irregularities are named corrugation. When the train speed increases, the dynamic interaction between the vehicle and the track becomes increase linearly with the speed of train and this gives rise to larger dynamic forces acting between the wheels and the rails. Once the rail corrugation has begun to develop, the dynamic forces in the train-track system will be further increase, and the deterioration and material removal rate of the track will increase.

When the train speed increases, the dynamic interaction between the vehicle and the track becomes more and more than this gives rise to larger dynamic forces between the wheels and the rails. When rail corrugation has begun to develop, the dynamic forces in the train-track system will be further increased, and also deterioration rate of the railhead will increase.

The irregularities of very short wavelengths are called corrugation. Unfortunately, different authors use different suggestion to classify the corrugation and irregularity in the rail and also use different classifications, and sometimes the word corrugation is used for all wavelengths. In paper the word corrugation is used for short wavelength railhead periodic irregularities of lengths 300 mm or less. A recent review of studies and calcification of on rail corrugation was presented by Sato et al [6] where a short historical survey on rail corrugation is also given.

The growth rate of corrugation mechanism is illustrated in Fig. 1-3 although a similar feedback loop block diagram has been widely used in this paper. Initially in the straight longitudinal rail profile excites a so-called wavelength-fixing mechanism which caused by the dynamic behavior of the train and also represents the dynamic behavior of the vehicle/track system. This mechanism 'fixes' not only the wavelength but also the position of the corrugation along the track.

Other parameters such as the tangential forces between the wheel and rail (traction) , braking force applied opposite to the traction and the allowable limit of these forces (friction) have some effect on this dynamic mechanism [14].

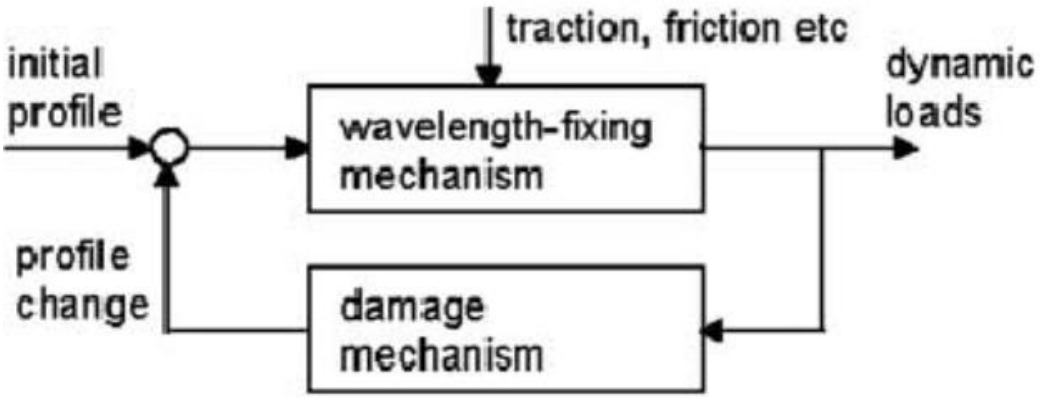

Figure. 1-3. A general corrugation mechanism. A general corrugation mechanism [14].

1.5.2 Classification of corrugation.

Rail irregularities are classified in different ways. In this paper, it classified as follow.

The irregularities of very short wavelengths are called corrugation and long wavelength irregularities so called waves. But is nominated different names for different authors use various classifications, and sometimes the word corrugation is used for all wavelengths. In this paper, the word corrugation is used for short wavelength railhead periodic irregularities of lengths 300 mm as explained above. The most common types of corrugation that have been documented in the

literature can be classified according to their wavelength-fixing and damage mechanisms, as Table 1.1 Types of corrugation, characteristics, references, and treatments [16]

In the studies, there are two definitions of corrugation are given in ("l'Union Internationale des Chemins de Fer, International Union of Railways"). The primary one says that corrugation is

						Treatment	
NO	Type	Wavelength fixing mechanism	Point of attack	Frequency	Damage mechanism	Demonstrably successful	Should be successful
1	Pinned-pinned resonance or roaring rail	Pinned-pinned resonance	Straight track and high rail in curves	400-1200Hz	wear	Hard rail, control friction	Increase pinned-pinned frequency so that corrugation would be < 20mm wavelength
2	Rutting	Second torsional resonance of driven axel	Low rails in the curves	250-400	wear	Friction modifier, hard rail and asymmetric profiling in curves	Reduce applied traction in curving, improve behavior of the vehicle, dynamics absorber
3	Other p2 resonance	P2 resonance	Straight tracks or high rails	50- 100	wear	Hard rails, highly resilient track forms	Reduce unsprang mass
4	Heavy haul	P2 resonance	Straight tracks and high rail in curves	50-100	plastic flow	Hard rail	Reduce cant excess when corrugation is on the low rail
5	Light rail	P2 resonance	Straight tracks or curves	50-100	Plastic bending	Increase rail strength and EI	Reduce unsprang mass

characterized by an almost regular sequence of shiny peaks and dark troughs generally spaced approximately 30 to 80 mm apart. For another type of corrugation, it is stated that "in this wave effect, there is no difference in appearance between the peaks and troughs of the waves", and "the wavelength generally varies between about 80 and 300 mm". Of the latter, the longer waves (300

mm) occur preferentially on the low rails in curves. Then the railhead irregularities are divided into two groups here, corrugation (30 to 80 mm) and short wavelength irregularities (80 to 300 mm). This corrugation thus develops on the railhead due to the train traffic.

Tassilly and Vincent associated the P2 resonance with longer wavelength corrugation on the rapid transit system (RATP) in Paris, although only as a factor that exacerbated the effect of the fundamental torsional resonance of wheelsets [17].

The frequency of both the P2 resonance and the first torsional resonance of wheelsets is commonly in the range 50–100 Hz, so it is unsurprising that severe corrugation can result where both resonances are excited. This can occur in tight curves in metro systems, as noted by Tassilly and Vincent.

1.5.3. Effect of the passenger car curving in rail corrugation.

The corrugations mostly occurring at curved tracks sites. In the present paper that has been took for the simulation of passenger car curving, a curved track with radius $R0$ = 300m and a half passenger car are selected, shown in Fig.2. The curve length of the curved track is 80m, the circle curve length is 100 m. The track gauge is 1437 mm. The sleeper space is 600 mm. The super-elevation of the outside rail of the track is 100 mm, the rail cant is 1/40, and the type of rails laid is 60 kg/m. The half passenger car is equipped with a bogie with two wheelsets and double suspension systems where used to model wheel rail interaction and study the cause of the rail way track irregularities. The nominal rolling radius of the wheelsets with worn profile is $r0$ = 457.5 mm the average speed of the train at the curving speed of passenger car is 80km/h. and the passenger care are assumed as below.

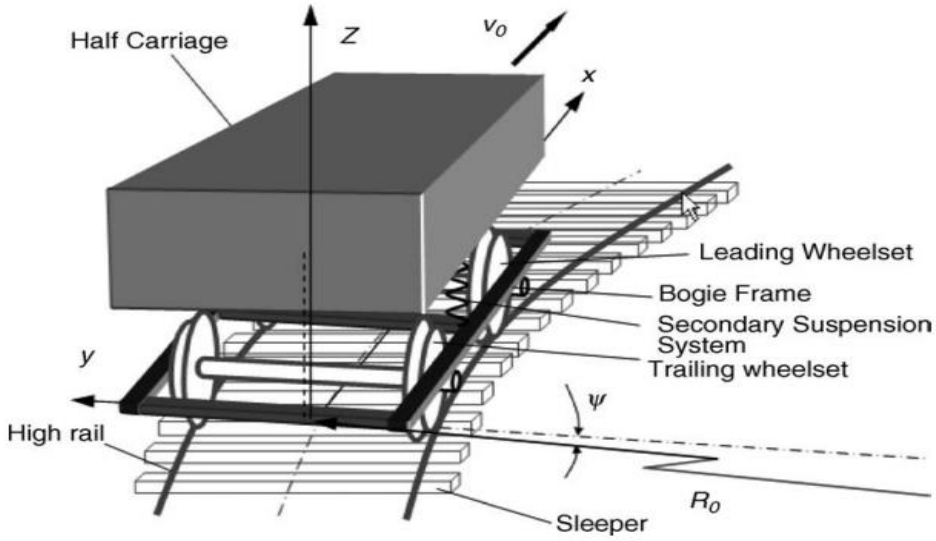

Figure 1.4. A half passenger car passing a curved track [18]

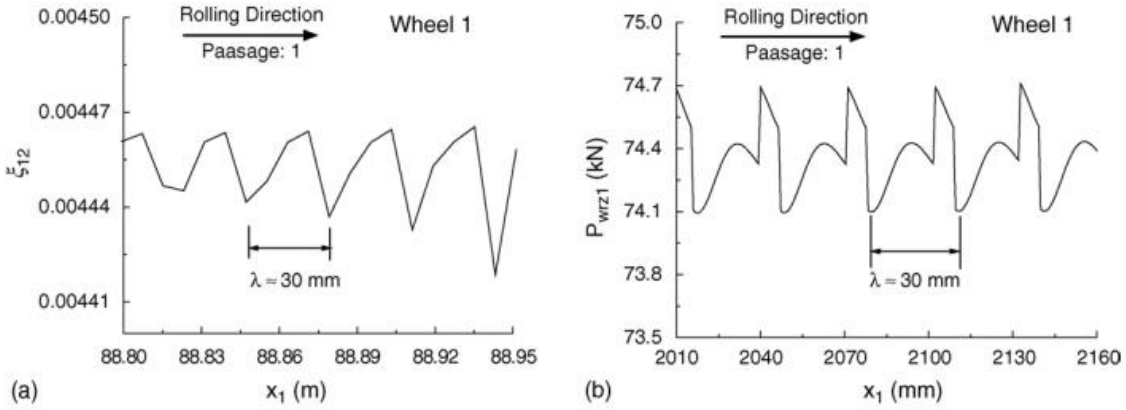

Figure 0-1.5. Lateral creepages and normal load in the length of corrugation calculation. (a) Lateral creepage zoom and (b) normal load zoom [17].

The result in the paper described that [18]. The defects mainly include scratches, the uneven initial running surface of rail, the gap between jointed rails and the uneven stiffness of rail supports. In this case, it is assumed that no such defects were existing on the curved track considered. It is well-known result, when a train is passing a curved track and the moving direction and inertia of the vehicles change continually due to the curved track direction.

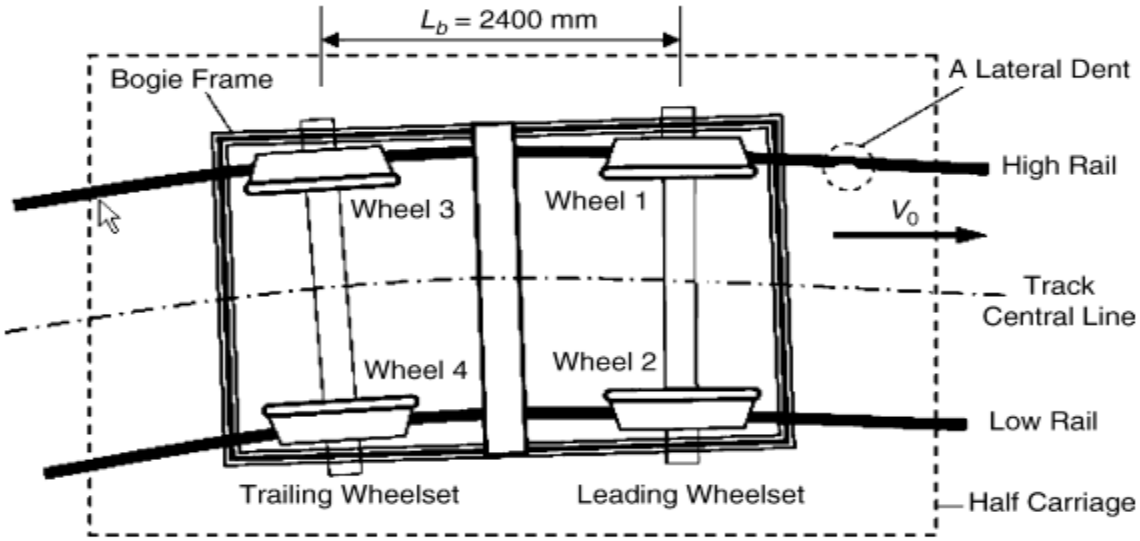

Figure 1.6. A half passenger car passing through the curve track with a lateral dent [18]

And also, found that, such change is random. A leading wheelset of the bogie attacks on the high rail of the curved track. In a situation, the high rail oscillates easily at some natural frequencies of the curved track. The rail oscillation causes a periodical variation of the normal load and creepages between the wheel and rail at the same frequencies. It is believed that the oscillating amplitude is very small without an excitation of the curved track defect.

1.5.4 Prediction of the growth of wear-type rail corrugation

Also, the aim of this research is to simplify and describe only the most critical dynamical characteristics of the system via appropriate assumptions. Corrugation where described by the conceptual block diagram of the key process components and the associated fundamental feedback interaction that is proposed for the modelling approach. The basic concept of the block diagram consists of a feedback interaction between wheelset/track vibrational dynamics, wheel/rail rolling contact mechanics and wear on the rail surfaces this paper discussed and develop mathematical model for the wheel/rail and interaction of the wheel and rail and is similar to that proposed in, Hempelmann and Knothe [19] and Igeland and Ilias

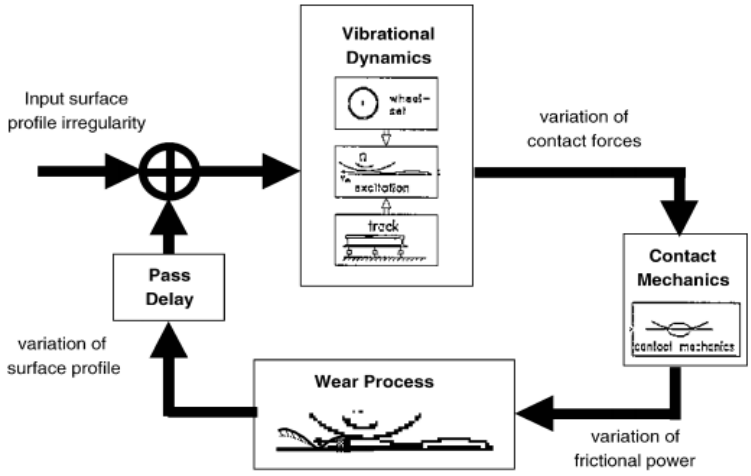

Figure 1.7. block diagram [19]

Result showed that after detial investigation of wear-type rail corrugation of the analytical growth predictions, numerical simulations were performed using simplified and finite element, time domain models. That Assuming simplified numerical model, based on a two degree of freedom representation of the vehicle/track dynamics. Details of this model and results showing good comparisons with the analytical growth predictions, are provided in Meehan et al. [6]. For a more comprehensive assessment of the accuracy of the analytical model, a finite element model was developed and tested using an internationally recognised benchmark test and is described subsequently.

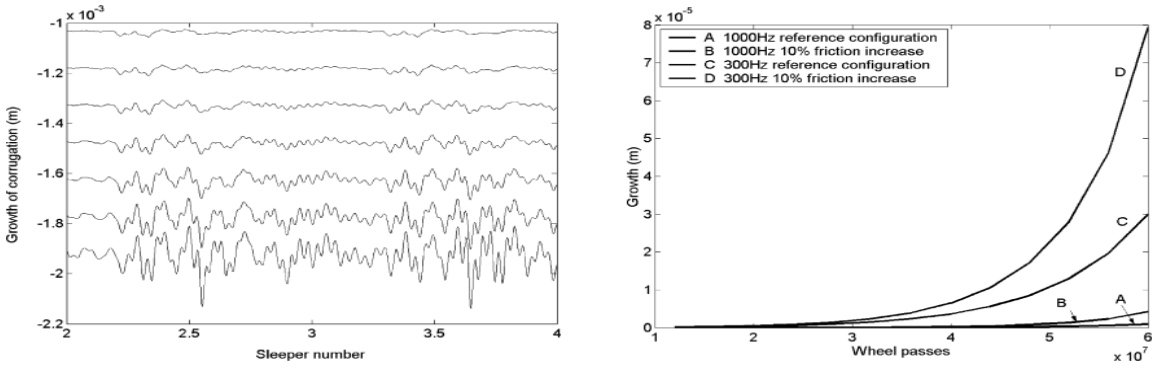

Figure 1.8. A) profile of worn rail v slipper number B) change in corrugation growth in 20m/s[6].

1.5.5 Effects of wheel passing frequency on wear-type corrugations

The most analytical model provides a useful means by which to predict the sensitivity of growth rate of corrugation. This sensitivity may be useful in order to predict and or control the growth of wear-type corrugations. As such, an analytical expression for prediction of the range of growth rate for any particular speed (or pass delay) is developed in this paper to understand and verify the effect of speed in the sensitivity of the wear. One of the result in this paper where analytical evaluation of straight line rail second part is prediction of the growth rate of the corrugation.

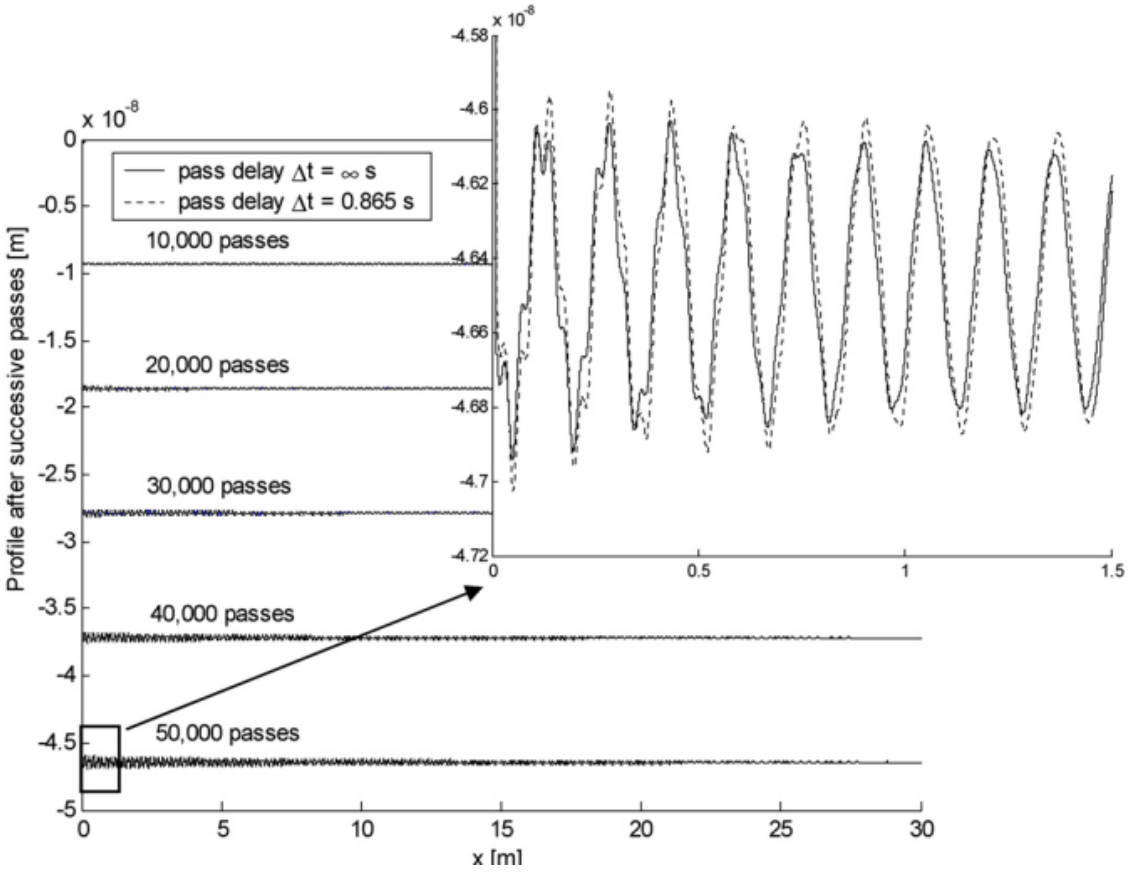

Figure1.9. . Corrugation growth over 50,000 passes. [20]

Corrugation growth over 50,000 passes.

The results for typical passes highlight that large variations in growth rate may occur due to passage delay effects, the particularly at speeds >30 km/h. This growth rate range prediction may be considered to be a confidence with which the growth rate can be predicted without precise knowledge of the mode-pass delay ratio. Alternatively, if the mode-pass delay ratio can be

controlled precisely considering the effect of speed then this closed form algorithm block diagram may be used to estimate the maximum reduction in corrugation growth rate achievable.

The prediction was found to straight track and insensitive to variations of railway parameters and hence applicable to most conditions. The model diagram is as follow. [20]

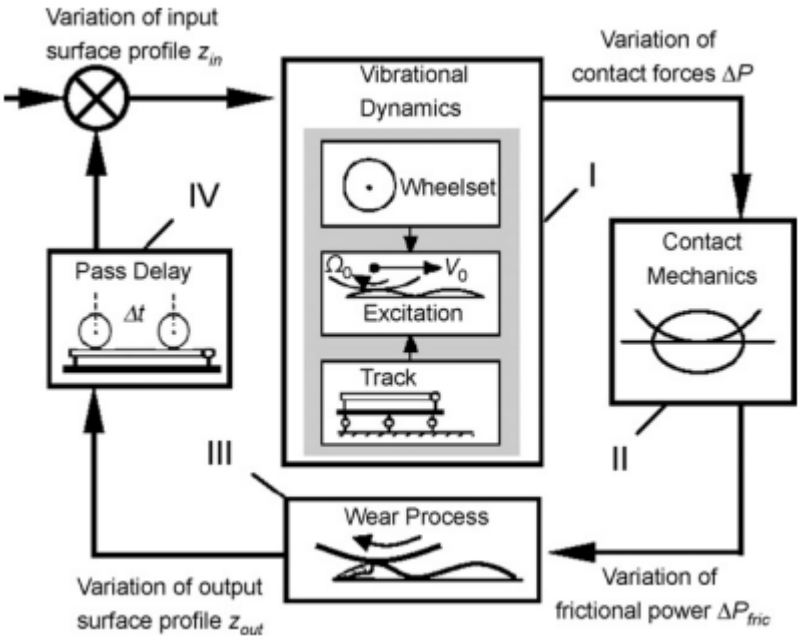

Figure.1.10. Feedback model for wear-type rail corrugation. [20]

1.5.6 Effects of variable pass speed on wear-type corrugation growth

Using the above diagram, the development of analytic solutions for the detailed rail profile history for a range of input profiles, where the vehicle speed changes on each pass. The development of a useful expression for quantifying the corrugation growth rate due to a distribution of train speeds. Using this expression an investigation into how different speed distribution shapes affect the corrugation growth rate has been provided.

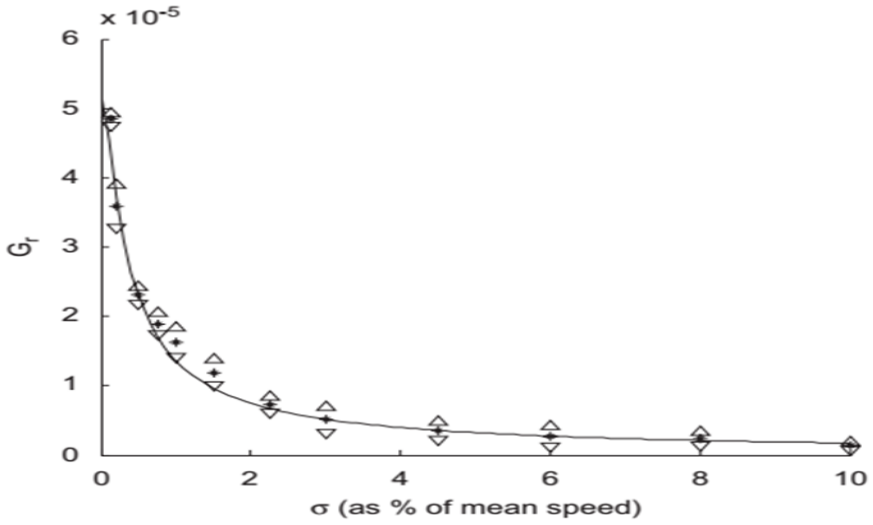

Figure 1.11. Growth rate vs. standard deviation [21].

A theoretical proof that maximum corrugation growth rate occurs under constant pass speed conditions. The development of a closed loop form expression of the error in growth rate induced by artificially accelerating the wear coefficient during numerical simulations.to this end the speed is express and quantified by the standard deviation by the probability curve as show in the figure

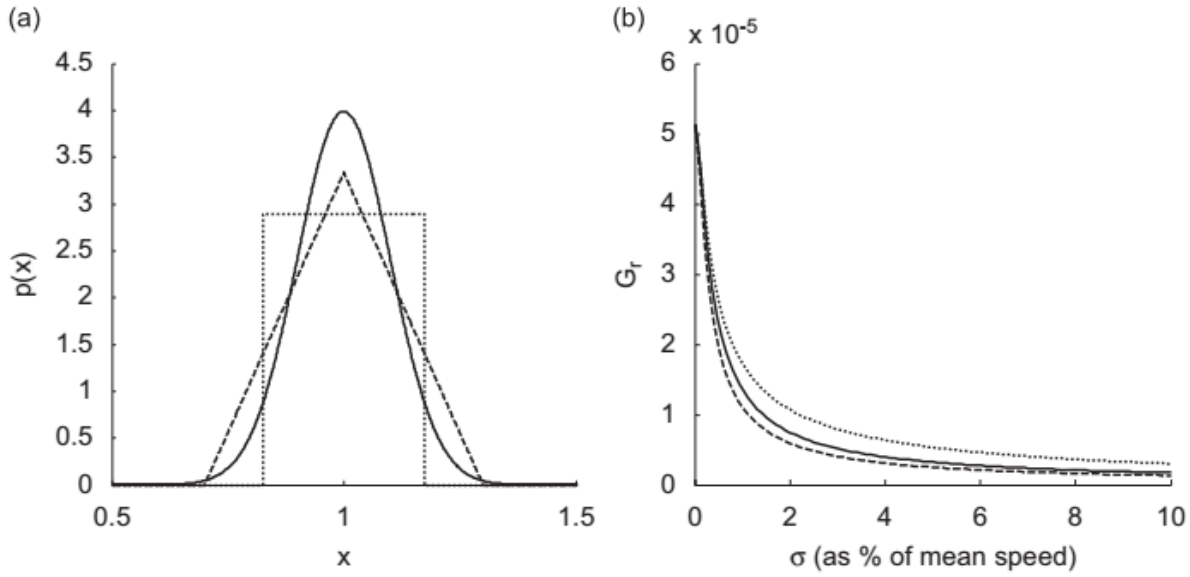

Figure 1.12 A). Probability distributions with matched variance B) growth rate vs. equivalent standard deviation. [21].

From this model, straight line track where assumed in analytical solutions for the rail profile under different corrugation initiators will first be developed and modeled. A transfer function between initial and final rail profiles in Laplace space will be described and finally used to derive a frequency response expression for the corrugation growth mechanism where mentioned. [21]

1.5.7 The effect of non-uniform train speed distribution on rail corrugation growth in cornering.

This part of the corrugation growth study analyzed the rate of corrugation growth in the curved track and described its effect by developing steady state analysis on the rail of 50m radius. This study says "train passing speed accelerates corrugation growth on straight track and conversely, widening the probabilistic train passing speed distribution can be used as a mitigation tool. The dominant mitigating mechanism is that different vehicle speeds lead to different wavelengths and positions of periodic wear along the track and therefore cancellation of corrugation growth". [22].

Figure 1.13. 1 – 9-month-old corrugated rail profile [22]

Assuming the train is curving in the 50m radius curve and with full axil load >11000 and using the static analysis for calculating the loads in the outer and inner rail where equally distributed traction effort also considered in the longitudinal direction but ignoring the motion in the lateral direction rather consider the lateral creepage. And the study will have focused on an existing frequency domain corrugation growth model was modified to investigate the effects of an asymmetric speed distribution on the maximum growth rate for trains in cornering. The model was equipped with a

numerical cornering model based on a bogie navigating large radius corners, and including the effects of weight transfer between the high and low rail due to centrifugal tipping torque from cant deficiency.

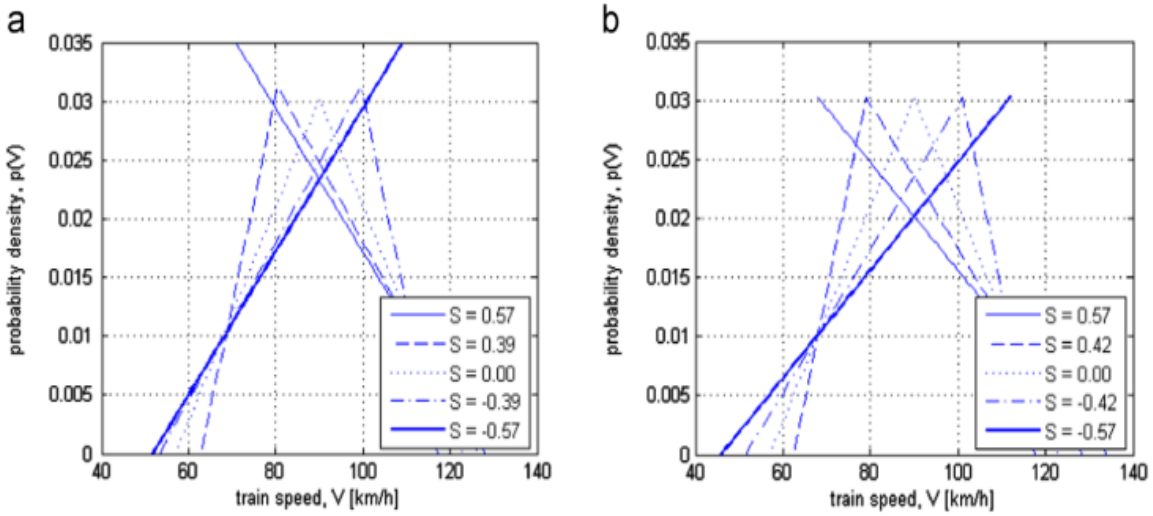

Figure.1.14 Simulated a) fixed standard deviation and b) fixed width speed distribution curves [22]

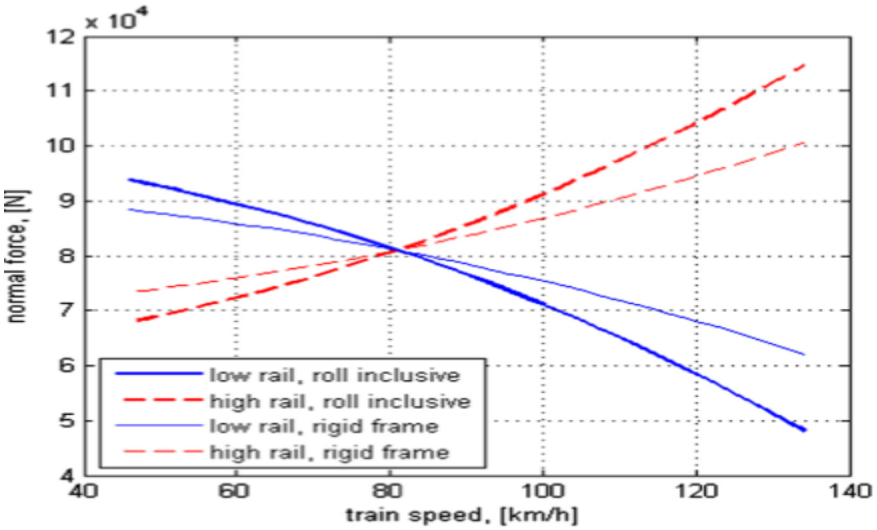

Figure 1.15. Normal force on rails with changing speed. [22]

1.5.8 Research gaps.

This review proposes some differences in classification of the phenomenon to take account of work undertaken above. The reviewed papers are mostly investigated in the mechanism of rail corrugation generation and developments also the variation of difference between wheel and rail reacceptance and Rail corrugation characteristics, causes, and treatments of effect in non-uniform train speed distribution on rail corrugation growth in cornering. However, these papers will investigate and analyze the effect of non-uniform speed for the cause of railhead corrugation growth in fine curve at 50m radius and straight line and specifically this project will rather investigate numerical and ABAQUS investigation of corrugation that comes from non- uniform speed of tram railway cars in curves and straight line and comparing the result.

1.6. Significance of the Research

This research will have a great advantage for future analysis and uses of rail and applications on the rail maintenance and driving quality also curve radius effect on the rail head corrugation due to speed of train. And the research will contribute on the studies that concerning the rail head damage due to speed and other dynamic parameters of tram cars.

In the future, it will add new knowledge about existing one with analysis of railway corrugation rail material removal, strain, deflection under vertical wheel load, which cause wear, fracture and deteriorations on the contacting interface of wheel and rail.

This research will also be important for railway engineers to improve their understanding of the designing the driving speed and the railway track of rail joints and maintenance of the rail by considering the effect of radius in tram car speed. However, this paper will provide the reference for designing of the railway train speed by showing the stress impacts on two rails (outer and inner) in curved track and straight track using MATLAB numerical MATLAB/SIMULINK Finite Element Method in ABAQUS to identify and observe the effect of speed in tram railway cars.

Chapter. 2

Methodology

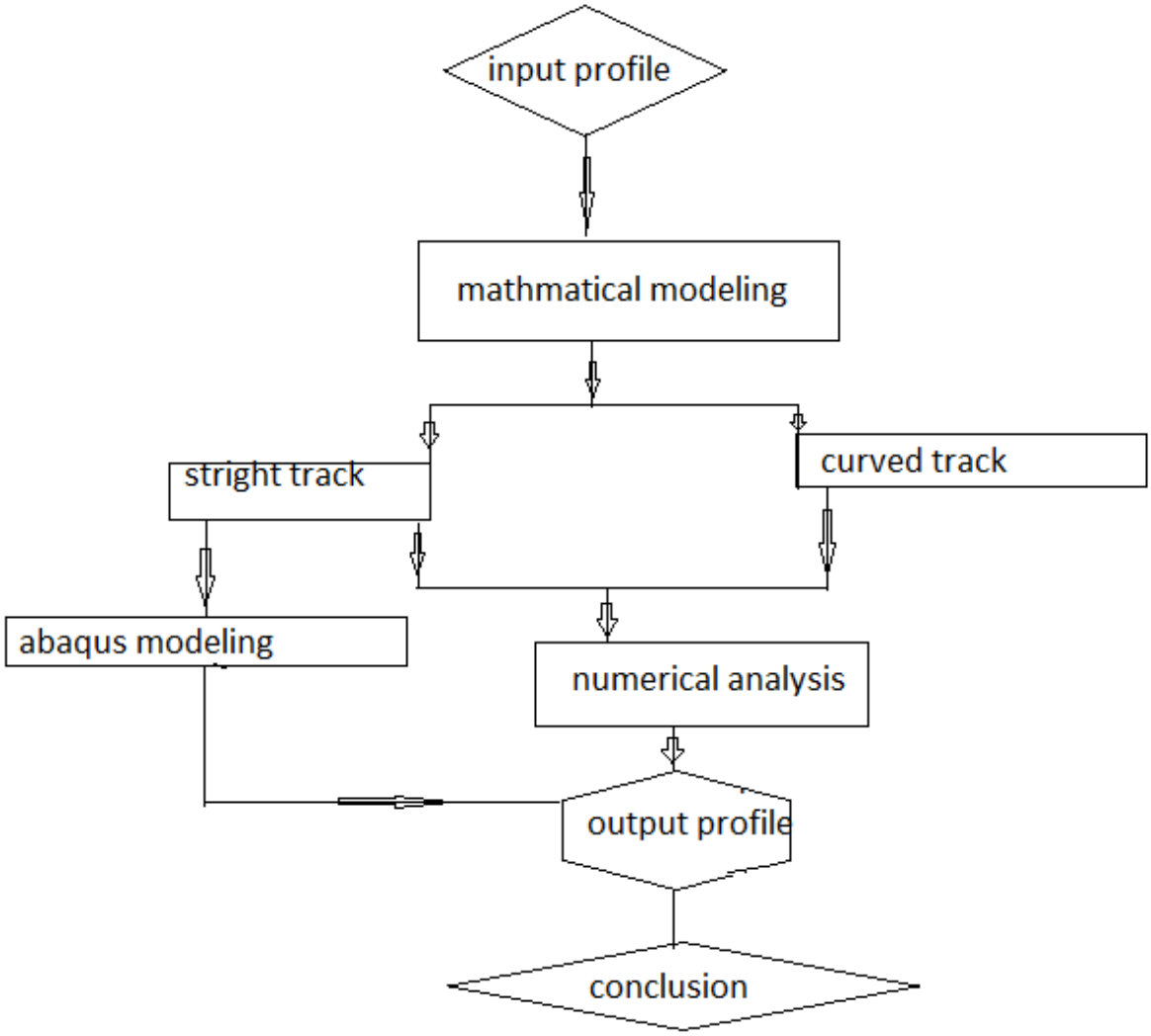

Figure. 2.1 Methodology to study Rail corrugation caused by nonuniform speed.

Chapter 3.

3. Corrugation modeling

3.1. Types of corrugation.

Both wheels and rails are prone to develop quasi-sinusoidal irregularities, which are known as corrugation when their wavelength is less than about a meter. If the wave length is greater than a meter is known as wave. Corrugation on rails give rise to noise, ground-borne vibration and more general dynamic loading, which increases damage of components of both vehicle and track. Corrugation that have been documented in the literature can be classified according to their direction of creep are horizontal and vertical.

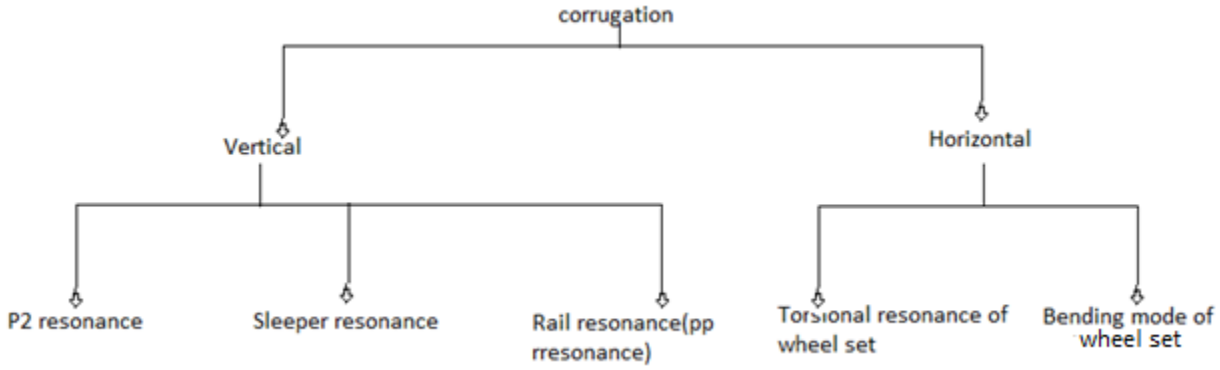

Figure 0-1.1. Different types of corrugation

3.1.1. Vertical Corrugation.

Due to the wheel-rail receptance the contact force in wheel which is rolling on the rail is unsteady state dynamic force F as shown in the fig below. [23] those with change in profile surface ΔZ and the wave length L.

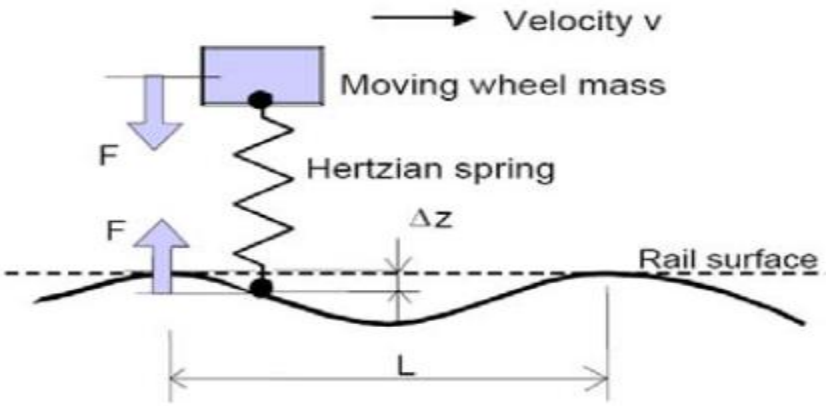

Figure 3.2. Vertical-longitudinal model [23].

*P*2 resonance is significant in heavy haul and light rail corrugation but also as one of the most frequent causes of corrugation on a wide variety of railways. For example, the longer wavelength corrugation in Fig below has resulted from excitation of the *P*2 resonant frequency, and this is the source of corrugation at 300–400 mm in the measurements (from the same railway) shown in Fig.3.2. [24]

i. Heavy haul corrugation.

Type of corrugation that had been found to exist on so-called heavy haul railways. The case of this type of corrugation is that plastic flow occurs more readily the higher the traction ratio and normal contact stress [25].

The reason for this is that plastic flow occurs more readily the higher the traction ratio and normal contact stress for a vehicle curving at balance speed the traction ratio is greater at the high rail than on the low rail for almost all circumstances. It is accordingly reasonable to expect that plastic flow would occur more readily on the high rail in these conditions, as in Fig.3.3. However, when a bogie curves with cant excess, the traction ratio on the low rail wheel increases significantly because the trailing wheelset moves in towards the low rail and the leading wheelset moves towards the high rail, thereby increasing the angle of attack. There are high lateral loads on the leading, low rail wheel and also high contact stresses, because contact tends to occur towards the field side of the wheel, which is often slightly convex. The direction of plastic flow, towards the inside of the curve is consistent with lateral forces arising from the angle of attack of the leading wheelset.

Figure.*3.3.* heavy haul corrugation b) spalling through heavy haul [25].

ii. Light rail corrugation.

This type of corrugation actually propagates from the welds and has the wavelength in the range 500–1500 mm. The principal difference between light rail and heavy haul corrugation is that the damage mechanism for the former is plastic bending of the rail, so that corrugation is measurable on both railhead and rail foot [26].

The treatment that has been adopted is to straighten welds and joints, thereby reducing the main irregularities that excite the P2 resonance, and to grind rails to eliminate existing corrugation. Modern rail steels and more robust rail sections have a sufficiently high bending strength to resist damage by this mechanism.

Figure 3.4. a) 'Pinned–pinned resonance' and 'P2 resonance' b) P2 resonance' corrugation on a tram system corrugation on the same rail[26].

The other case of p2 resonance corrugation is first torsional resonance of wheelsets is commonly in the range 50–100 Hz, so it is unsurprising that severe corrugation can result where both resonances are excited. This can occur in tight curves in metro systems, as noted by Tassilly and Vincent.

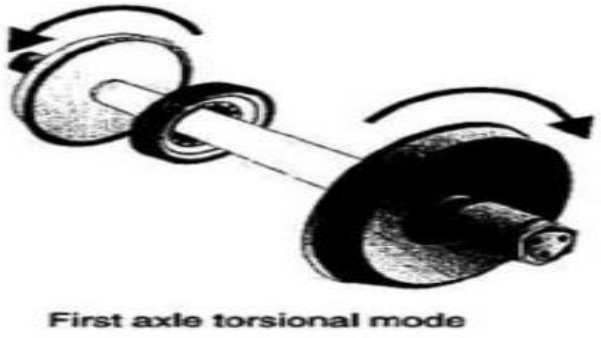

Figure 3.5. first axle torsional resonance mode[26].

iii. Sleeper resonance.

The parameters used in deferent civil engineering works for each type of track are standard parameters. However, currently many types of ballasted track and slab track are developed so that the range of track parameters, vertical and lateral stiffness and damping, of both

ballast and slab track are enlarged as much as possible. It must also be kept in mind that the ballasted tracks as well as the slab tracks have some variations due to the combination of all possible rail fastening systems, and all this could lead to variation in rail profile.

iv. Pinned- pinned resonance corrugation.

pinned–pinned resonance corrugation occurs primarily in straight track and gentle curves, where curving is undertaken with minimal flange contact. It associated also with track carrying relatively light axle load traffic, i.e. <20 tone. [27,28,29].

Figure 3.6. roaring rail from a metro system and from the UK main-line railway [27]

White phase is first sign of corrugation and will developed as result of the rapid heating and quenching of the rail surface during wheel slip.

The damage mechanism for pinned–pinned (roaring rail) resonance corrugation is wear. It can be shown from relatively simple dynamic models of the track and vehicle.

The case of pinned-pinned (roaring rail) corrugation are resonance the rail vibrates as if it were a beam that was almost pinned at the sleepers.

v. Rutting

Rutting is special type of corrugation as the research studies this kind of corrugation will happened inside rail although will occur in straight line of the track as shown in the fig below.

The case of this type corrugation is specially the place where the breaking and the traction is severe [30].

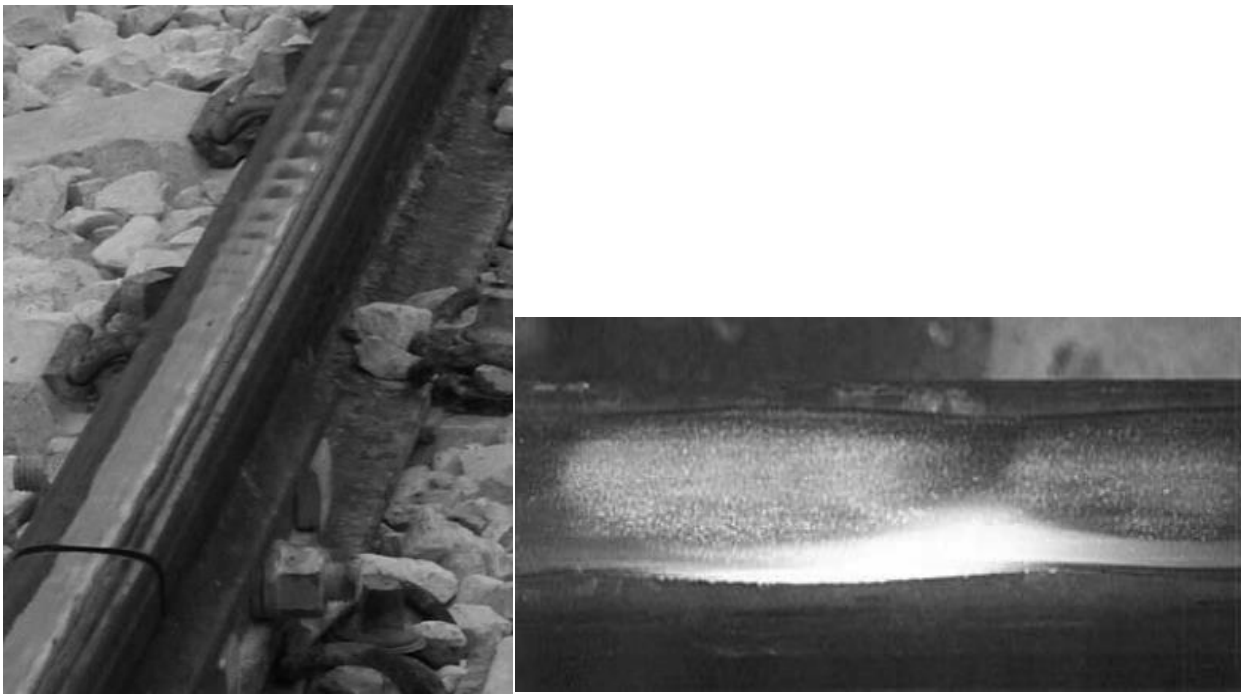

Figure 3.7. a). Rutting on the inside (low) rail in a curve b) Rutting showing development of plastic flow[30].

Discrete irregularities such as welds and joints (e.g. Fig.3.7. above) are common triggers for corrugation and often fix the position of corrugation along the rail. Rutting usually has an extremely uniform wavelength and appearance and can develop quickly to a depth of tenths of a millimeter. Wear debris is sometimes apparent to the naked eye and Plastic flow can occur on a well-developed corrugation (Fig.3.7. b).

The case of this kind of corrugation is where identified on North America transit system, it was found that rutting in inside rail in curves was not only the most common corrugation mechanism but was also associated with second torsional resonance of driven wheelset as shown in figure below.

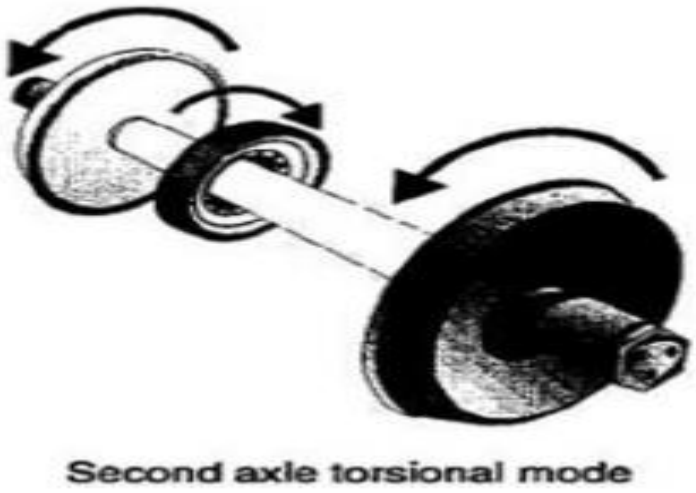

Figure 3.8. second torsional resonances of wheelset [31]

The study explained frequency of the second torsional resonance is commonly about 250–400 Hz. A frequency of 250 Hz corresponds to a corrugation wavelength of 50 mm for vehicles at 45 km/h, which is a common speed for metro vehicles.

Rutting occurs where the traction ratio (the ratio of tangential to normal force) on one wheel is close to the friction limit, so that this wheel slips and drives the opposite wheel in the wheelset in a roll–slip oscillation.

The damage mechanism for rutting is clearly wear, which is quasi-periodic with high peaks corresponding to the slip phase of a roll–slip oscillation. The importance of longitudinal slip is illustrated by the longitudinal scuffing marks in Fig. below. which shows the low rail of a 200-m radius curve on a suburban railway.

Figure 3.9. Longitudinal scuffing apparent in friction modifier in low rail of 200 m radius curve [30].

3.1.2. Horizontal corrugation.

The most common types of corrugation that will happened in horizontal directional. The dynamic force creep is Torsional resonance of wheel set and bending mode of wheel set.

Torsional resonance of wheel set.

Increasing the difference in tangential force across the wheelset and exacerbating the stick–slip oscillation. These influences are illustrated in Fig.3.10 [32,33], which shows the traction ratio at both wheels on leading and trailing axles of a bogie as a function of curve radius and for two values of applied traction. The traction ratio shown comprises

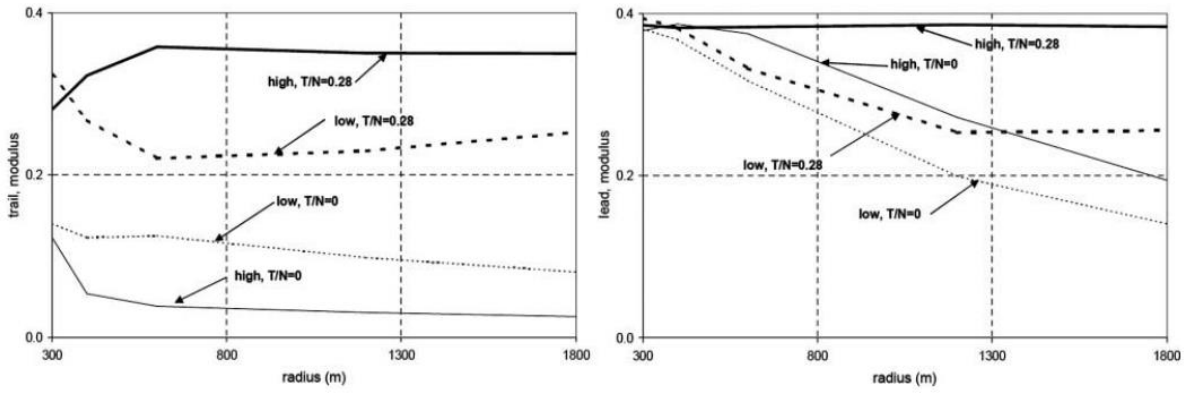

Figure 3.10. Traction ratio on leading and trailing wheelsets of a bogie resulting from curving and applied traction [from 16].

3.2. Numerical modelling of corrugation.

The variable speed model used in this paper is an extension of the model used in Song and Meehan [34]. The system diagram for this feedback model can be seen in fig below. And this model diagram is described the modeling in four stages.

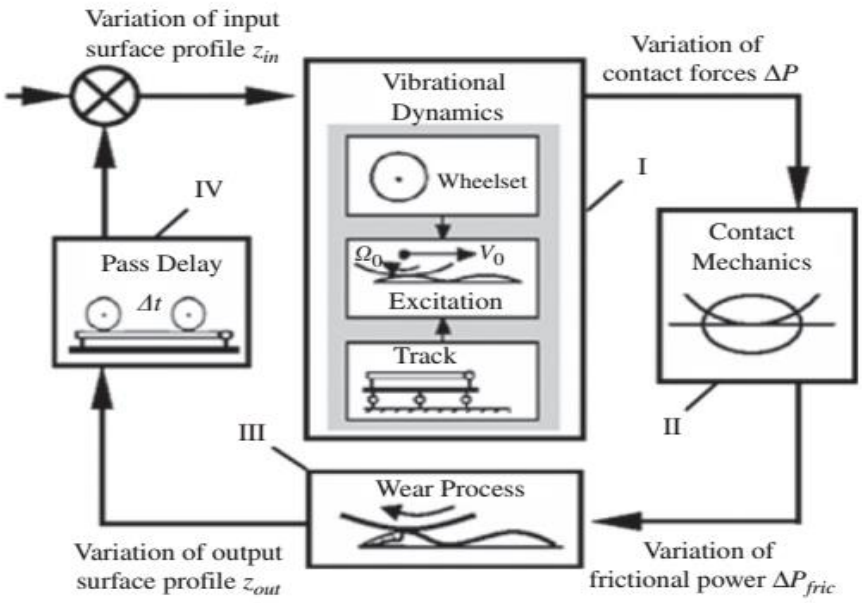

Figure 3.11. block diagram [34].

1. The initial rail profile excites the dynamic components of the wheel–rail system. This leads to a variation in contact forces, which in turn affects the contact mechanics.
2. The variable contact mechanics leads to a variation in the wear process.
3. And 4. fed back into this system over successive passages.

This Song and Meehan general representation of corrugation formation used to derive mathematical model by considering.

- Wheel-rail dynamics.
- Linear contact mechanisms.
- Wear process.
- Finite passage delay for the feedback process.

3.2.1. Wheel-rail dynamics.

wheel–rail dynamics and its modal approximation is provided in Meehan et al. [35]. where a modal decoupling of the vertical dynamics due to the pinned–pinned rail mode and a contact spring is performed to yield a two degree of freedom model of the system, which can be used to highlight the advantages of using a wide distribution of pass speeds.

Assuming that the wheel is acting like a linearized contact spring and is exciting the first pinned–pinned rail mode.

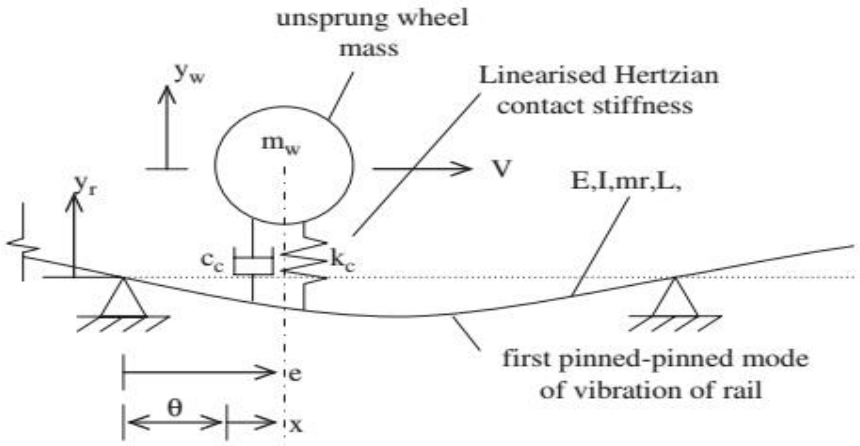

Figure. 3.12. Schematic diagram representing simplified vertical wheel/rail dynamics [35]

To initiate the discussion, let us consider a simple spring-mass damper system, as shown in Fig.26 below. We might consider this as a simple mechanical-measurement system where x1(t) is the input displacement variable which acts through the spring mass damper arrangement to produce an output displacement x2(t). Both x1 and x2 vary with time.

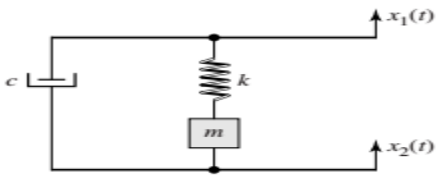

Figure. 3.13. Simple spring-mass damper system

We assume that the damping force is proportional to velocity so that the differential equation governing the system is obtained from Newton's second law of motion as.

$$my'' + cy' + ky = f(t)\text{----------1}$$

$$y'' + \frac{c}{m}y' + \frac{k}{m}y = \frac{f(t)}{m}$$

And decoupled modal description for the wheelset–track vibrational dynamics, I, may be utilized based on experimental and theoretical evidence of an approximately constant corrugation pitch associated with a dominant mode of system vibration. The equations for any given mode i may be described as [36]

$$y''_i + 2\zeta i\omega i y'_i + \omega^2 y_i = \frac{kc}{mi}(Pi - 1)Zin\text{----------2}$$

each yi is a component of the modal displacement of the wheel/rail system, Kc is the contact stiffness and ζi, ωi, mi represent the modal damping, natural frequency, and mass for a particular mode i where *pi* is the modal contribution factor These relate to the actual wheel and rail displacement by

$$y_w = \sum_{i=1}^{M} Piyi \qquad y_r = \sum_{i}^{M} yi\text{----------3}$$

for i = 1 to M, where M is the number of modes and assuming time independent.

$kc(Pi - 1)zin$ represents the modal excitation force arising from the incoming variation in wear, Zin.

3.2.2. Linear contact mechanisms

There are two aspects to the model of the contact mechanics. The first is the use of Hertzian theory to calculate the dynamic contact force of the wheel on the rail. The dynamic component of the contact force is defined such that compression is positive and may be expressed as [37]

$$\Delta p = k_c(y_r + z(x) - y_w) + c_c(\dot{y}_r + \dot{z}(x) - \dot{y}_w)\text{----------4}$$

ΔP from nominal steady state conditions are assumed and for a nominal contact force P0and corresponding displacement δ0, the linearized Hertzian contact stiffness is

$$k_c \equiv \frac{\partial p}{\partial \delta} = \frac{3p0}{2\delta 0} \text{ ----------5}$$

where the distance δ0 by which two points (one in each body, in the unreformed regions) approach after first contact of the bodies is given by Johnson [36] as

$$\delta o = [\frac{9po^2}{16RE^2}]^{\frac{1}{3}} F2 \text{ ----------6}$$

where R and E are the equivalent radius of curvature and elastic moduli of the two bodies, respectively, and F2 is a curvature function approximately equal to 1 as defined in .

The second aspect to the contact mechanics is the calculation of the variation in slip (or creep) Δξ resulting from contact force variations, ΔP. If small variations from nominal conditions ξ0, P0 are assumed, this may be described by the linear relationship

$$\frac{\Delta \xi}{\xi 0} = c_\xi (\frac{\Delta P}{P0}) \text{----------7}$$

Where $c_\xi = \frac{-2(2-\frac{\xi 0}{\xi \max})}{3(1-\frac{\xi 0}{\xi \max})^2}$

$$\xi 0/\xi \max = 1 - (\frac{1-Q}{\mu Po})^{\frac{1}{3}} \text{ ----------8}$$

Cξ is the sensitivity of lateral creep to normal force fluctuations μ is the limiting coefficient of friction, Q the tangential contact force that is assumed to be constant and ξmax is defined in [38]

3.2.3. Wear process.

The wear model is based on the frictional work hypothesis [39] that states that the wear rate (mass removed per second) is proportional to the frictional power. The resultant variation in longitudinal profile zout(x) exiting the rolling contact region due to the variation in frictional power $\Delta \dot{W}$ friction from nominal conditions may be obtained using

$$\frac{Zout - Zin}{\Delta Z0} = \frac{\Delta \dot{w}_{fricr}}{w_{fricto}} \text{----------9}$$

where Δz0 is the nominal steady state change in profile per wheelset pass, and is given by

$$\Delta z0 = \frac{-k0Q0\xi0}{2\rho b}$$

$$\dot{w}_{fric} = Q_0 \xi_0 v$$

$$\Delta z_0 = \frac{-k_0 \dot{w}_{fric}}{2b\rho v} \text{----------10}$$

and k0 is known as the wear proportionality factor or steady wear coefficient and Q0 is tangential force (traction force). Assuming that the tangential contact force and the wheelset linear velocity is constant, the variation of frictional power from nominal steady state conditions is proportional to the variation in creep such that [from reference 37]

$$\frac{\Delta \dot{w}_{fricT}}{w_{fricto}} = \frac{\Delta \xi}{\xi 0} \text{----------11}$$

The equations governing the contact mechanics and the frictional wear process for can be combined as using equation (4) as follow

$$\Delta p = k_c[(y_r + \dot{y}_r) - (y_w + \dot{y}_w) + z(x) + \dot{z}(x)]$$

Recalling equation (3):

$$\Delta p = k_c(y_i - y_i p_i) z_{in}) = k_c(y_i(1 - p_i) z_{in}$$

There for the equation govern contact mechanics and wear process:

$$\frac{Zout - Zin}{\Delta Z0} = \frac{\Delta \xi}{\xi 0} = c_\xi (\frac{\Delta P}{P0})$$

$$\frac{\text{Zout}-\text{Zin}}{\Delta \text{Z0}} = \frac{c\xi\ (kc\ (yi\ (1-pi\ )+zin)}{po} \text{----------12}$$

where Δz0 is the nominal steady state change in profile per wheelset pass, P0 the nominal normal contact force and Cξ the non-dimensional sensitivity of creep variations to contact force variations.

The system equations of motion are now completely described by equation (2,12). To obtain the characteristic behavior of the system it is convenient to express the equations of motion (2), (12) and in Laplace form using a non-depersonalized complex variable S defined by the transform,

$$\frac{z_{outi}}{z_{ini}} = 1 + \text{kb}(1 - \frac{kc_i}{s^2+2\xi is+1})$$----------13

Where:

$$k_b = \frac{\Delta z0\ C\xi kc}{p0} \quad \text{and kci}=\frac{kc(1-pi)^2}{mi\omega i^2}$$----------14

Above equation represents the dynamic behavior of the system over one wheelset passage *K*b represents the sensitivity of wear variations to wheel/rail contact deflection variations and *Kci* may be shown to represent the modal sensitivity of the wheel/rail relative displacement to a change in input longitudinal profile.

For realistic railway parameters, *K*b, *Kci* and ζi are always positive valued. Under these assumptions, it may be easily shown, using renowned stability analysis techniques [40], that the second-order system of equation (13) is always stable.

3.2.4. Finite passage delay for the feedback process

The corrugation growth feedback loop is closed when the change in profile height for each pass, ΔZn, is added to the existing profile, Zn, to become the input profile for the next pass, Zn+1. A single wheel pass transfer function can be created by multiplying each of the major steps in the corrugation growth feedback diagram of Fig.as

$$\frac{z_{n+1}}{z_n} = 1 + \frac{\Delta z_n}{z_n}$$----------15

Let say $\Delta z_n = \Delta z$ and

$$\frac{Zout - Zin}{\Delta Z0} = \frac{\Delta\xi}{\xi 0} = c_\xi\left(\frac{\Delta P}{P0}\right) = \omega = \frac{v}{\lambda}$$

$$k_b = \frac{\Delta z0\ C\xi kc}{p0} \quad \Delta z_0 = \frac{p_0 k_b}{C\xi kc} = \frac{\Delta p k_b}{\omega k_c}$$

$$\frac{z_{n+1}}{z_n} = 1 + \frac{\Delta p k_b}{\omega k_c z_n}$$----------16

It is important to consider here that conditions alternate between each successive wheelset pass as every bogie will have a leading and trailing wheelset, each under different steady state cornering conditions. A growth rate for a single equivalent wheel pass may be calculated based on an averaging of a full bogie pass as,

$$\frac{z_{n+1}}{z_n} = \sqrt{\frac{z_{n+2}}{z_n}} = k_{b/eq}\frac{\Delta p}{\omega z_n k_c} + 1 \text{ ----------17}$$

Where:

$$k_{b/eq} = \frac{k_{b(n+1)} + k_{b(n+2)}}{2}$$

Probabilistic speed distribution

single wheel pass it is sufficient to leave it in terms of frequency, ω. When multiple wheel passes at varying speeds are considered, this frequency must be broken down to a ratio of speed to fixed wavelength, λ. When a probabilistic speed distribution, p(V) is introduced [from reference 22], the growth rate of corrugation for a single equivalent wheelset pass then becomes

$$G_r = \frac{z_{n+1}}{z_n} - 1 = exp\int_{-\infty}^{\infty} ln\left| k_{\frac{b}{eq}}(v)\frac{\Delta p}{z_{in(\omega)}k_c} + 1\right| p(v)dv - 1 \text{----------18}$$

The probabilistic speed distribution would specifically be studied in curves,50m minimum curvature for different passing speed of the wheel which is between Vmax and Vmin, and the probability of the speed which could fall between this gab are identified by standard deviation.

$$s = \sum_{i=1}^{n}\frac{(vi - Vavg)}{(n-1)\sigma^3} = \text{----------19}$$

Probabilistic passing speed

triangular probability density function is used to investigate the effects of speed distribution asymmetry on growth rate. Two constraint cases were defined as being constant average with constant standard deviation, and constant average with constant domain width. Limits of statistical mode were chosen as full right-angled left and right skewed curves and domain extremes were calculated to maintain the defined constraint cases. Probabilistic distribution of speed, p(V), over

many vehicle passages with labels of domain limits, Vmin and Vmax, mode, Vm and maximum height, defined as follow.

$$p(v) = 2\frac{(v-v_{min})}{(v_{max}-v_{min})(v_m-v_{\min})} \quad if v \le v_m \text{----------20}$$

$$p(v) = 2\frac{(v-v_{min})}{(v_{max}-v_{min})(v_{max}-v_m)} \quad if v > v_m \text{----------21}$$

On the probability distribution graph, standard skewness(S) is defined as the second moment of a data set about the mean and is used as a standard measure of statistical spread asymmetry and it will have described below.

$$s = \frac{\sqrt{2}(v_{min}+v_{max}-2v_m)(2v_m-v_{max}-v_m)(v_{min}-2v_{max}-v_m)}{(v_{min}^2+v_{max}^2+v_m^2-v_{min}v_{max}-v_{min}v_m-v_{max}v_m)} \text{----------22}$$

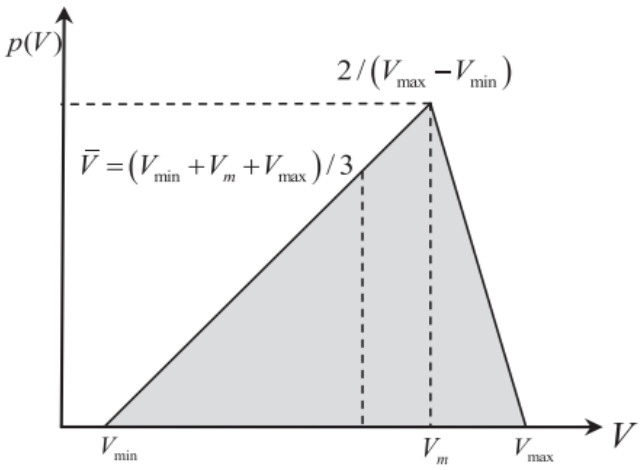

Figure.3.14. speed distribution curve used in the simulation [from reference 22]

Different passing speed data in the curves and straight lines of tram cars from AALRT(km/h)

Table 3.1. speed distribution

Number of pass	vmin	Vmax	Vm	S
1	35	65	40	6.1943
2	33	63	42	4.7129
3	31	61	44	1.8560
4	29	59	46	-2.0286
5	27	57	48	-6.1631
6	25	55	50	
7	23	53	52	

The table below is data from ERC kality depot some mechanical property universal standard that used for corrugation simulation.

Table 3.2. parameters Constant value parameters [41] and from reference 22].

Parameters	**Values**	**Parameters**	**values**
Minimum speed (km/h)	35 in straight and 25 in curves	Track length(m)	10
Wheel mass(kg)	350	Rail density(kg/m^3)	7800
Wheel radius(m)	0.46	Curve radius(m)	50
Wheel load(KN)	66	Coeff of friction	0.4
Young's modulus (steel) (N/m^2)	$2.07x10^{11}$	Primary rail damping ratio	0.01
Poisons ratio	0.3	Contact damping ratio	0.0021
Shear modulus (Pa)	$7.76x10^{10}$	Sleeper spacing (m)	0.6
Curve cant(rad)	0.1040	Mass of the train total	Loaded 11000kg

Table 3.3. Constant parameters

B	creep equation exponent 0.02
C22	Kalker coefficient 3.46
F22	lateral creep coefficient (N), defined as GabC22 6.79×10^6
G	acceleration of gravity (m /s^2) 9.81
Ω	
Ko	wear coefficient 2×10^{-9}
R’	longitudinal relative radius of curvature of contact (m) 0.605
R’’	transverse relative radius of curvature of contact (m) 2.400
μ0	maximum coefficient of friction 0.4
μ∞	coefficient of friction at infinite slip 0.3
Mb	mass of bogie per wheelset (kg) 3000
Mv	mass of vehicle plus payload per wheelset (kg) 8800
Mu	unsprang mass per wheelset (kg) 970
Hb	height of bogie center of mass from the rail (m) 0.25
Hv	height from the rail to geometric roll center of the vehicle (m) 0.5
Hvc	height of vehicle center of mass from the roll center (m) 1.35
W	track gauge (m) 1.435
kroll	rolling stiffness of the wagon at its roll center 402000

The standard skewness is defined as the second moment of a data set about the mean and is used as a standard measure of statistical spread asymmetry. For continuous distributions like the ones above, this can be evaluated as an integral of the distribution function, p(V). For the triangular distributions used, and analyzed using MATLAB plot as follow

Twenty-one different, oddly spaced statistical models were chosen above on the table between the domain limits for fixed standard deviation and 7 speeds were integrated within the domain of each associated distribution curve. All sets maintain an average of 45km/h with symmetric fixed standard deviation curve (i.e. s= 0). Fig.) shows a selection of seven speed distribution curves for fixed standard deviation

And the railway speed of the tram car where had taken from the Addis Ababa light rail vehicle data railway from on station to other station

Table: 3.4 variable speed pass

Number of pass	Station 1	Speed A	Speed B	Speed C	Speed D	Station 2
1	0	35	65	45	35	0
2	0	33	63	45	33	0
3	0	31	61	45	31	0
4	0	29	59	45	29	0
5	0	27	57	45	27	0
6	0	25	55	45	25	0
7	0	23	53	45	23	0

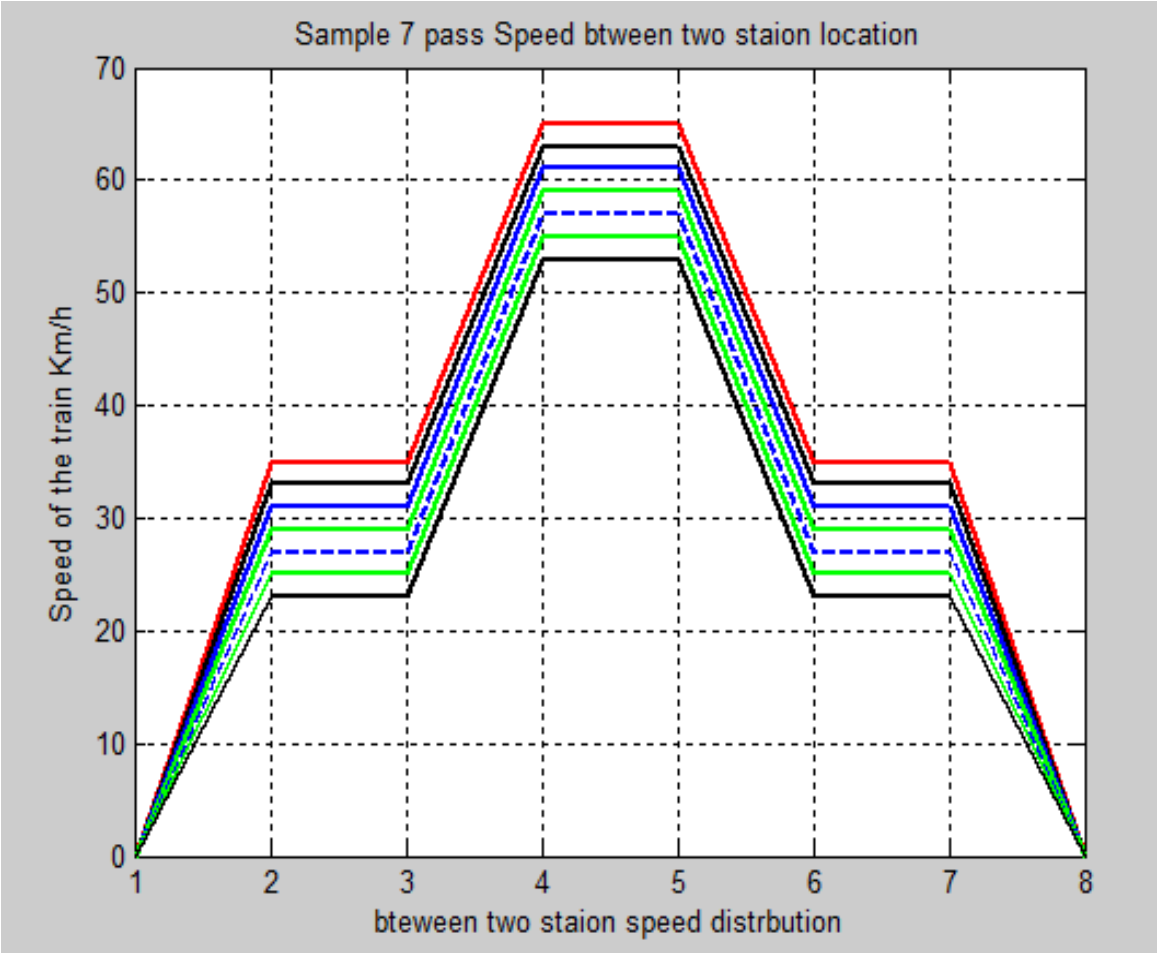

Figure: 3:14b variable passing speed between two station location

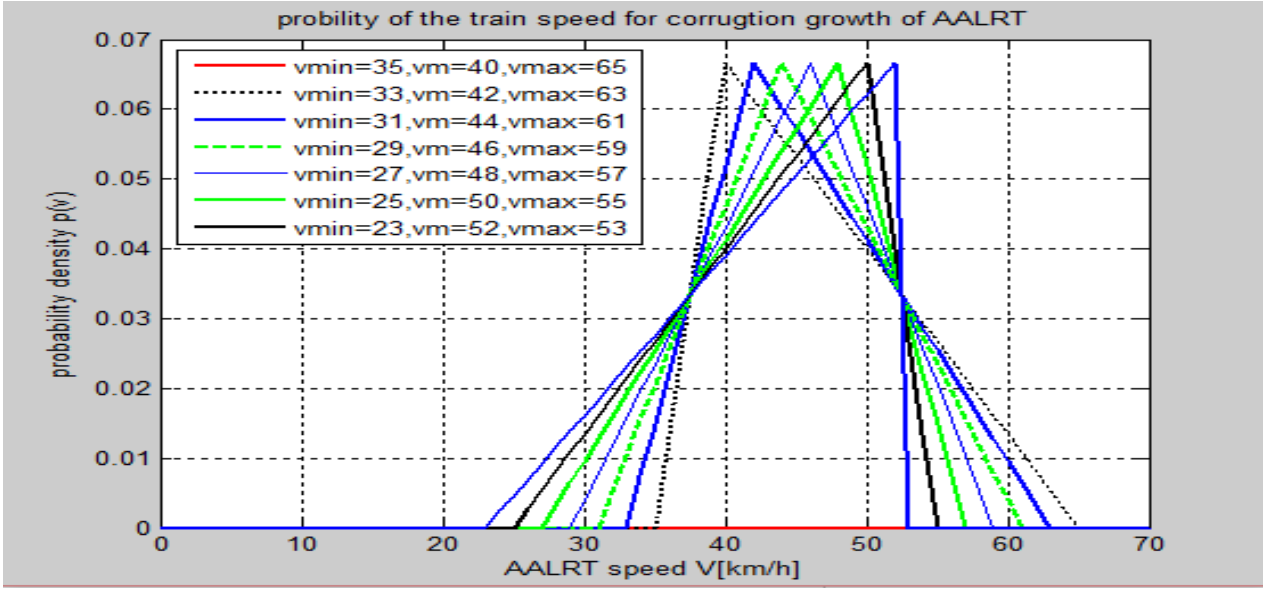

Figure 3.15. Simulated fixed width standard deviation and speed distribution curves

3.3. Corrugation growth in straight track

Corrugation in straight track would happened mostly by the time of the traction and breaking are severe and cause railhead deflection and material removal also by the resonance wheelset that will lead for the wave length fixing type of corrugation.

The load and the velocity relation in the straight track are describe as follow by the rolling resistance and traction effort also by breaking force and wheel sliding. The train free body diagram is described by the free sketches to specify the force and the point of attack in the track line of both curved and straight lines

In straight line, the corrugation is mostly happened by the severe braking and traction time, the corrugation will develop by the dynamic effect of the whole vehicle. In breaking time, specially in the emergence braking the wheel will skid in the track for a longer distance, this will lead the rail for removal of the material and also in the straight track one another effect of speed is the train run by high speed the rail will affected by the dynamic effect of the train, so this all will discussed and analyzed below.

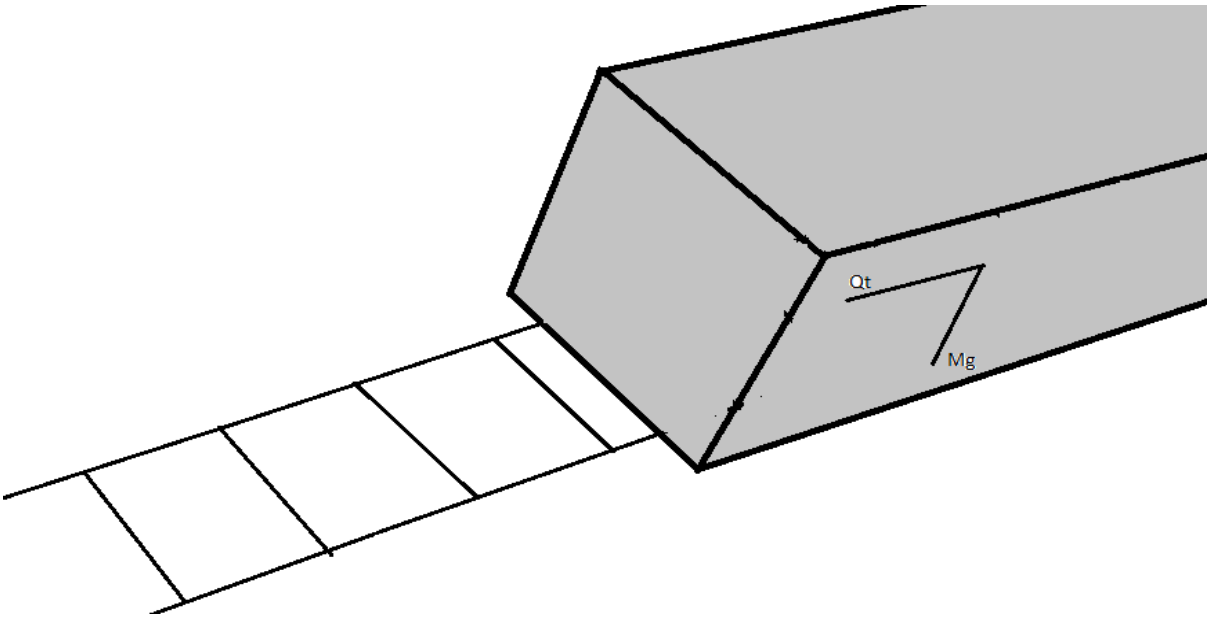

Figure.3.16. The side view of the train in the straight line to describe the direction of the traction effort.

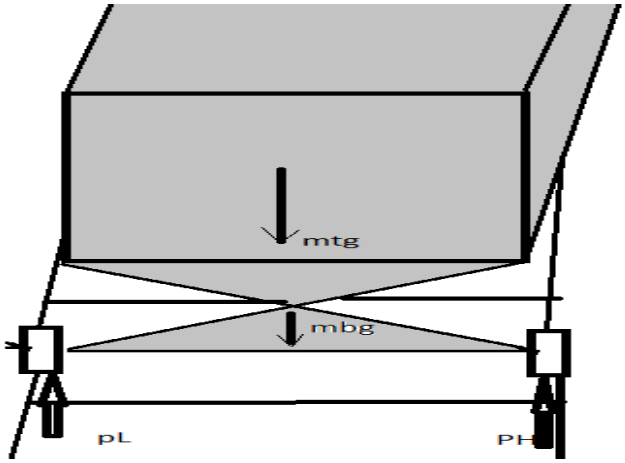

Figure .3.17. The front view of the train to describe applied in the wheel and rail in straight track.

Tractive effort on the longitudinal direction in straight line is shown as

$$TE = \frac{HP \times 308}{v}(Ib - f) = \frac{229675.56}{v} watt$$

Assuming the moment in clockwise direction for tractive effort TE; then applying the moment as follow

$$\sum m@P_L = 0$$

$$-p_H \times 1.435 + \frac{TE}{2} + (984 \times 9.81 \times 0.7175)$$

$$p_H = \frac{TE \times 0.5 + (984 \times 9.81 \times 0.7175)}{1.435}$$

$$p_H = \frac{\frac{229675.56}{v} + (6926.1)}{1.435} = p_H = \frac{160052.655}{v} + 4826.6$$

$$\sum m@P_H = 0$$

$$p_L = \frac{160052.655}{v} + 4826.6$$

3.3.1. Plastic deformation caused by the forward velocity.

Not all solid surfaces perfectly elastic or plastic. The material of bodies in freely rolling contact undergoes a cycle of loading and unloading as flows through the region of contact deformation as shown in fig below.

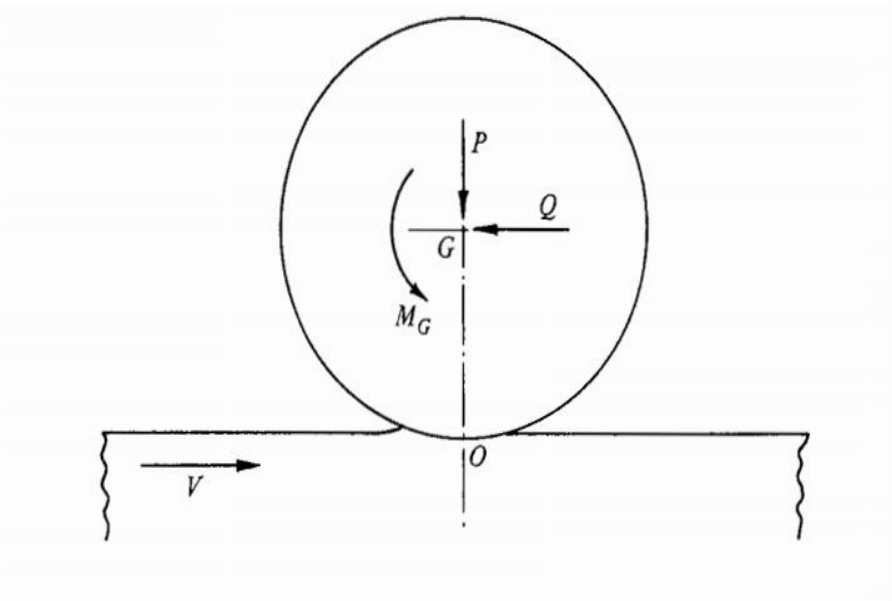

Figure. 3.18. The wheel/rail in plastic deformation

3.3.2. Traction, acceleration and braking

For a railway to operate efficiently and safely, its locomotives should be powerful enough to accelerate their trains rapidly to the maximum allowed line speed, and the braking systems must be able to bring a train reliably to a standing at a station or in emergency braking time. Calculating railway train accelerations and decelerations in order to predict the rate of corrugation growth for AALRT tram.

When the train speed increases the dynamic interaction between the car body and the track this gives to rise the larger dynamic forces. The force requires to move a train in straight line is rolling resistance.

Rolling resistance is friction related, including the resistance of wheels to rolling and it varies with the increase as the speed increase.

The resistance for train movement on straight and level track can be determined by W.J. Davies formula

$$R = A + Bv + Cv^2$$

Whereas R, Train rolling resistance A, rolling resistance component independent of train speed B, Train resistance dependent on speed C, drag coefficient based on the shape of the front of the train and other features affecting air turbulence. And v, is train speed.

This resistive force caused in straight track in track issue are the rail-flange forces vary with speed and quality of the wheel tread and rail as well as the tracking effect of the trucks. The relationship between speed and traction speed are described below in the graphs the track. The Davis Equation has been substantially updated to reflect the resistivity of the train, but its basic form is the same.

$$R_0 = 1.5 + \frac{18N}{w_t} + 0.03v + 0.006v^2$$

From Davies formula above Ro, resistance. Number of Axle W, Total Weight in Tons of Locomotive or Cars V, Velocity of Train. AALRT have three bogies in the one tram car the number of axle will be 6(six) and also the total Wight of the car will be 11000kN and the power of the train from standard 1450KW.

Q=1450000/12= 120830 and this also divided to each wheel of the train = 60415

3.4. Curving

In case of cornering for each speed within the domain of the chosen distribution curves, the steady state parameters of the train are obtained by numerically solving. During curving the train runs in

$$TE = Q = ma = \frac{mv^2}{r}$$

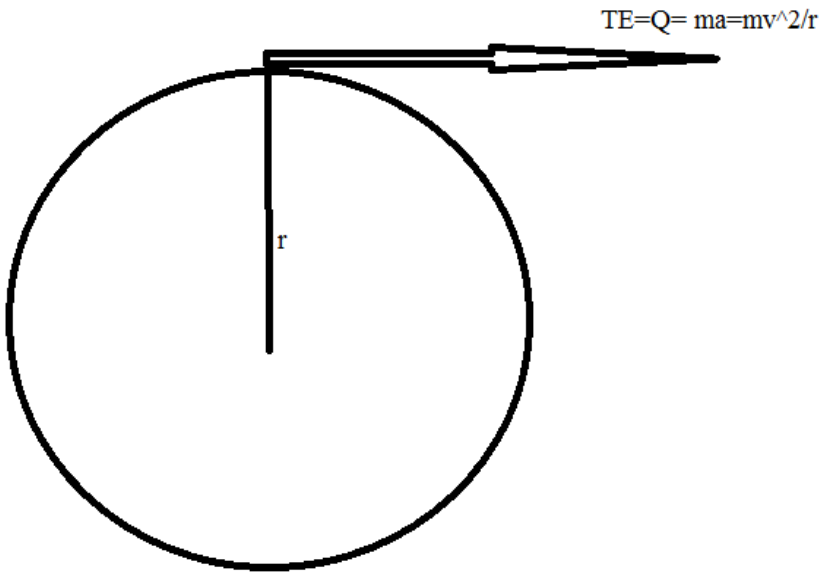

Figure: 3.19. traction in curving

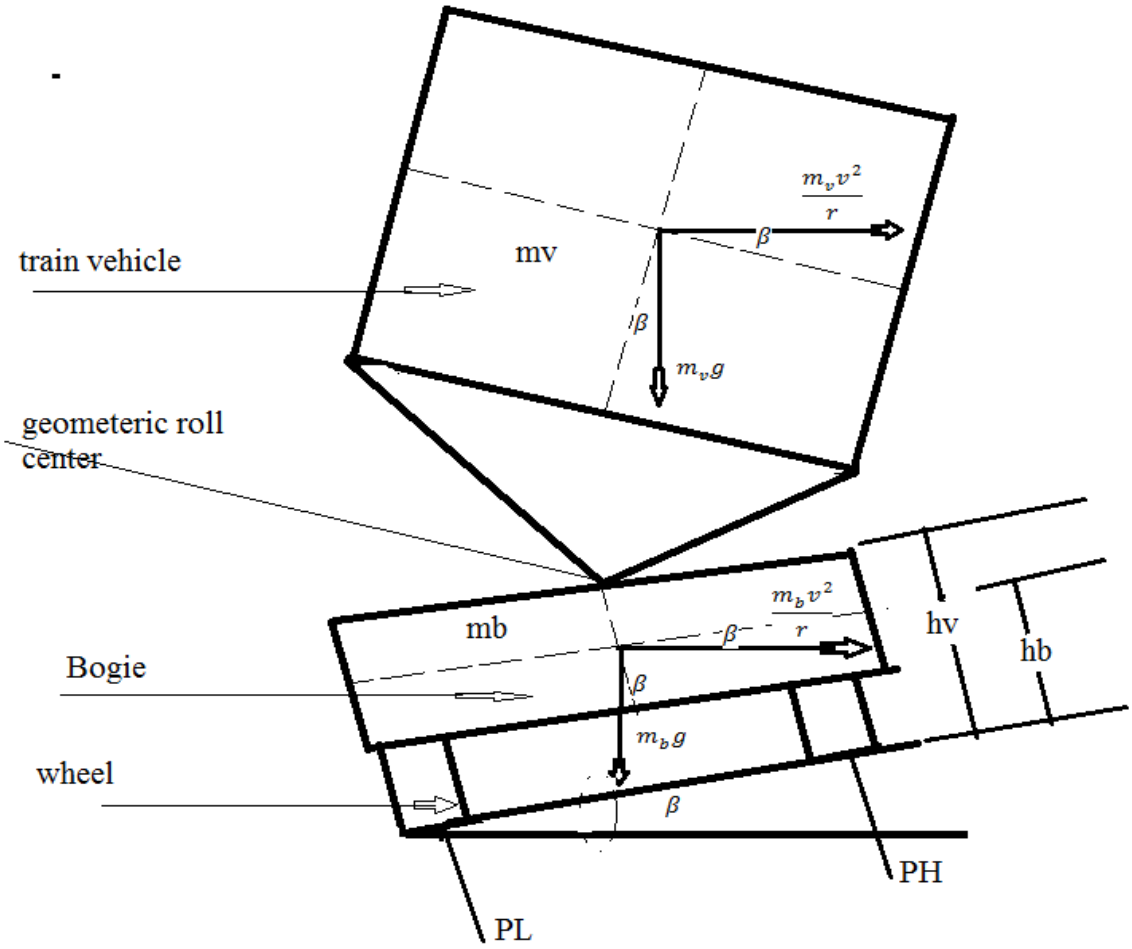

Figure.3.20. train free body in the curve

Assumption has been taken in the vehicle free body diagram

- Static analysis
- At geometric roll center is reactive force for the vehicle PL and PH are also reactive forces
- Traction is towards the high rail due to the load of the train is mostly on the high rail

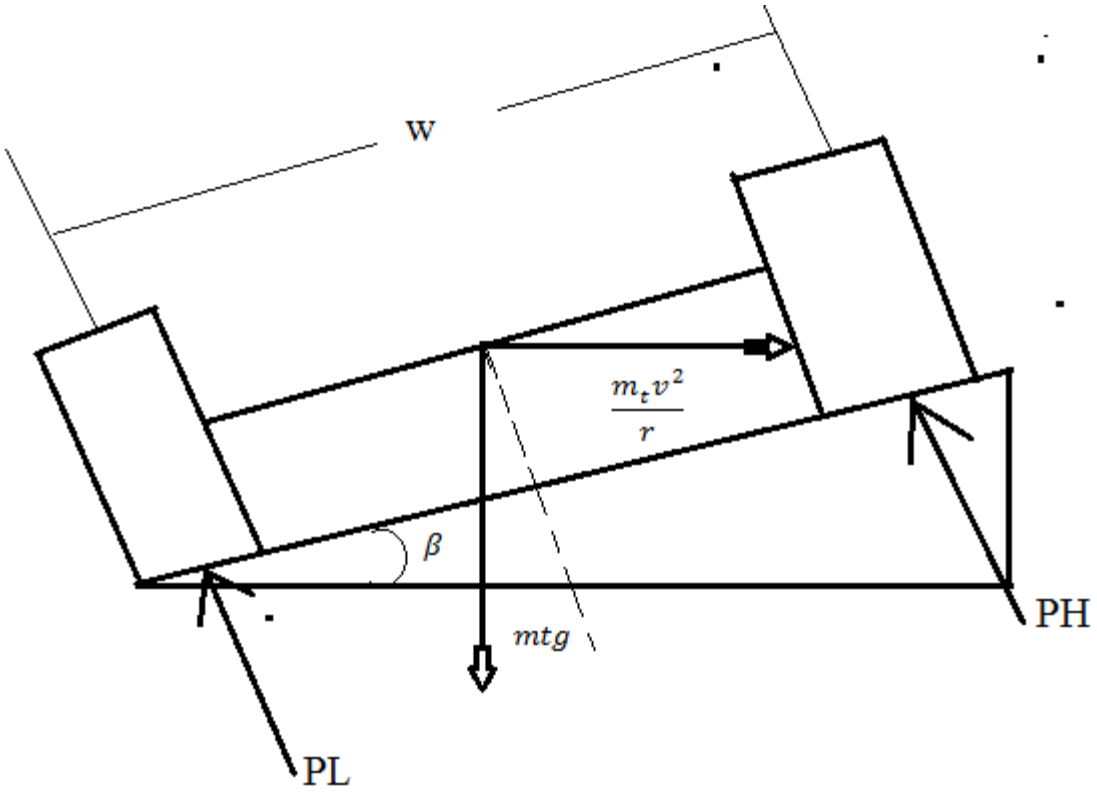

Figure:3.21 Total vehicle free body diagram

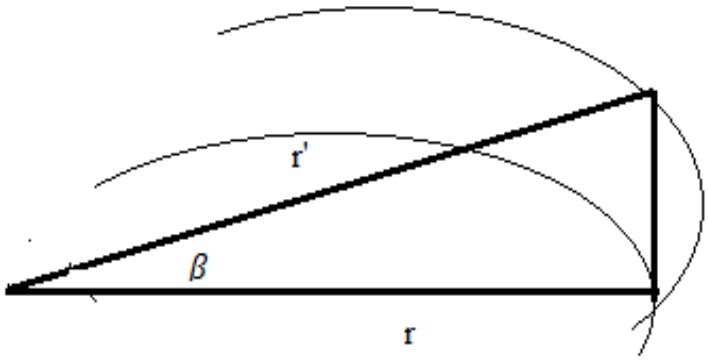

Figure.3.22. the cant of the curved rail

$$r' = \frac{r}{cos\beta}$$

The total lateral traction is equal to:

$$\sum_{i}^{yn} Q = \frac{m_t v^2 cos\beta}{r} + m_t g sin\beta$$

$Q_{(v)} = \frac{m_t v^2 cos\beta}{r} + m_t sin\beta$----------22

$$Q(v) = 22.52v^2 + 6094.6$$

The mass, cant angle and radius of the curvature is given in the table 3 above at skewness s=0 at table 2:

$$Q_0 = \frac{(11000kg)\ (45km/h)^2(cos(5.9374^0)}{50m} - (11000kg)(9.81m/s^2)\sin(5.9374)$$

$Q_0 = 45889\underline{\text{N}}$ traction effort in the s=0

From the figure above the normal force of total train:

$$p_0 = m_t g sin\beta$$

$$p_0 = (11000kg)(9.81)(sin(5.9374)$$

$p_0 = 11{,}162N\ downward$ load of the train in s=0

Normal force of the PH (high rail) and PL (low rail):

Applying the moment in the PL:

Assuming the moment in clockwise direction

$$\sum m@PL = 0$$

$$-wp_H + \frac{mtgw}{2} cos\beta + \frac{m_t w v^2}{2r} sin\beta + \frac{m_v h_v v^2}{r} cos\beta - m_v h_v g sin\beta + \frac{m_b h_b v^2}{r} cos\beta - m_b h_b g sin\beta + \alpha = 0$$

$$p_H = \left(\frac{mtg}{2} + \left(\frac{m_v h_v + m_b h_b}{wr}\right) v^2\right) cos\beta + \left(\frac{m_t v^2}{2r} - \left(\frac{m_v h_v + m_b h_b}{w}\right) g\right) sin\beta + \frac{\alpha}{w}$$----------23

$$\sum m@PH = 0$$

$$wp_L - \frac{mtgw}{2} cos\beta - \frac{m_t w v^2}{2r} sin\beta + \frac{m_v h_v v^2}{r} cos\beta - m_v h_v g sin\beta + \frac{m_b h_b v^2}{r} cos\beta - m_b h_b g sin\beta + \alpha = 0$$

$$p_L = \left(\frac{mtg}{2} - \left(\frac{m_v h_v + m_b h_b}{wr}\right) v^2\right) cos\beta + \left(\frac{m_t v^2}{2r} + \left(\frac{m_v h_v + m_b h_b}{w}\right) g\right) sin\beta - \frac{\alpha}{w}$$----------24

Gravitational forces above the roll center are balanced by the rolling stiffness, kroll, combined with the angular deflection, α such that, [40]

$$\alpha(v) = \frac{h_{cv} g\beta - \frac{v^2 h_{cv}}{r}}{g h_v - \frac{k_{roll}}{m_v}}$$----------25

There for solve for PH(v) & PL(v):

$$\alpha(v) = 0.0006621v^2 - 0.0303$$

$$p_{H(v)} = \left(\frac{11800x9.81}{2} + \left(\frac{8800x0.5 + 3000x0.25}{1.435x50}\right) v^2\right) \cos(5.937) + \left(\frac{11800xv^2}{100} - \left(\frac{8800x0.5 + 3000x0.25}{1.435}\right) 9.81\right) \sin(5.937) + tan^{-1}(0.0004614v^2 - 0.02111)$$

$$= 100320 + 67.463v^2 + 40.12v^2 + tan^{-1}(0.0004614v^2 - 0.02111)$$

$$p_{H(v)} = 107.58v^2 + 100320N + tan^{-1}(0.0004614v^2 - 0.02111)$$---------26

$$p_{L(v)} = \left(\frac{11800x9.81}{2} - \left(\frac{8800x0.5+3000x0.25}{1.435x50}\right)v^2\right)\cos(5.937) + \left(\frac{11800xv^2}{100} + \left(\frac{8800x0.5+3000x0.25}{1.435}\right)9.81\right)\sin(5.937) - tan^{-1}(0.0004614v^2 - 0.02111)$$

$$= 124260 - 67.463v^2 + 40.12v^2 + tan^{-1}(0.0004614v^2 - 0.02111)$$

$$p_{L(v)} = -27.343v^2 + 124260N - tan^{-1}(0.0004614v^2 - 0.02111)\text{----------27}$$

The critical slip ratio, ξmax, is a function of the contact patch dimensions of major and minor semi axes, a and b, as well as normal force, P0, shear modulus, G, effective friction coefficient, μ, a Kalker coefficient, C22, for lateral traction, Poisson's ratio, ν, and Young's modulus, E, such that [40]

$$\xi_{max} = \frac{3\mu p0}{c22Gab} \text{ =(3x0.4x36575)/ (6790000) = 0.0065}$$

$$GabC22 = 6.79\ X\ 10^6$$

$$a, b = \frac{6.79\ X\ 10^6}{(3.46)(7.76\ X\ 10^{10})} = \ 0.2529\ X\ 10^{-4}$$

Using equation. (8)

$$\xi 0/\xi \text{ max} = 1 - (\frac{1-Q_0}{\mu_0 Po})^{\frac{1}{3}}$$

$$\xi 0/\xi \text{ max} = 5.6684$$

and

$$\xi 0 = 0.0368$$

where Cξ is the sensitivity of lateral creep to normal force fluctuation given by:

$$c_\xi = \frac{-2(2-\frac{\xi_0}{\xi max})}{3(1-\frac{\xi_0}{\xi max})^2} = 0.1122$$

Using equation (10).

$$\Delta z0 = \frac{k0Q0\xi 0}{2\rho b} = \frac{(2\ X\ 10^{-9})(22.52v^2 - 6094.6\ )(0.0368)}{2(7800)(\ 0.2529\ X\ 10^{-4})}$$

$$\Delta z0 = 4.2015X10^{-9}v^2 - 1.1370X10^{-6}$$

The normal contact force variation, ΔP using equation (5) and (6)

$$k_c \equiv \frac{\partial p}{\partial \delta} = \frac{3p0}{2\delta 0} = \Delta p$$

$$\delta o = [\frac{9po^2}{16RE^2}]^{\frac{1}{3}} = \frac{9(11{,}162)^2}{(16)(50)(2.07X10^{11})^2} = 3.1981\ X\ 10^{-6}$$

$$\Delta p = \frac{3(11{,}162)}{2(3.1981X10^{-6})} = 5.2352\ X\ 10^{9}$$

Sensitivity of wear variations to wheel/rail contact deflection in low rail.

$$k_b = \frac{(8.4746\ X\ 10^{-5})(0.1122)(5.2352\ X\ 10^{9})}{-70.18v^2+61{,}158N-tan^{-1}(0.0004614v^2-0.02111)}$$

$$k_b = \frac{49779}{-70.18v^2 + 61{,}158N - tan^{-1}(0.0004614v^2 - 0.02111)}$$

And sensitivity of the wear variation in the high rail

$$k_b = \frac{49779}{(107.58v^2 + 100320N + tan^{-1}(0.0004614v^2 - 0.02111))}$$

$$\Delta p = k_c(y_i - y_i p_i) + z_{in}) = k_c(y_i(1 - p_i) + z_{in}$$

Resulting from an input surface profile height variance Zin, taken ass zero initial profile

$$\frac{\Delta p}{z_{in}} = \frac{k_c}{1+k_c(y_i+y_i p_i)} \text{----------2}$$

$$z_{in} = 1 + k_c(y_i + y_i p_i)$$

The expressions governing the behavior of the quarter car model with different passing speed of the vehicle taken as follow are as follows:

Table 3.5. sum of mode (Quarter car model) 42][Appendix B]

	Speed V=20km/h	Speed V=40km/h	Speed V=60km/h
Mt	11000kg		
Kt	169380kg/sec^2	679010 kg/sec^2	1527800 kg/sec^2
Ct	30522kg/sec	611111kg/sec	91667kg/sec
Mw	350kg		
Kw	10779kg/sec^2	43210 kg/sec^2	97222 kg/sec^2
Mr	50kg		
Kr	1539.8kg/sec^2	6172.8 kg/sec^2	1388.9 kg/sec^2
Cr	277.47kg/sec	555.55kg/sec	833.33kg/sec

$$y_{i(\omega)=} \sum_{i=1}^{5} \frac{1}{k_i} + m_i(2\pi\omega)^2 + 2\pi\omega c_i$$

$$y_{i(\omega)} = 0.0585 + 9.4248\ X\ 10^7\omega^2 + 5.3721\ X\ 10^6\omega$$

$y_i p_{i(\omega)} = unsprang\ mass$---------- the wheel act as unsprang mass in the rail

$$z_{in(\omega)} = 1 + 5.2352\ X\ 10^9(0.0585 + 9.4248\ X\ 10^7\omega^2 + 5.3721\ X\ 10^6\omega + 970)$$

$$z_{in(\omega)} = 3.0723\ X\ 10^5 + 4.9341\ X\ 10^{14}\omega^2 + 2.8124\ X\ 10^{13}\omega \text{ ----------29}$$

Finally, the growth of the corrugation becomes using equation 17

$$Z_{1+n} = k_b(1 + \frac{k_c}{4\zeta(1+\zeta)})$$

$$= exp \int_{-\infty}^{\infty} ln \left| k_{\frac{b}{eq}}(v) \frac{\Delta p}{k_c} + 1 \right| p(v)dv - 1$$

$$exp\int_{-\infty}^{\infty} ln\left|\frac{\Delta z0\ C\xi kc}{(107.58v^2+100320N+tan^{-1}(0.0004614v^2-0.02111))}+1\right|p(v)dv$$
$$-1$$

train at curve rigid geometric roll center $tan^{-1}(0.0004614v^2-0.02111=0$

$$exp\int_{-\infty}^{\infty}\ln(\frac{49779}{(107.58v^2+100320)})+0.065)\,dv$$

Integrating the above expression for the high rail.

$$\exp(\frac{\left(107.58v^2+100320N+tan^{-1}(0.0004614v^2-0.02111)\right)}{145.26v}\left(ln\frac{(3235.6)}{(107.58v^2+100320N+tan^{-1}(0.0004614v^2-0.02111)0)}-1\right)+0.065v$$

And the integrating the expression for the low rail

$$\exp(\frac{-27.343v^2+124260N-tan^{-1}(0.0004614v^2-0.02111)}{141.36}\left(ln\frac{(3235.6)}{(-27.343v^2+124260N-tan^{-1}(0.0004614v^2-0.02111))}+1\right)+0.065v$$

The corrugation growth feedback loop is closed when the change in profile height for each pass, ΔZn, is added to the existing profile, Zn, to become the input profile for the next pass, Zn+1. A single wheel pass transfer function can be created by multiplying each of the major steps in the corrugation growth feedback diagram of above on the in the figure 3.11.

Chapter 4

Abacus Modeling of corrugation

Abacus is a commercial software for dynamic and static simulation of mechanical multibody systems (MBS). Abacus has become one of the most used software tools for simulating different mechanical system including railway vehicle dynamics. The Abacus enables setup of a model by usage of simple elements such as rigid bodies, dynamic bodies springs, dampers, constraints and joints. More advanced components such as flexible bodies and wheel-rail contacts can also be used. Specifically, the wheel-rail contact element takes care of everything concerning the contact such as contact detection, normal and tangential force distribution and revolution of the wheel at given time and direction.

It can also handle contact point of wheel-rail. The structural flexibility of bodies in the mechanical system needs to be accounted for through input from other FE-software. The solver also visualized and plotted in the Abacus 6.13 software.

4.1. Rail

Rail that is simulated in the paper is standard chin rail which is used in the Addis Ababa light rail transit. The following are all standard and specification of chains rail that is utilized in Addis Ababa tram railway cars.

LRT rail	Height (mm)	Weight (kg/m)	Bottom width (mm)	Head width (mm)	Middle thickness (mm)	Length (mm)	Standard
50kg	152	50	132	70	15.5	12.5-25	TB

Table.4.1. dimensional specification of AALRT [41].

And the AALRT rail has its own mechanical and chemical composition which is stated in the table below. Simulation input data for the rail for material property. Data obtained from kality depot Addis Ababa.

Mechanical property						Chemical composition				
Yield strength		Tensile strength		Elongation	Hardness	C	Si	Mn	S	P
MPa	Kg/mm^2	MPa	Kg/mm^2	min	HB				<<	<<
460		880min		9	260	0.65-0.77	0.15-0.35	1.10-1.50	0.04	0.04

Table.4.2. mechanical property and chemical composition of the rail [41]

The physical sketch of the rail is as follow

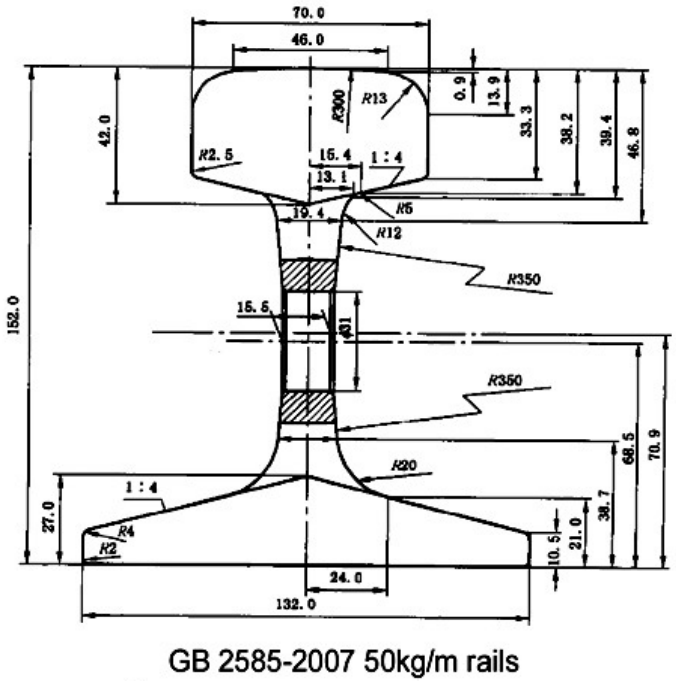

Figure 4.1. detail dimensional sketch of the AALRT rail [41].

First, to study the growth rate of corrugation which is caused by non-uniform speed of the train in abacus understand which output parameter is needed the basic output for the corrugation is plastic deformation of the rail. FE-based dynamic wheel-rail contact modelling and simulations was

developed. Abaqus solve and the part assemble for configuring, meshing and loading a parametric wheel-rail model.

The meshing can be based on measured wheel and rail profiles, i.e., worn profiles. The kinematic constraints are enforced with the ABAQUS contact element and the material models are treated as elastic-plastic with kinematic hardening. The dynamic explicit loads were obtained from train dynamic calculations with special purpose MBS software.

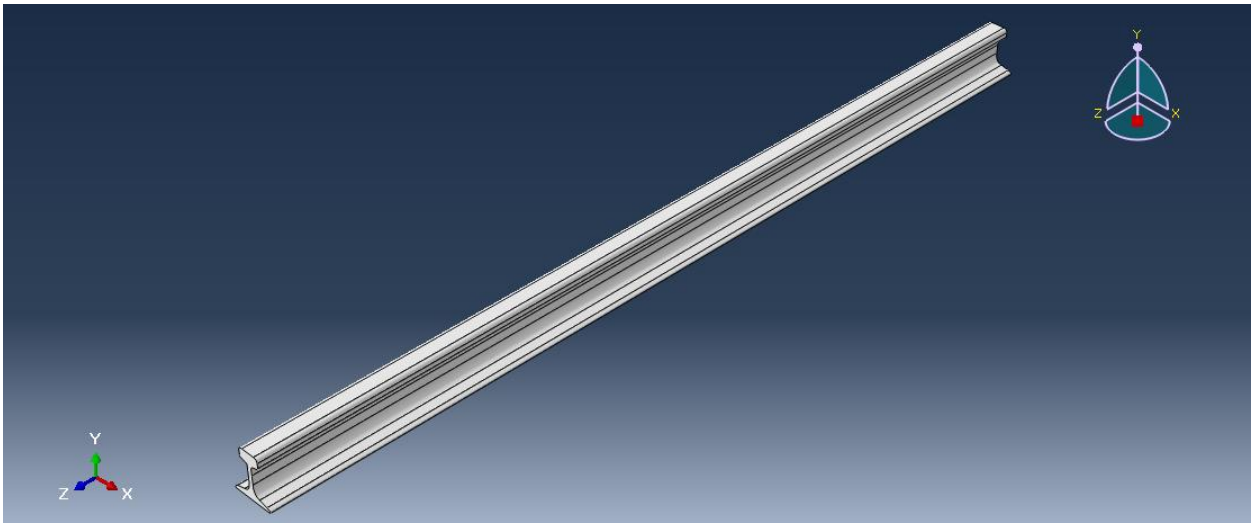

Figure 4.2. ABAQUS rail part.

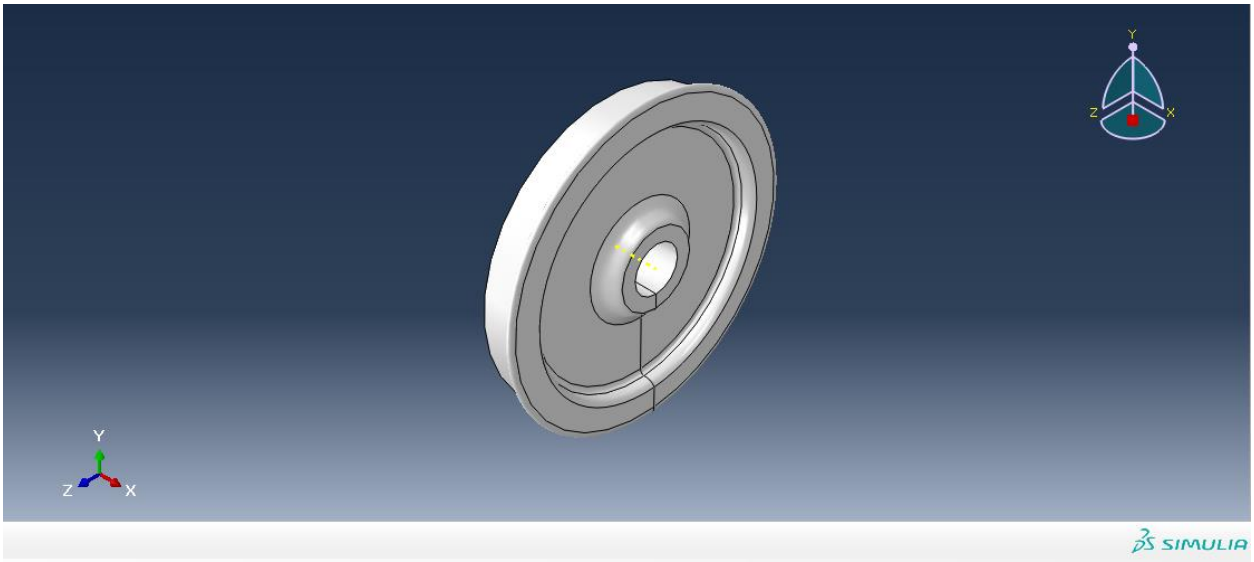

Figure.4.3. ABAQUS wheel part.

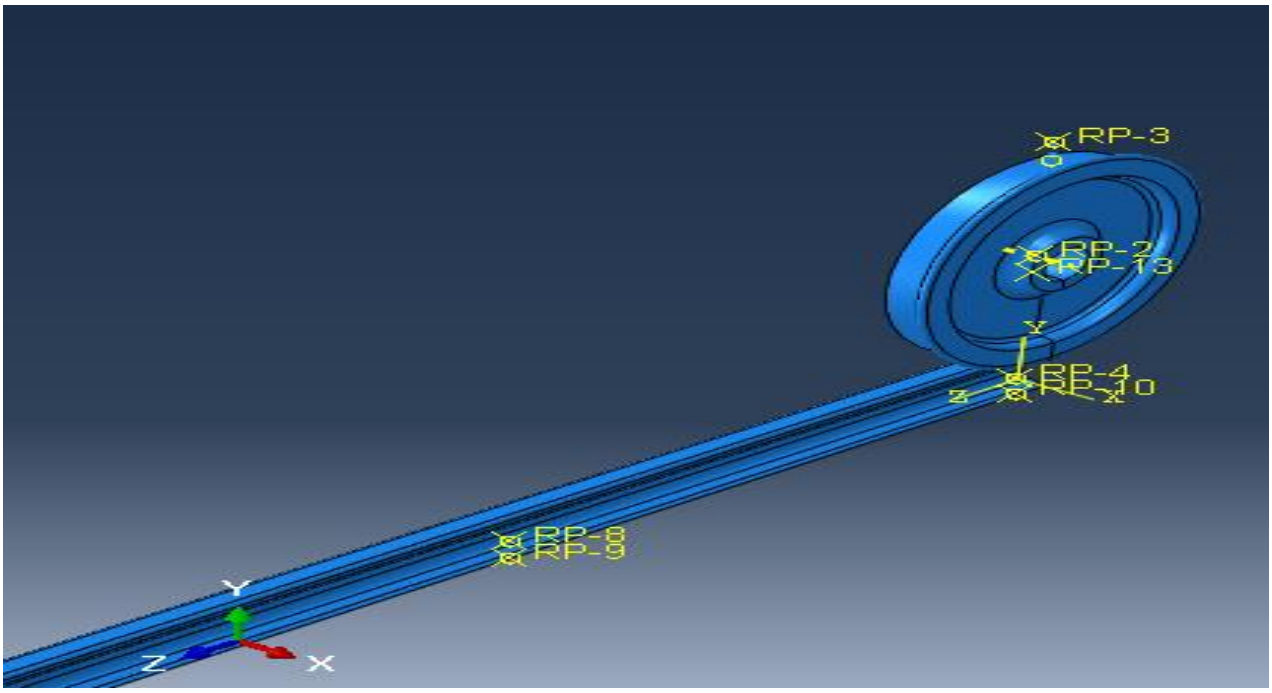

Figure.4.4. ABAQUS wheel-rail contact assemble.

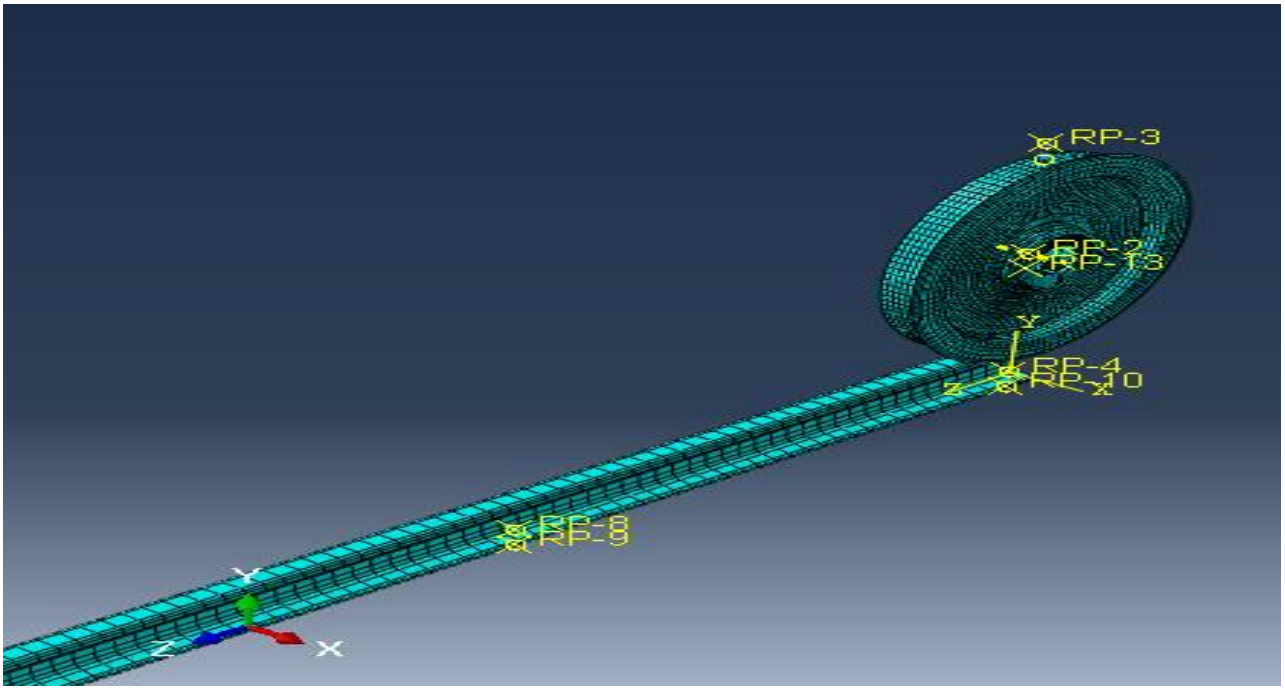

Figure.4.5 ABAQUS mesh

Chapter 5
Result and discussion

Simulation parameters were implemented to represent Addis Ababa LRT which have ballast track. MATLAB and ABAQUS simulation where done in curve radius 50m and the gage is 1435mm and 0.1040rad cant, [from table 3.2] Speed of the train is between 20-70km/h but taking most(skewness) of the speed is take place at average 45km/h. The bogie has a wheelbase with 2.5m and carries almost one half the mass of one loaded passenger train with full loaded condition 11000 kg above the train geometric roll center assuming dry contact conditions with a coefficient of friction of 0.4 at full sliding and 0.3[table3.2] at high slip. For each speed within the domain of the chosen distribution the simulation has been done

5.1. Corrugation caused on straight line.

The first part of the results section will show the increasing rate of corrugation in straight line, using ABAQUS analytical solutions and MATLAB/SIMULINK numerical straight track simulation, which is described.

In regarding to the load on the two wheels on the straight line carries the same load [Appendix 3].

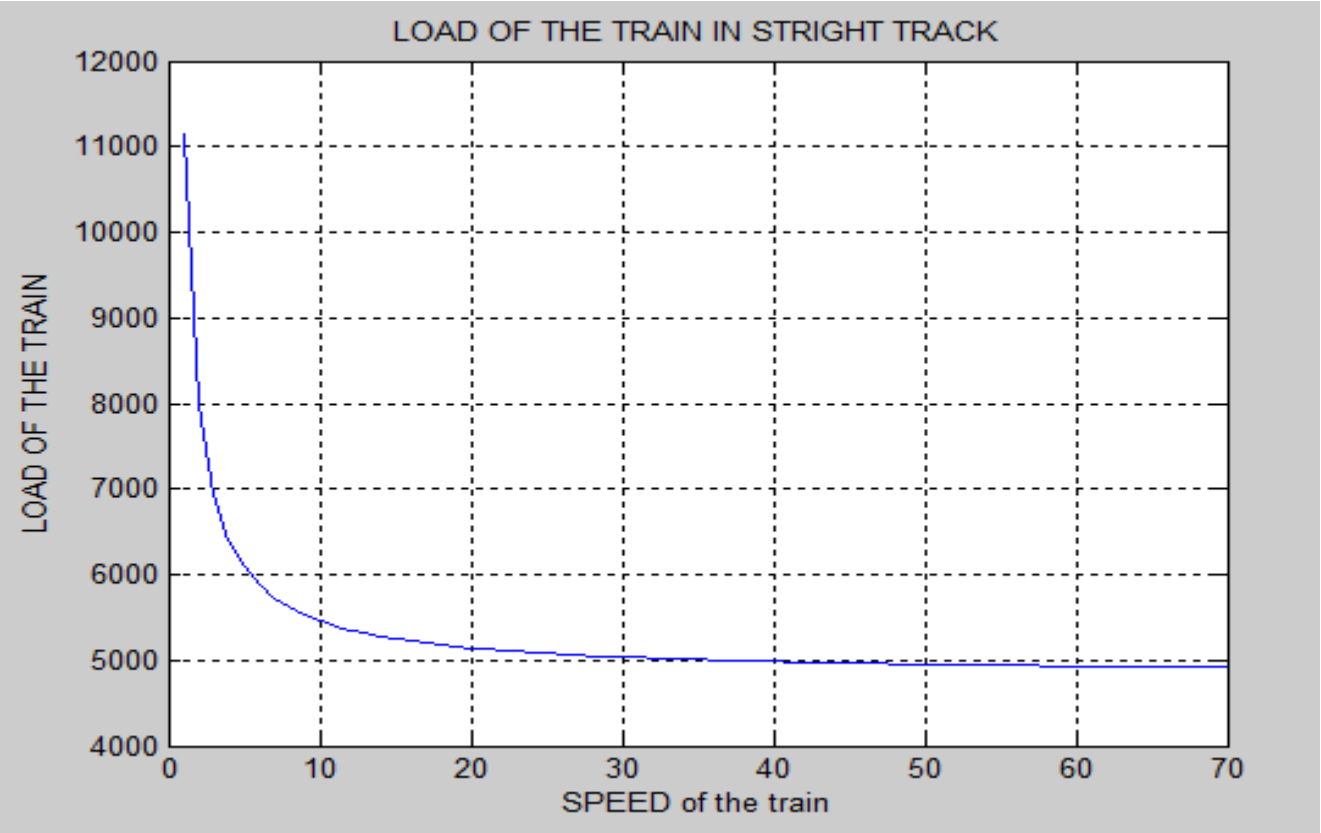

Figure.5.1. the effect of load in straight line

As shown seen in the graph above at very low speed the load of the car are extremely high. the speed increases the contact between rail and wheel decrease. This load decrease because of the friction between the wheel and rail decrease because of the forward speed of the train as observed in the graph fig;5.1.

And also, the traction effort is comparatively high at low speed, this is so because of the kinetic and potential energy created during the motion of the train that would overcome the resistance that will increase at the high speed. [Appendix 4];

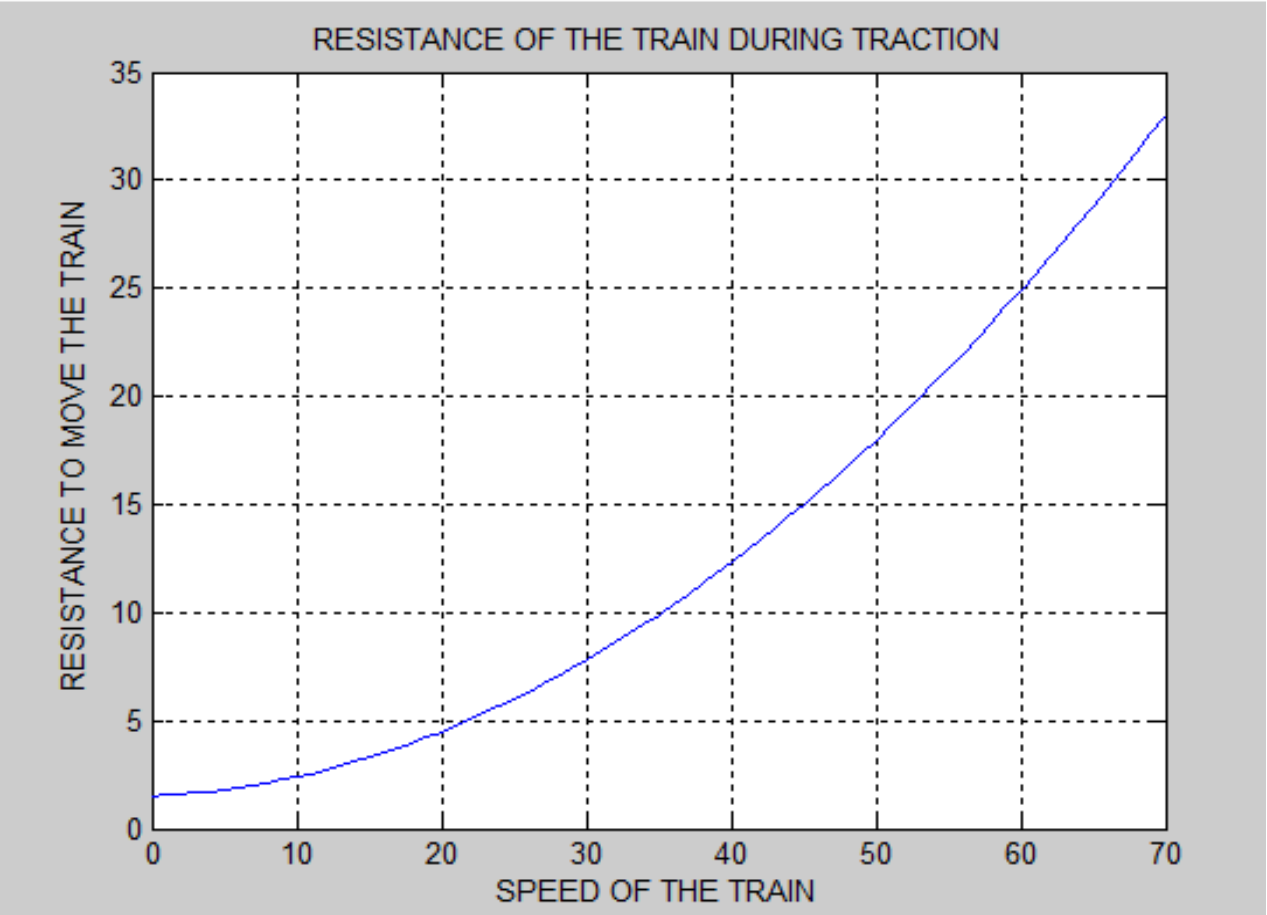

Figure 5.2. Resistance of the train running in the straight

Resistance is the combination of forces that work against a train's movement. The primary resistant force that trains must overcome is friction. If the weight, w, is great enough to overcome the static friction, the car will start to move. Resistance increases significantly as the speed increases this is so because of the opposite forces that applied against the train [Appendix 5].

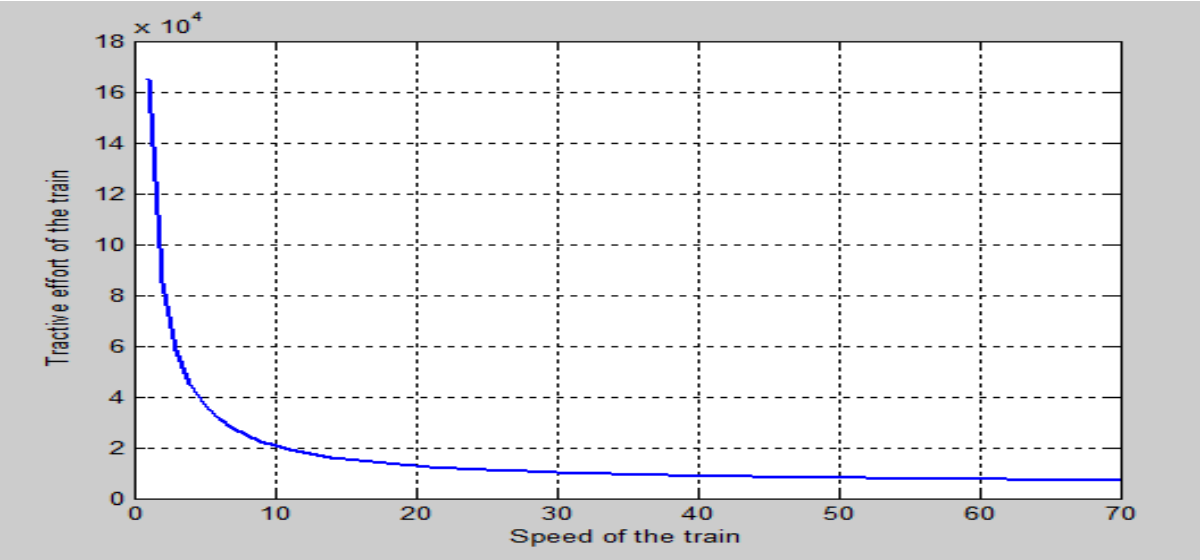

Figure.5.3. The traction change with speed in straight

Using equation of motion described above in equation (1) to obtain this corrugation and input is frequency input because of the dynamic effect of the vehicle and that the wheel is acting like a linearized contact spring.

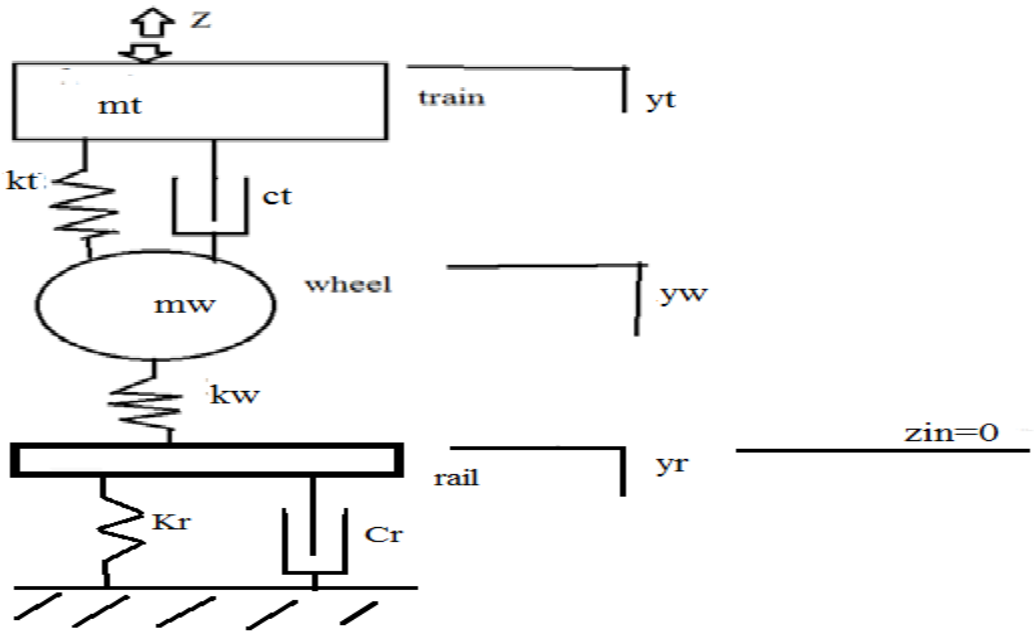

Figure:5.3-wheel rail dynamics Freebody diagram

to calculate the corrugation growth generated by dynamic of vehicle system, a quarter car system will be implemented using MATLAB software. The expressions governing the behavior of the quarter car model are as follows: [42] using newtons second law of motion in figure 5.3

$\sum Fy = 0$ taking the initial profile Zin =0

F0-F1-F2=0

$$F2 = m_t y_t'' = c_t(y'_t - y'_w) + k_t(y_t - y_w) - c_t z + k_t z$$

$$F1 = m_w y_w'' = k_w y_w$$

$$F0 = m_r y_r'' = c_r y'_r - k_r(y_w - y_r)$$

And

$$F0 = m_r y_r'' - \left[c_t(y'_t - y'_w) + k_t(y_t - y_w) + c_r y'_r + k_r(y_w - y_r) - z(c_t + k_t)\right] + k_w y_w = 0 \text{----------30}$$

Z the input which represents the modal excitation force arising from the incoming vibration and taking the sin wave source block because it relates with the vibration

$$m_r y_r'' - c_t(y'_t - y'_w) - k_t(y_t - y_w) + z(c_t + k_t) + k_w y_w - c_r y'_r - k_r(y_w - y_r) - = 0$$

$$y_r'' = \frac{c_t}{m_w}(y'_t - y'_w) + \frac{k_t(y_t - y_w)}{m_w} - \frac{z(c_t + k_t)}{m_w} - \frac{k_w y_w}{m_w} \frac{-c_r y'_r - k_r(y_w - y_r)}{mw}$$

Using table 3.4 developing the Simulink model for the tram car exited in the straight-line track and observing the result by 20,40 and 60km/h which is the speed doubled and tripled and calculating the resulting resonance corrugation in the rail head.

Once rail vertical displacements have been calculated, by renaming V=L/t using this where V is the tram speed and t is time, they are differentiated twice with respect to kg to obtain the desired speed.

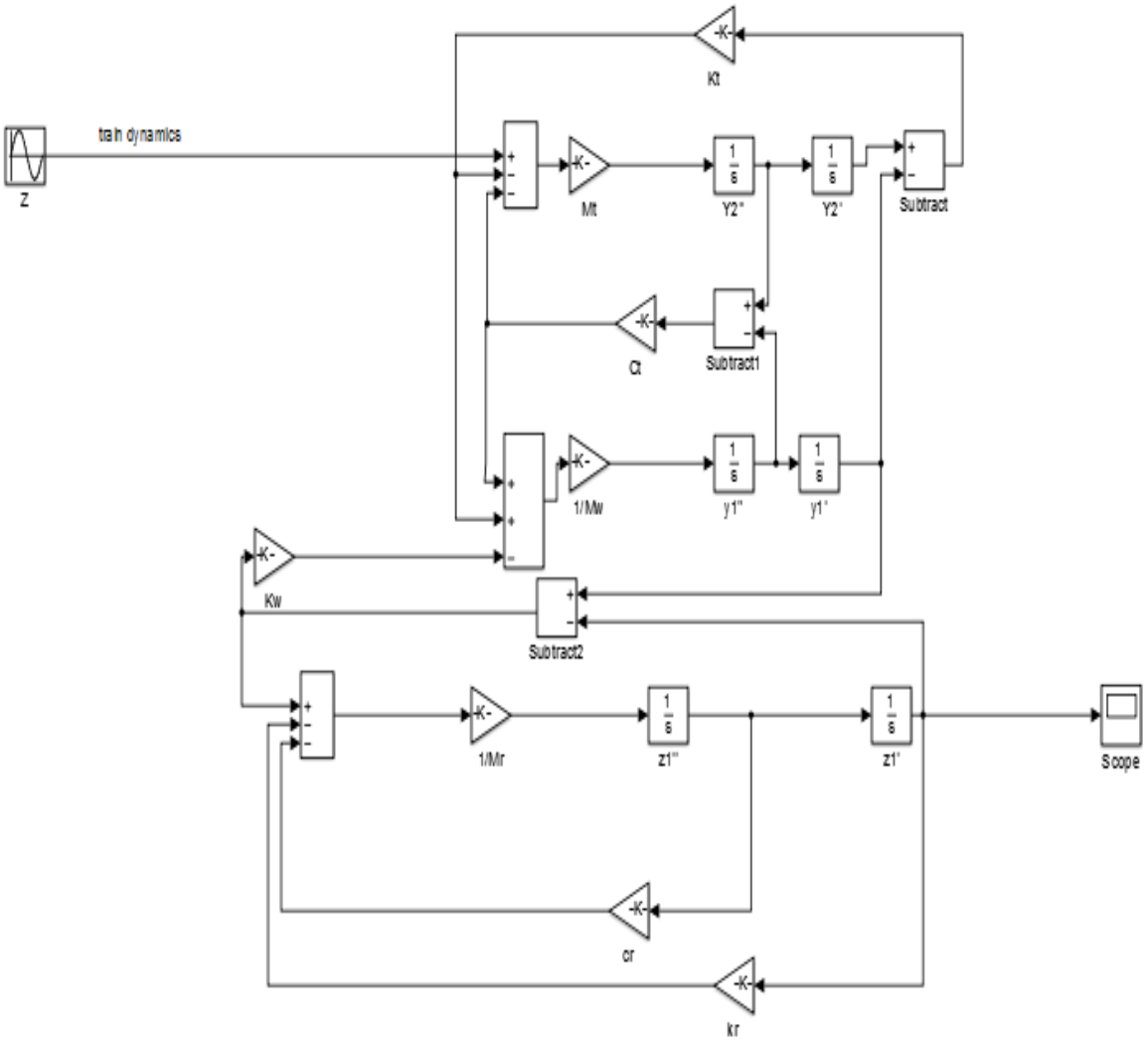

Figure.5.4. Simulink model for straight line track corrugation

Take three speeds from the speed rang of AALRT

Using MATLAB Simulink. From the figure 3.12 the taking unit length m had assumed by the beam deflection and for different types of corrugation then taking the 20,40,60km/h (5.55, 11.11, 16.66m/s) speed for sampling the growth rate of corrugation in straight line.

The procedure will be as follows: the growth of corrugation caused by the presence of dynamics of the train on the rail will be calculated by using an auxiliary quarter car model and then the influence in dynamic overloads of parameters which define rail irregularities will be discussed

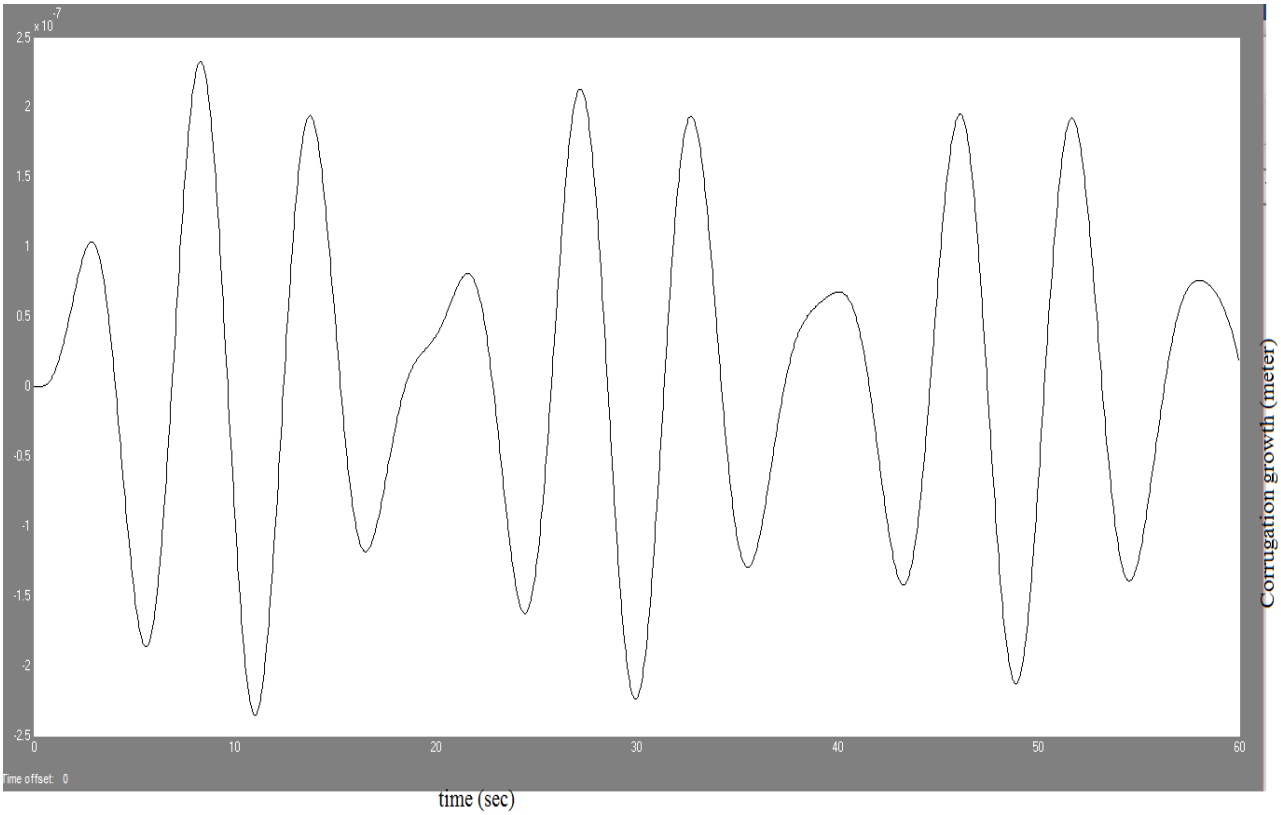

Figure 5.5. The growth rate of the corrugation in straight track at the speed 20km/h.

Normally observing the result on the graph above where: mw: unsprang mass per wheel, cw: contact stiffness, mt: sprung mass per train , kt: primary stiffness of train suspension , cr: primary damping of the rail, L: displacement of the ith mass, ith: velocity and ith damping, and: ith acceleration of the mass.

Boundary condition for the railway train acting like frequency response in the rail track and taking sine source block and initial surface is taking like liner which is initial rail profile is assuming zero or no irregularity or deformity in the rail head and with quarter car model simulation result showed up that the upper amplitude of the irregularity is due to dynamic effect of the vehicle which is running at 20km/h for single pass of the train is approximately $2.5\times10^{-7}m$

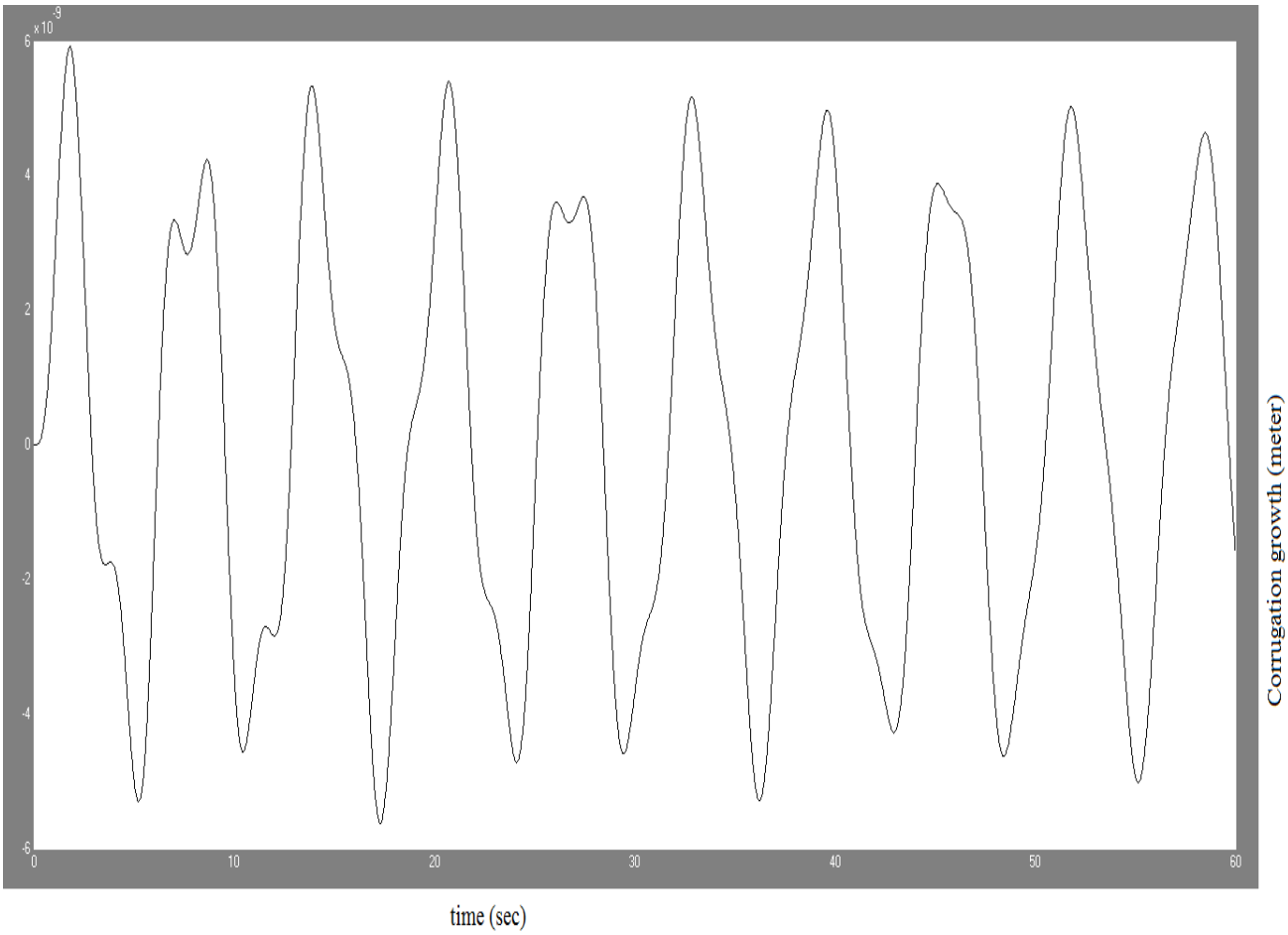

Figure 5.6. The growth rate of the corrugation in straight track doubled speed 40km/h

For the same Boundary condition for the railway train acting like frequency response due to the 40km/h speed in the rail track and taking sine source block and initial surface is taking like liner which is initial rail profile is assuming zero or no irregularity or deformity in the rail head and with quarter car model simulation result showed up that the upper amplitude for single pass of the wheel ,the irregularity is due to dynamic effect of the vehicle is approximately $6\times10^{-9}m$ per pass this showed that the speed doubled the amplitude growth will decrease .

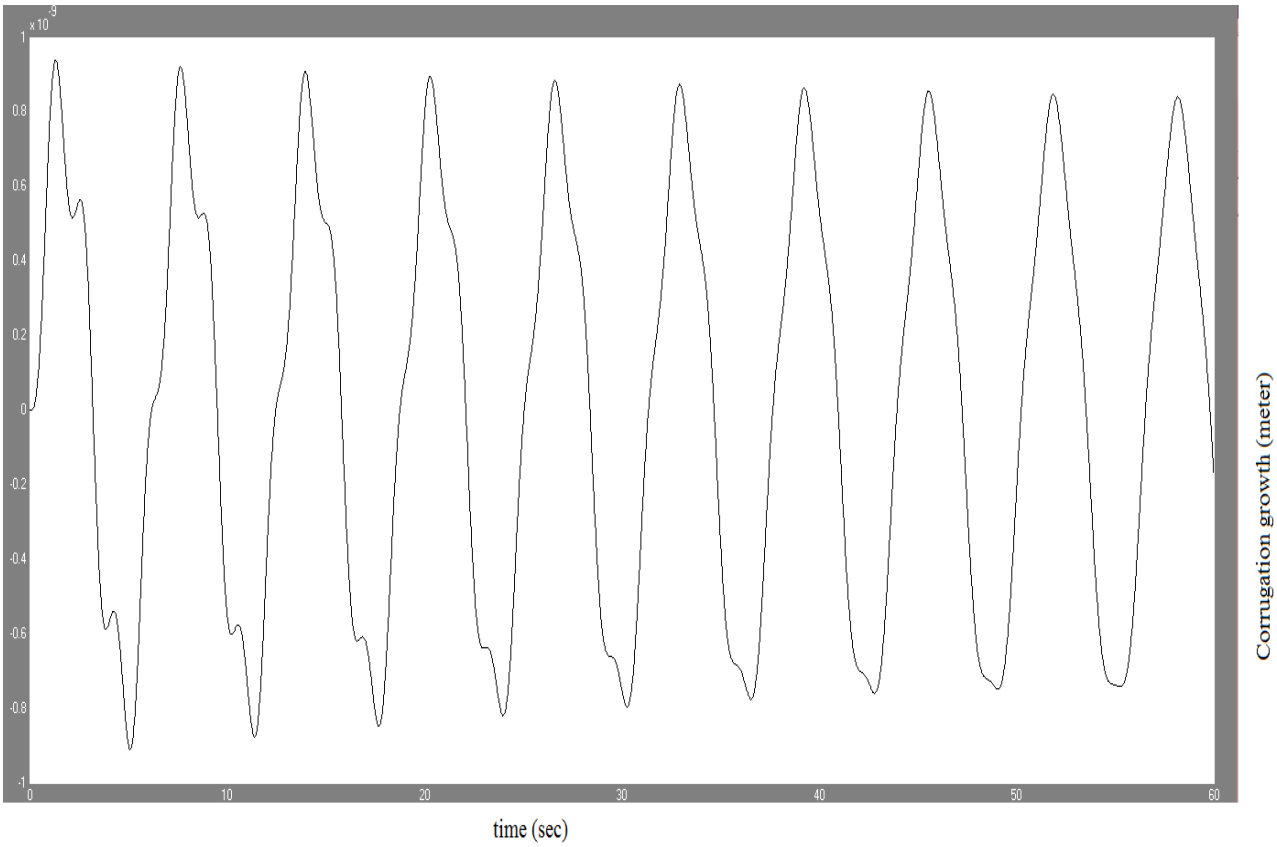

Figure 5.7. The growth rate of the corrugation in straight track 60km/h

from the above graphs, which were analyzed using newtons equation of motion to see the effect of the profile irregularity (corrugation growth) in the straight line of tram railway car the growth of amplitude will decrease to $1\times10^{-9}m\ per\ pass$.

Then as we see three simulation that analyzed at 20,40,60km/h and using the same damping ratio and radius of the wheel for three simulations. At the result of the simulation we can see that the speed increases the corrugation growth rate decrease as observed, this shows the friction between wheel and rail decreases at very high speed. The peak of the y the amplitude of irregularity in y axis is approximately $2.5\times10^{-7}m\ per\ pass$ and then the rate slightly decreases as the speed increase 40km/h y axis become $6\times10^{-9}m\ per\ pass$ and in final simulation takes at 60km/h y axis becomes $1\times10^{-9}m\ per\ pass$.

When the speed increases the contact between wheel and rail decreases and the frequency of the vehicle decrease, the increase of vehicle dynamics will lead to the pinned-pinned resonance and p2 resonance corrugation growth.

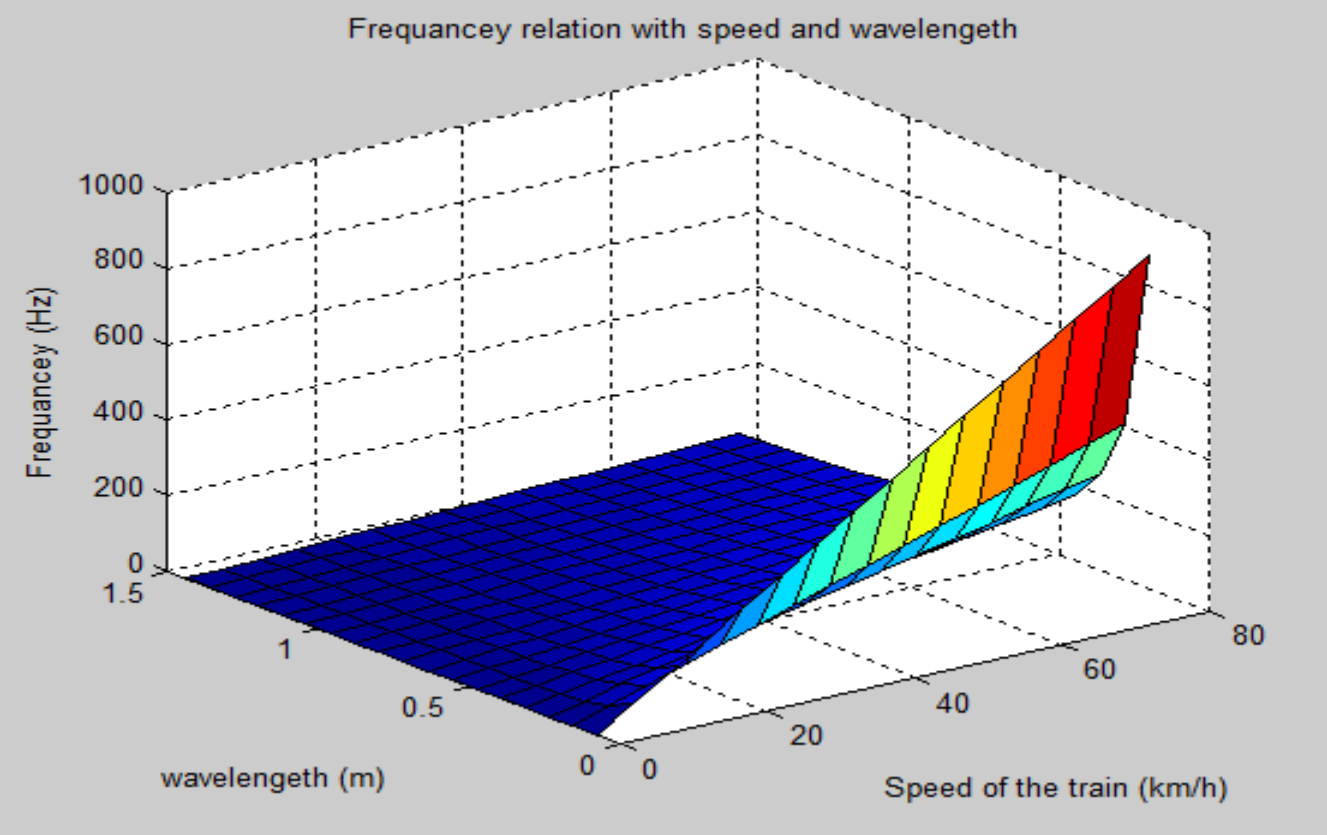

Figure:5.8. Relation between frequency, speed and wavelength. [Appendix 6]

From the above graph easily see the relationship between wavelength speed and frequency. Frequency would be affected in both wavelength and speed when speed increase frequency of the vehicle due to wavelength increase. This means at very low speed the irregularity will cause little resonance at high speed the irregularity will cause high resonance in whole vehicle.

There for the frequency that propagated from welds and rail joints are studied for the development of railhead corrugation and observed the result.

Table 5.1. corrugation and speed simulation result

Speed of tram car	20km/h	40km/h	60km/h
Corrugation growth	2.5×10^{-7}	6×10^{-9}	1×10^{-9}

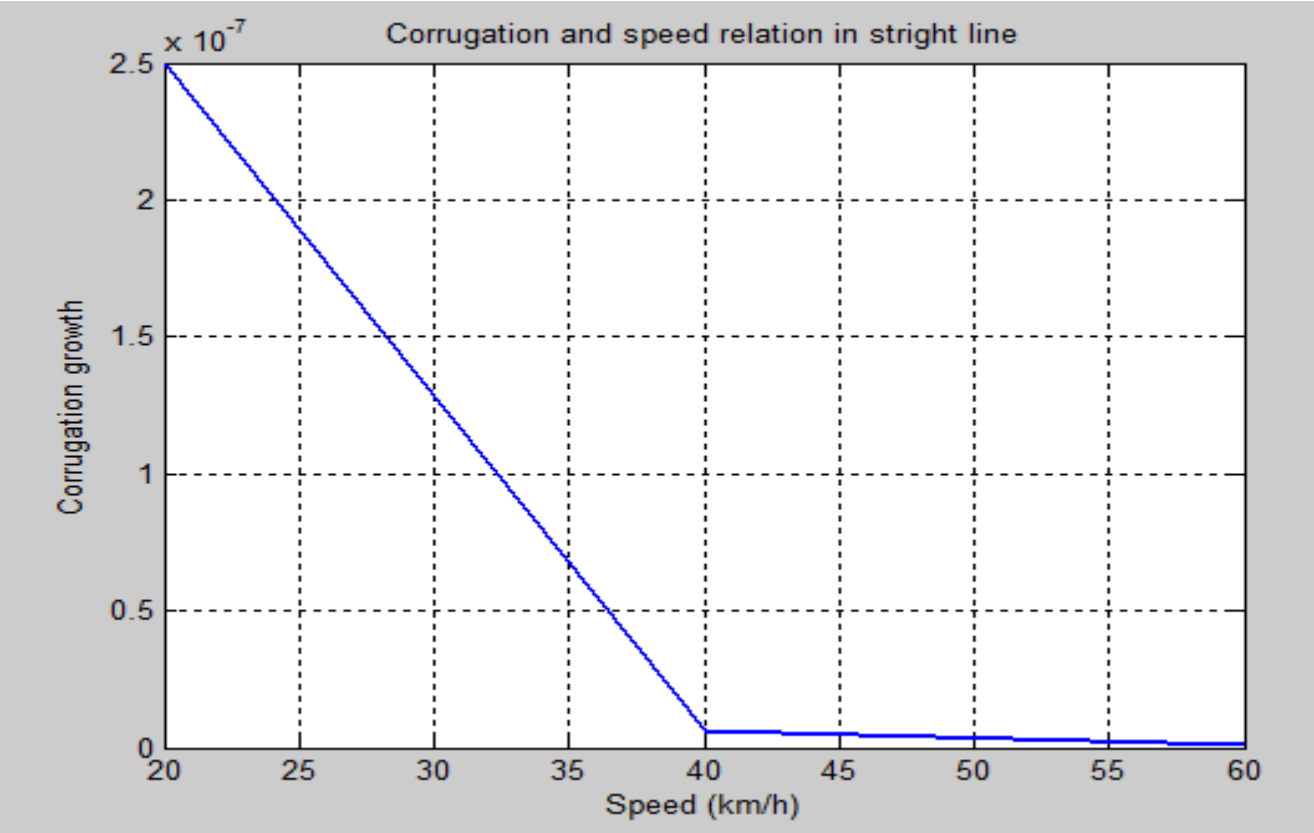

Figure:5.9. Comparison of Corrugation growth at speed 20,40,60km/h. [Appendix 7]

As observed in the graph the speed increase the rate of corrugation in straight track will decrease and this show that when at low speed the contact between wheel and rail is higher and then in high speed the contact load decrease and the friction will decrease, this is the basic to decrease the corrugation growth.

5.2. Corrugation growth in curved track

The curve is very sensitive to is place to the corrugation growth in railways. Because in the curving of the train the load of the vehicle will not be the same in high rail and low rail because of the centrifugal force of the whole vehicle. The load on wheels in the cornering are not the same like in straight rail do. [Appendix 8]

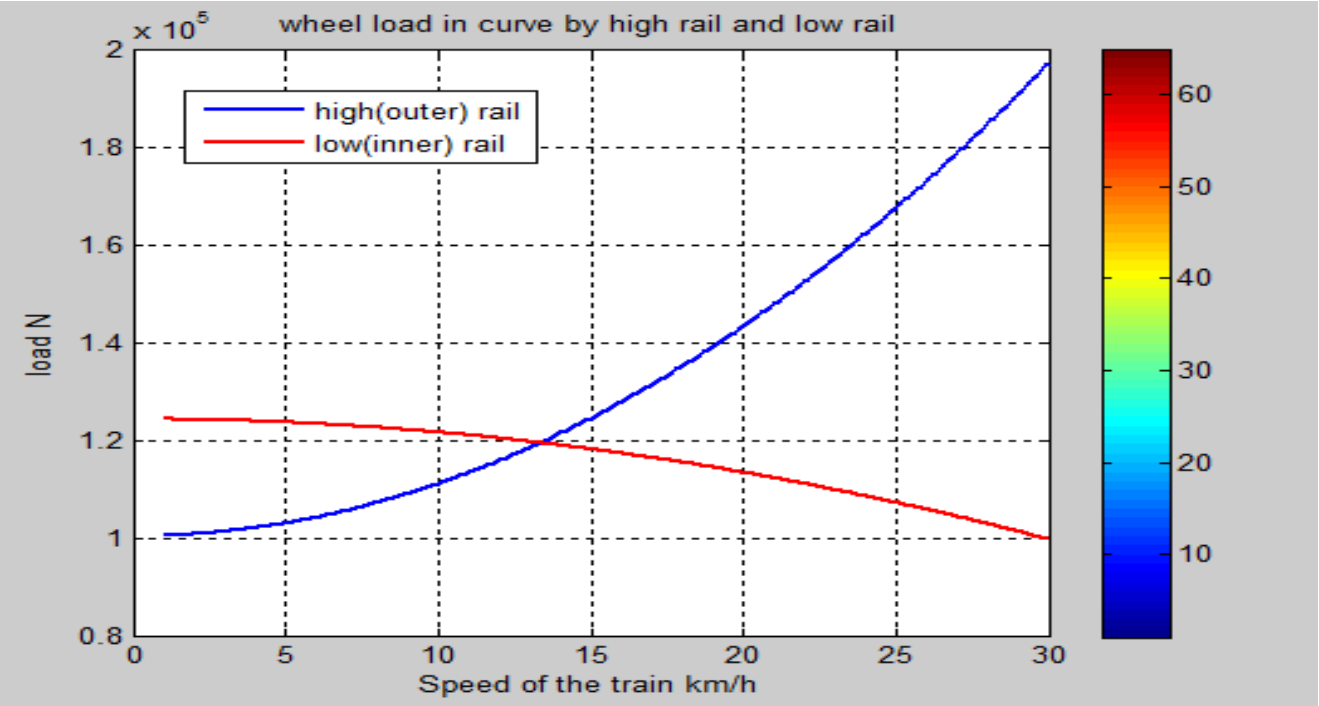

Figure 5.11. The load in higher and low rail of the train and neutral speed

The neutral curving/cornering speed is the speed under which the cant neutralizes the centrifugal force experienced by the cornering train. The neutral speed in the tram railway car AALRT taken as sample case is approximately 10km/h. as shown in the graph above the load in the high rail and low acting oppositely when the speed of train increase after the neutral speed. After the 20km/h the load on the wheels are varied extremely and after the speed of 30km/h the derailment will would be resulted because load in the law rail become 0N in the 30/h.

The traction of the train 50m radius cornering. [Appendix 9]

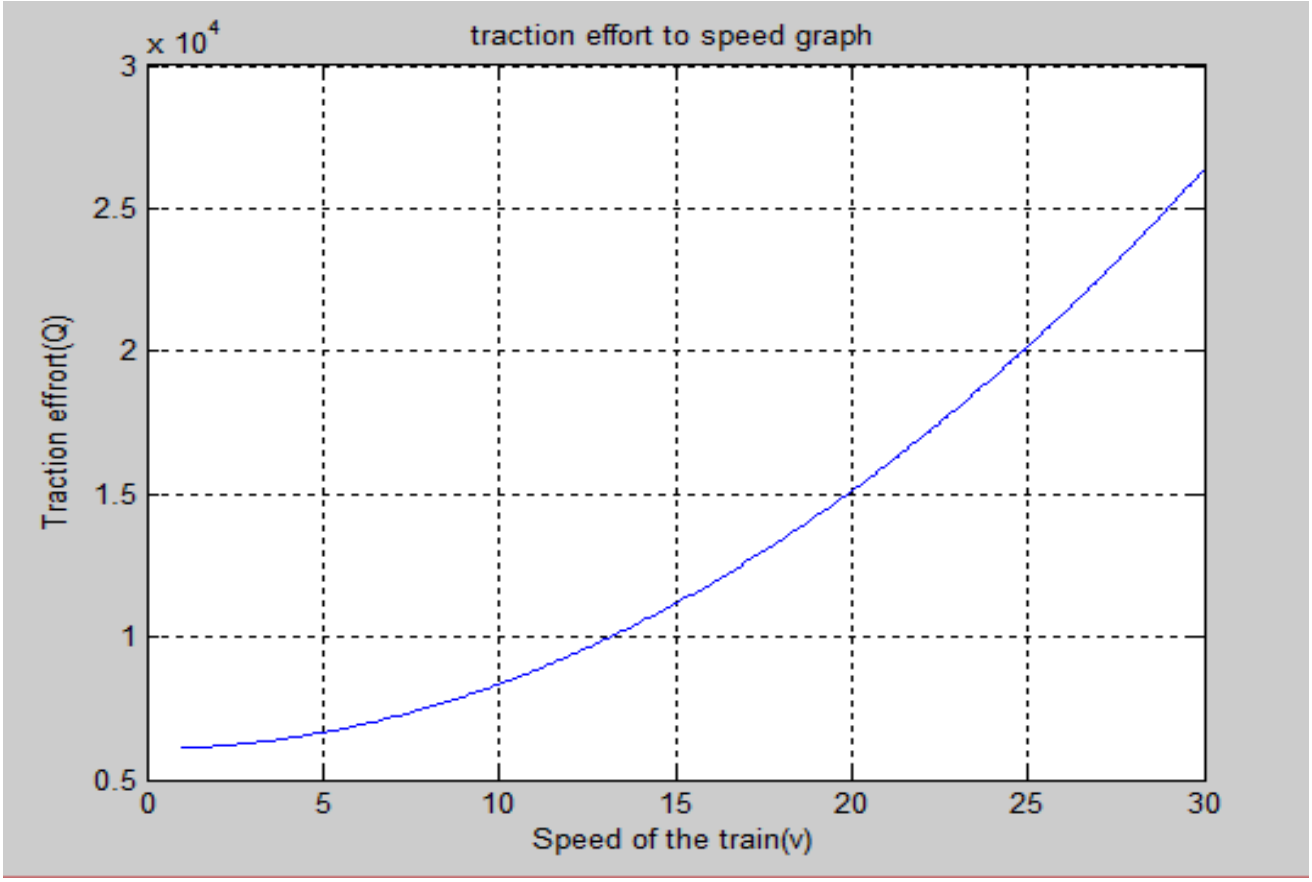

Figure.5.12. Traction effort in the curved rail

Then the train pass by different speed the vehicle thee profile of the rail head will affected by the different passing speed of the train [Appendix 10]

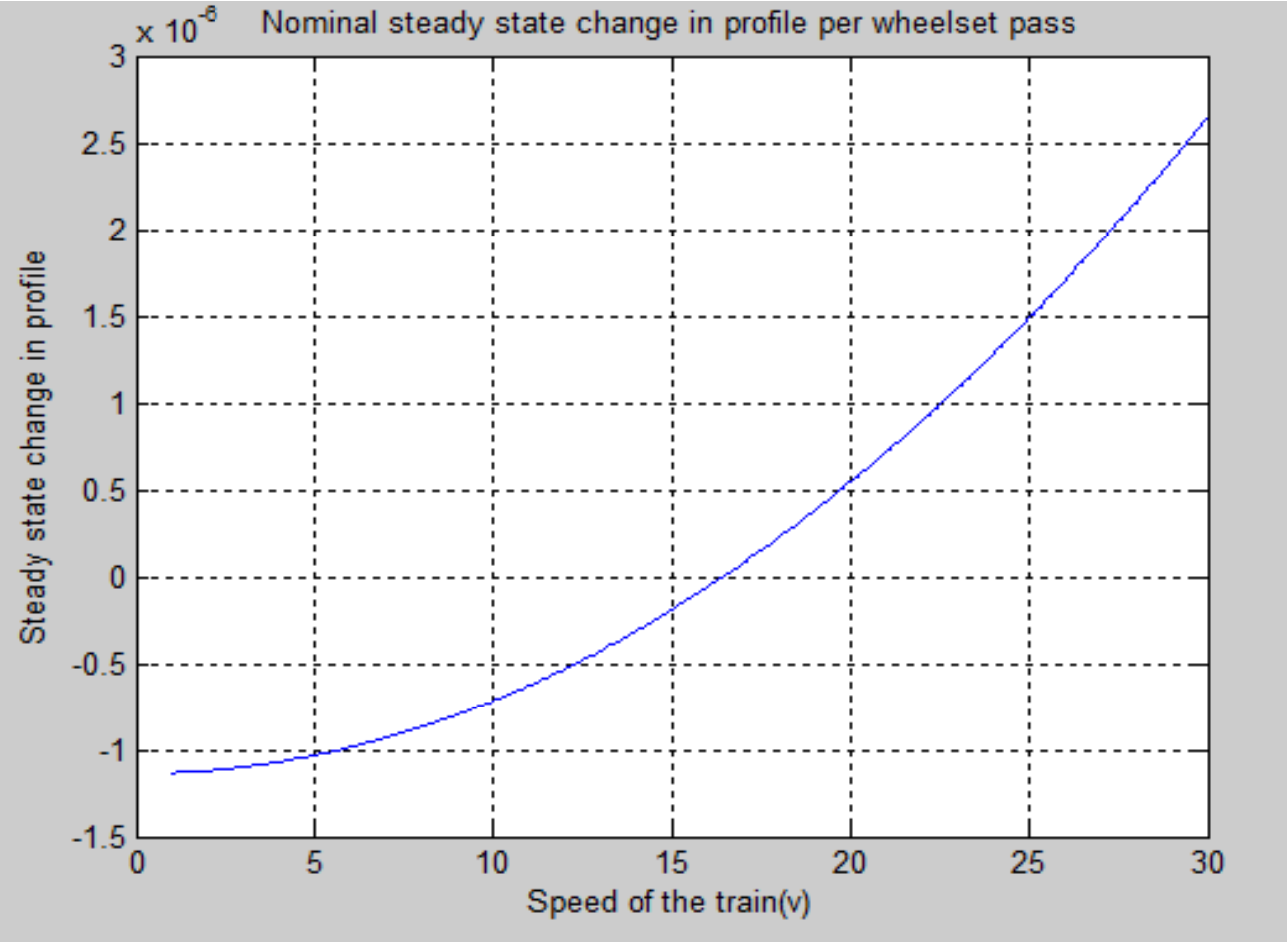

Figure.5.13. The profile change in the curved rail

And other parameter that are studied for the wheel and rail contact by varying speed is that the wear sensitivity of the higher and lower rail when the train is curving the sensitivity of the wear that the wear would be happened in both outer and lower rail has been studied. [Appendix 11]

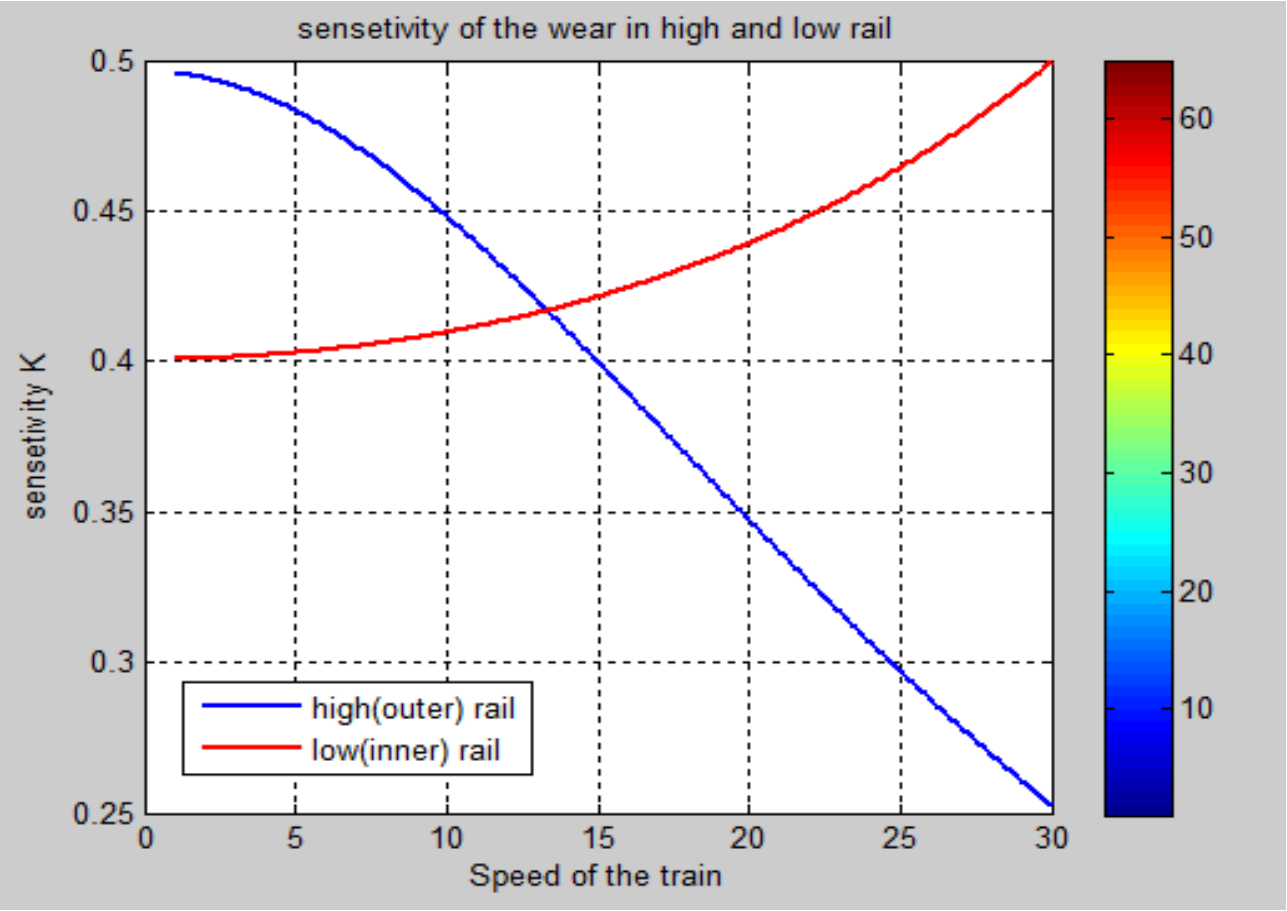

Figure.5.14. wear sensitivity in high rail and low rail

The speed increase will increase the damage sensitivity in the outer and lower rail and this sensitivity of the wear were exaggerated in the low rail rather than high rail, this so because of pitching motion of low rail.

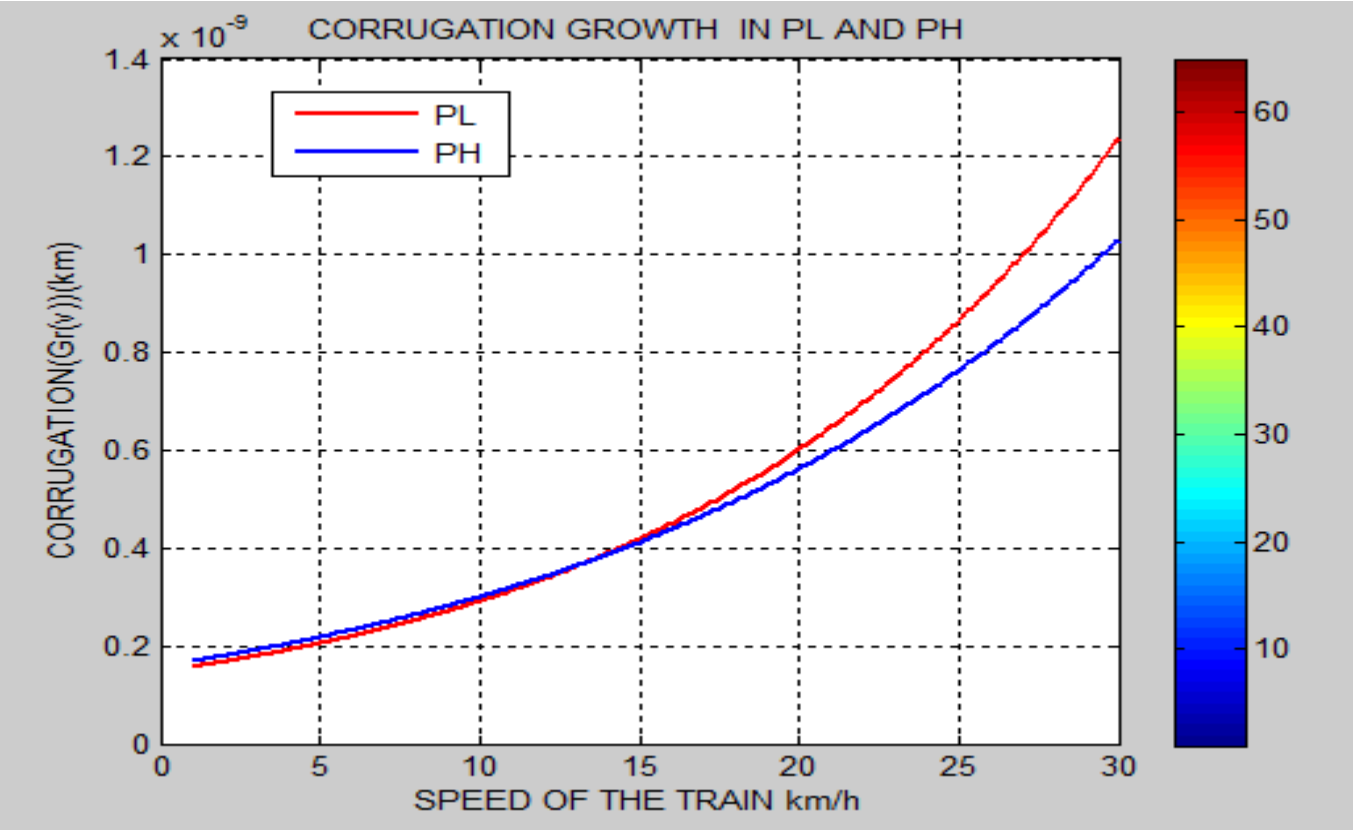

Figure.5.15. The growth of corrugation during cornering

Results showed that corrugation growth rate changed with the change of the speed during curving Based on the literature reviewed and analyzed the rate of corrugation in the curve is higher than the straight one. corrugation growth having a nonlinear relationship with speed in cure due to centrifugal forces and dynamic response frequency and corrugation wavelength. These effects of non-uniform speed could be decreased significantly with decreasing the sensitivity of single pass growth rate and this will have achieved by either widening the corner radius of the tram car or decreasing the cant deficiency for the nominal speed.in current condition decreasing the cant deficiency is the recommended idea.

5.3. Braking and acceleration

i. During severe acceleration

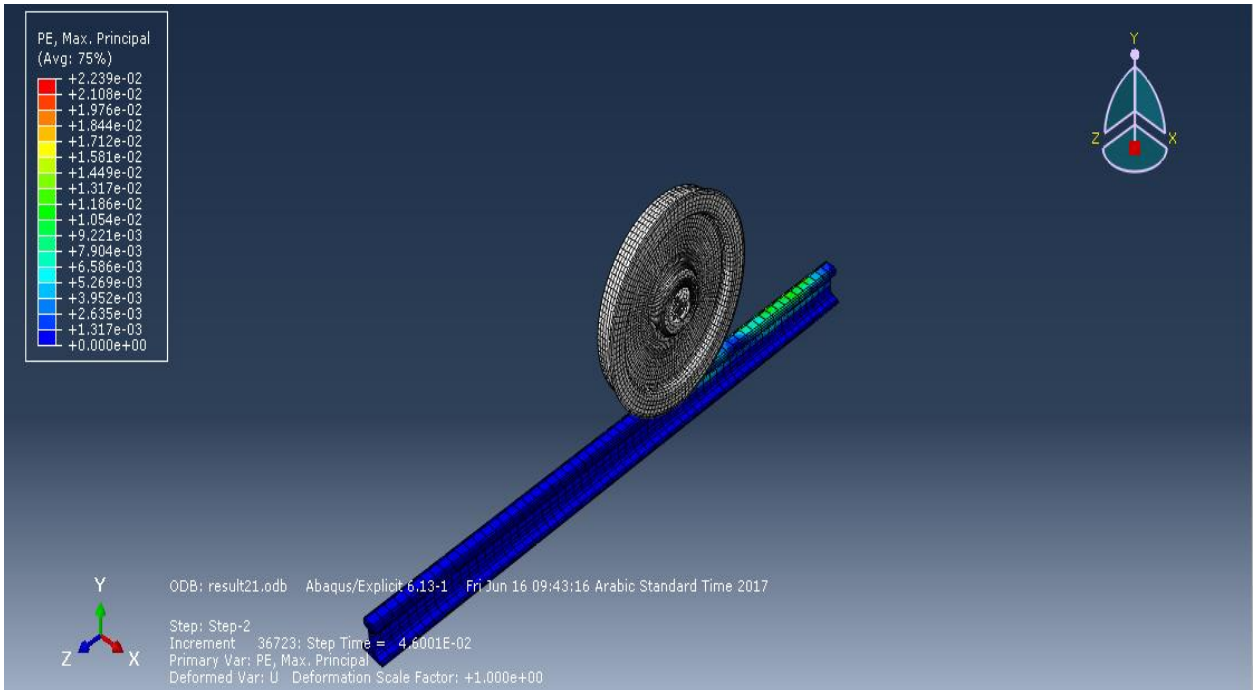

Figure 5.16. maximum principal stress on the rail during breaking

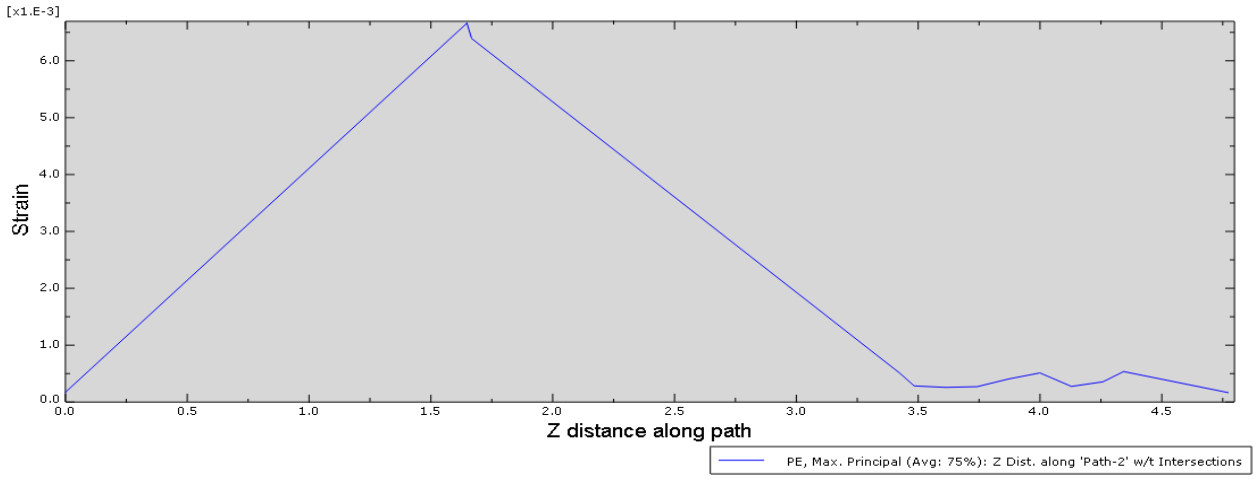

Figure. 5.17 Strain to longitudinal distance in straight line

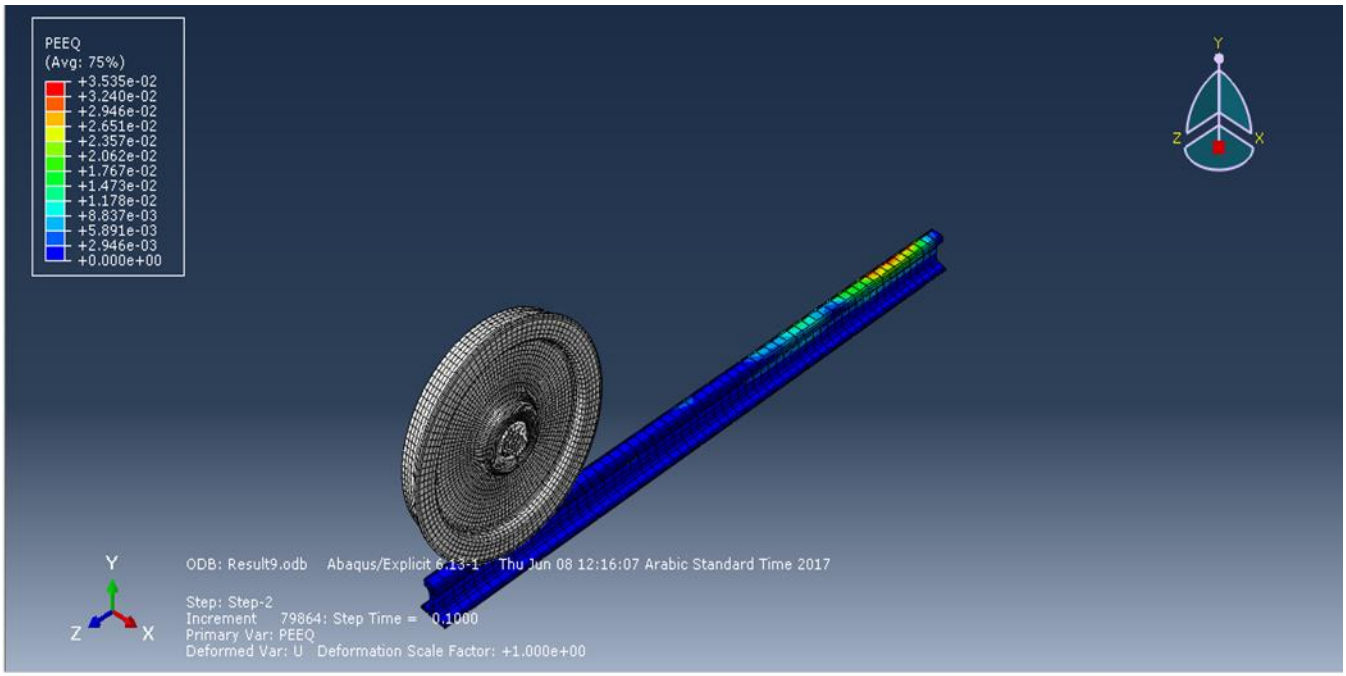

Figure.5.18. The plastic strain in the straight line of the rail track

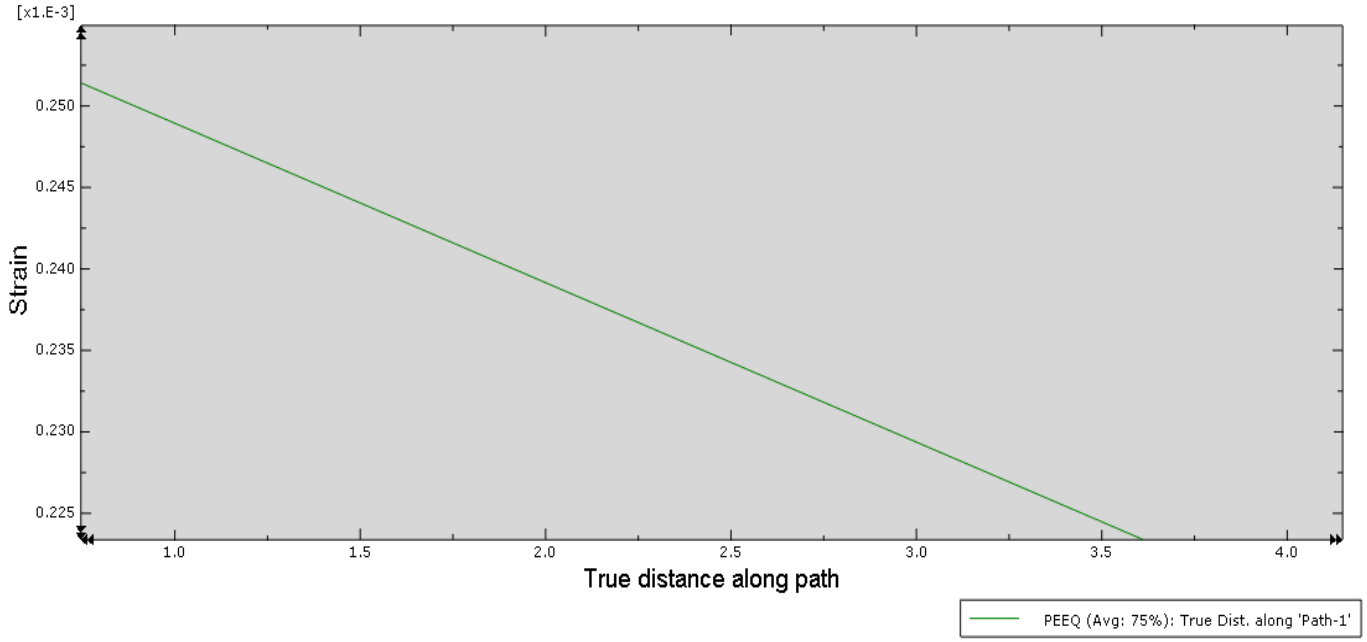

Figure.5.19. Strain to distance of the track

ii. Braking

The braking capacity of a railway vehicle depends on numerous factors and some of the most important are: running speed, weight, type of brakes, constructive and Functional characteristics of the brake rigging, braking characteristics, thermal phenomena, etc

During the traction in non-uniform speed plastic deformation occurs where the traction ratio (the ratio of tangential to normal force) on one wheel is close to the friction limit, so that this wheel slips and drives the opposite wheel in the wheelset in a roll-slip oscillation as shown in the result of the ABAQUS.

For Abaqus modeling to simulation of the breaking and traction of the tram vehicle has been studied. Considering the material property density and other chemical and mechanical property of the train. That showed that the wheel was running at speed at step one was of 5rpm and in step two it becomes 0rpm vise versa for severe traction.

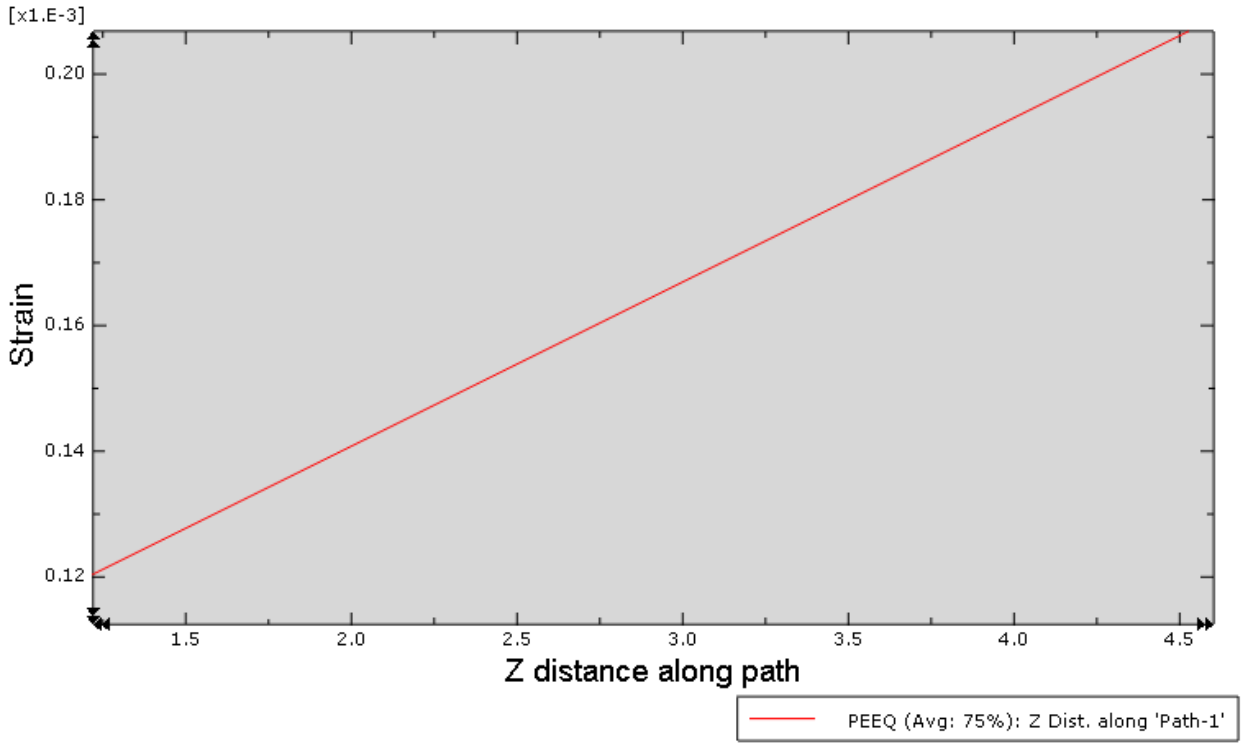

Figure.5:20: strain growth in time of severe breaking

5.3. Validation

5.3.1. Straight track

From paper Effects of wheel passing frequency, for all the distributions considered, the theoretical growth rate can be increased with increasing of the speed distributions [from referance20].

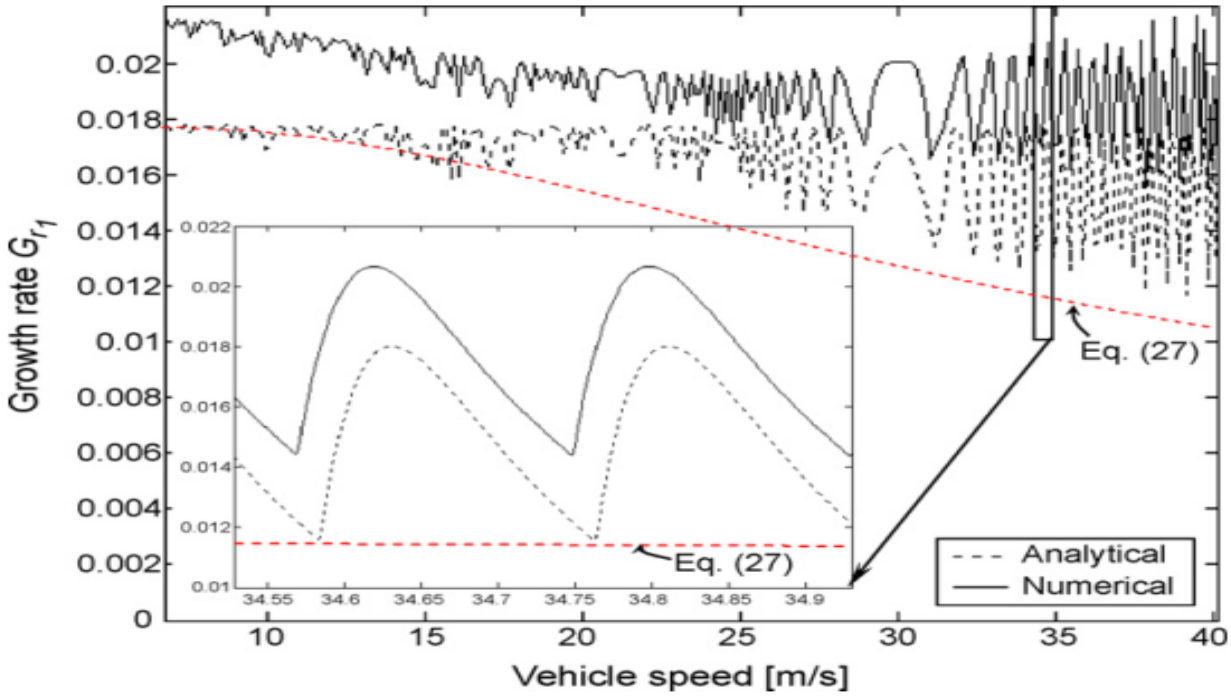

Figure; 5:21 Speed distribution and growth rate

Results of this analysis for realistic parameters indicate that substantial reductions in growth rate may be achieved by increasing the ‘‘width’’ of the speed distribution, and in case of this paper the growth of corrugation will also decrease with increase of speed.

5.3.2. Cornering

From the international paper “The effect of non-uniform train speed distribution on rail corrugation growth in curves/corners” the paper where studied typically have ballasted track (700 mm crushed basalt) consisting of 50 kg m/h rail (AS1085.1-1995) on Austrak M220 narrow gauge mono block concrete sleepers 272 kg) spaced at approximately 0.66 m with Pandora fist fasteners and rubber rail pads. The traffic is composed of 3 and 6 carriage electrical multiple unit (IMU/SMU) trains

travelling at an average of 90 km/h and the load of the wheels on the rail are as shown in figure below.

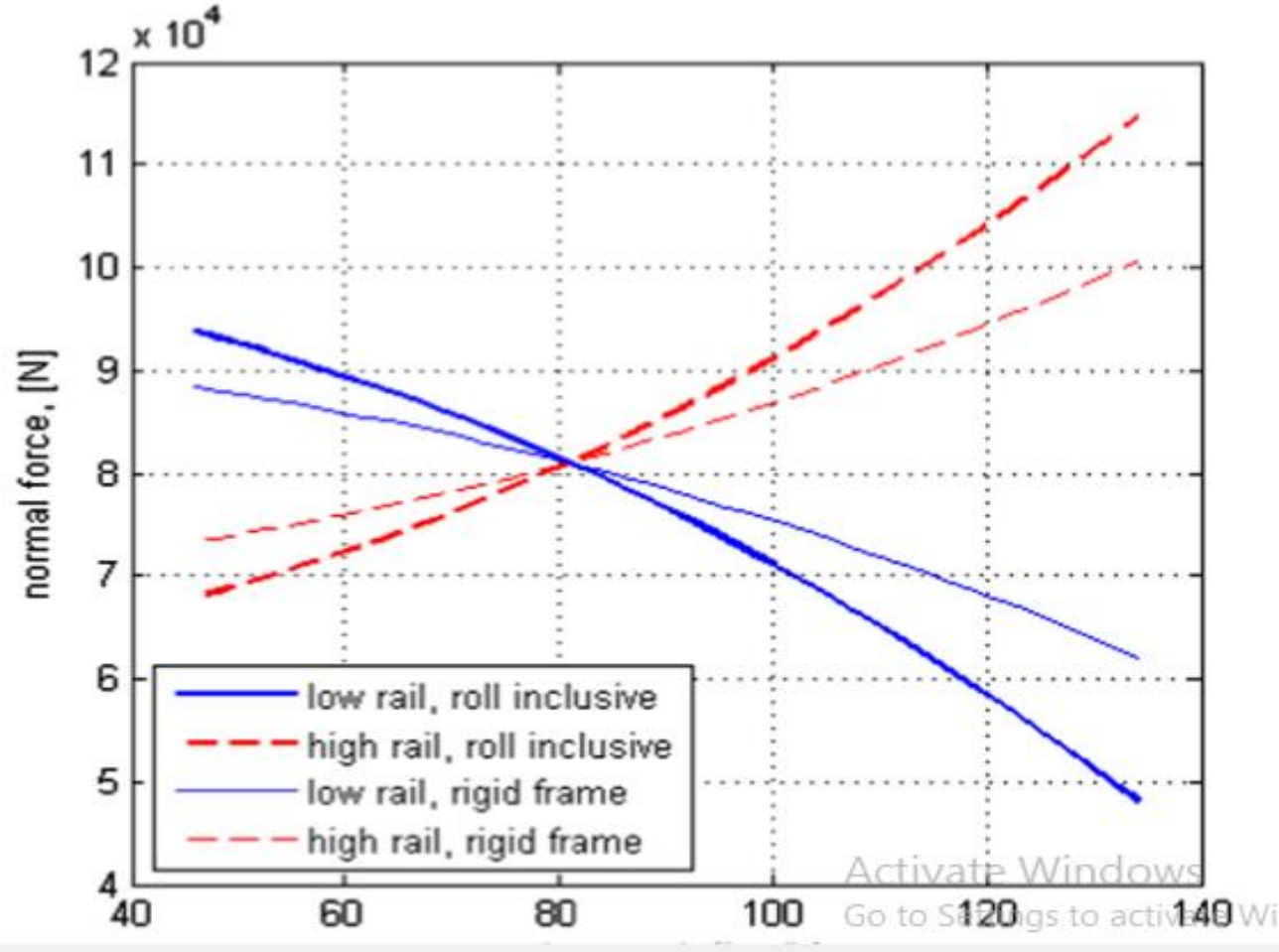

Figure 5.22 load to speed validation

The graph showed in that curving of the train the load of low rail decreasing and the load of high rail increasing continuously, this is so because of the centrifugal force of the train which is moving in the curve

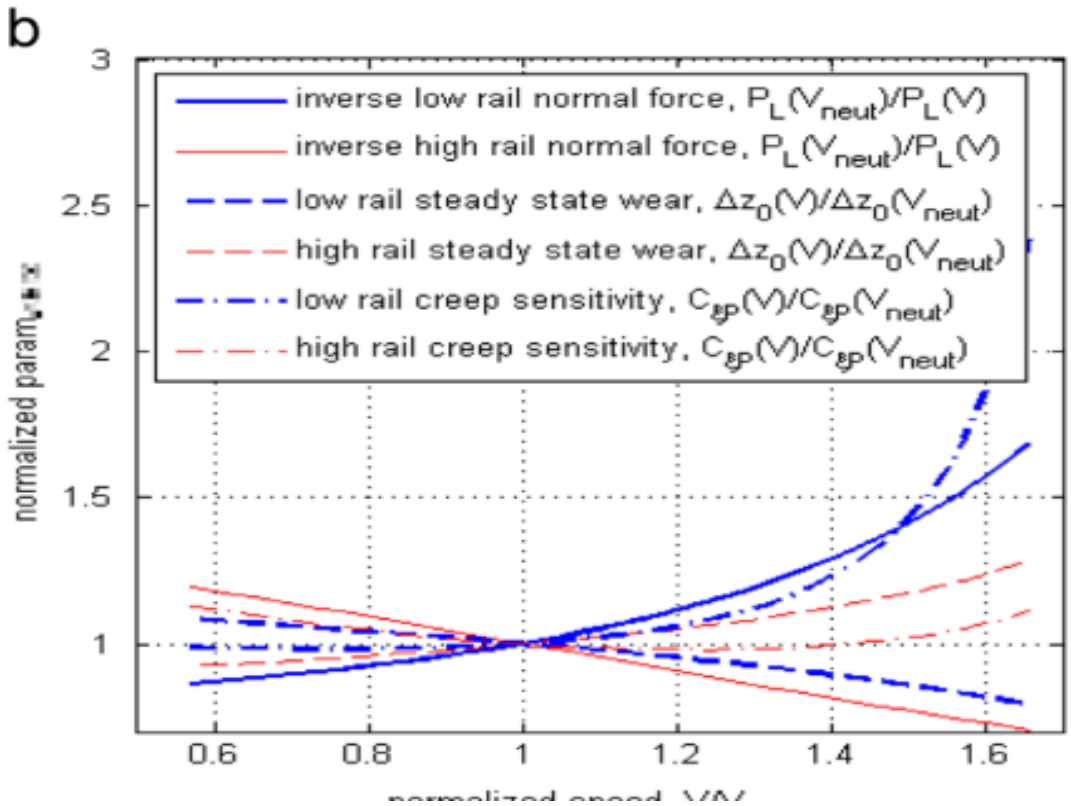

Figure 5.23: Speed to different Parameters for validation

This also showed that the creep sensitivity and corrugation growth rate in curving of passenger train. The neutral curving/cornering speed is the speed under which the cant neutralizes the centrifugal force at 1 or when the speed is at 90km/h experienced by the cornering train. Fig. highlights that the normal forces, creep sensitivities and steady state wear on both front and back wheels and high and low rails are equal at the neutral cornering speed.

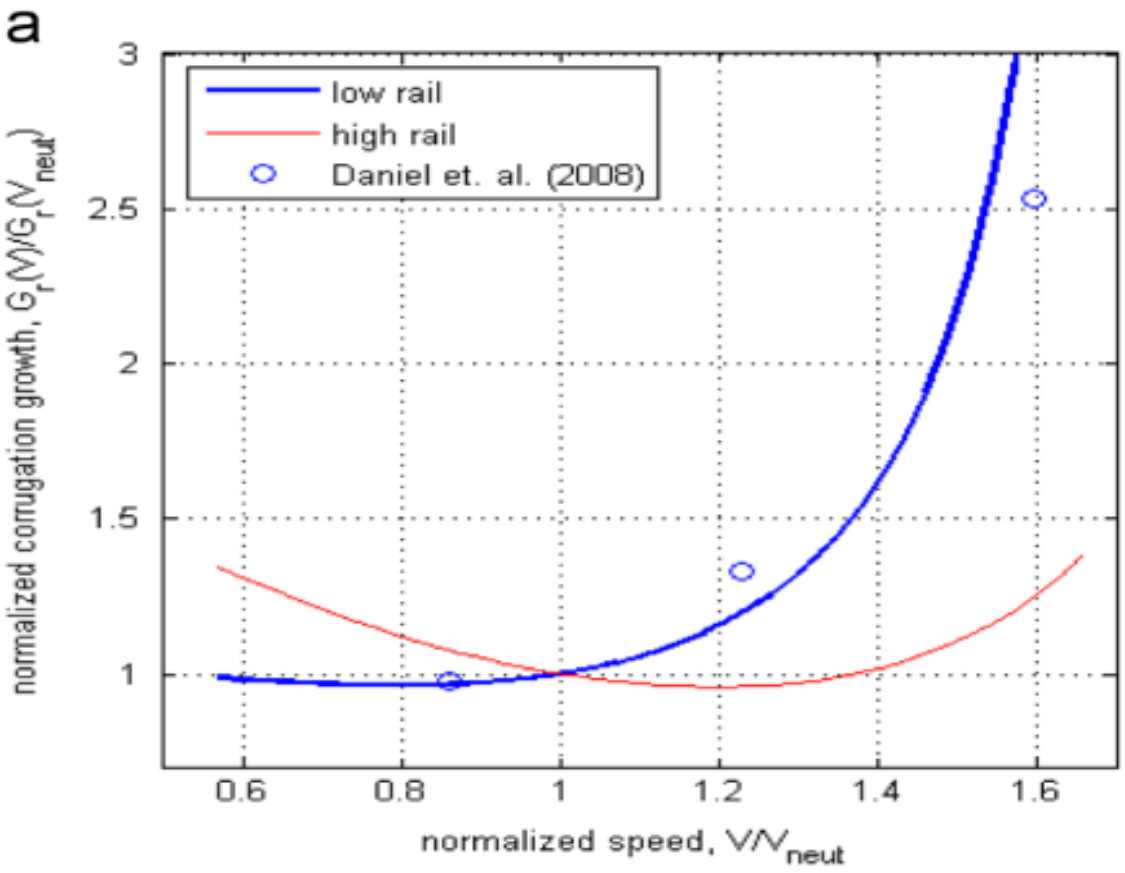

Figure 5.24. corrugation growth rate for validation

Analytical predictions have been developed for the growth of wear-type rail corrugation showing the effect of the non-uniform speed between successive multiple wheel passages. These predictions are based on a simplified feedback model that described above most critical interactions occurring between the wheel/rail structural dynamics, rolling contact mechanics and rail wear. the effect of passage velocity on corrugation growth due to require linear, steady-state (sinusoidal) solution assumptions. And comparing the result obtained by analyzing the radius of 50m for Addis Ababa light rail transit and observed the result numerically the same analysis that took by the radius of 200m with neutral velocity 95km/h.

Chapter 6

Conclusion and recommendation

6.1. Conclusion

In this study, the growth of a corrugation in railhead are determined under static and dynamic loads, the results are assumed to be significant. The analysis can include corrugation growth in curve and straight-line due to the speed of the train. The analysis is taking into account by using curved and straight line of the tram railway car ballast track.

From the results obtained in the static numerical and dynamic SIMULINK and ABAQUS analysis, of the three-different mechanism of corrugation are studied and identified.

The first one is Pinned-pinned and p2 resonance corrugation has been studied in MATLAB SIMULINK to understand the influence of non-uniform passing speed effect on the straight ballast track for a train in single wheel per single pass. And as the result showed at speed smaller speed 20km/h the maximum corrugation growth is approximately $2.5\times10^{-7}m$ and then the rate slightly decreases the speed increase 40km/h growth rate become $6\times10^{-9}m$ and in final simulation takes 60km/h growth becomes $1\times10^{-9}m\ per\ a\ single\ pass\ of\ simulation.$

The second is on the cornering at radius of 50m and the neutral speed in 50m radius of AALRT case is approximately 14km/h. as shown in the graph figure:5.11 above the load in the high rail and low acting oppositely when the speed of train increase after the neutral speed. After the 20km/h the load on the wheels are varied extremely and the growth rate of corrugation in the curving in 50m radius will be increase with the increase of the speed of the train. On the high(outer) rail, the corrugation growth is not much compared to low rail. In low rail corrugation growth 30km/h per pass is about $1.21\times10^{-9}km$ and in high(outer) rail $1.1\times10^{-9}km$ this would cause, the traction ratio is greater at the high rail than on the low rail for almost all circumstances. Because of it, reasonable to expect that plastic flow would occur more readily on the high rail. However, when a bogie curves with cant excess, the on the low rail wheel increases significantly because the trailing wheelset moves in towards the low rail and the leading wheelset moves towards the high

rail, thereby increasing the angle of attack. There are high lateral loads on the leading, low rail wheel and also high contact stresses on the low rail and corrugation will exceed in low rail.

Third result conclude that the rate of corrugation which is came by the breaking and speed change in the traction obtained that the plastic deformation happed at the step change of the wheel in the traction because of the rotation of the wheel increase in step two in the abacus and happened plastic removal of rail head has been observed.

Finally, conclude that the speed increase will maximize growth rate of corrugation and derailment in curve but in straight line due to dynamic effect of the train speed increase will decrease Corrugation growth this will happened in straight line because of decrease of the friction between wheel and rail.

6.2. Recommendation

The recommendation the study described as:

- Even though the result found for effect of speed in rail corrugation and irregularities index developing in a curved track and straight, the wear index value that predict the wear rate found high excessive. Therefore, to alleviate this problem optimized speed of AALRT wagon at curved and junction between intermediate & circular track shall be maintained.
- Predominantly at straight track with deferent passing speed according to result at speed >30km/h are comparatively low corrugation development. But in the cornering the speed of the train should not exceed 20km/h.
- Also, the train in cornering will not be exceed at described speed above because it will increase the corrugation and also increase the risk of derailment

6.3 Future work

The future work that proposed after the end of this paper will be; -

- The effect of the load in the corrugation growth in cornering of the train.
- The effect of vehicle dynamics in the growth rate of corrugation.
- Study on the material property of the rail that will cause corrugation.

Appendix

1.

```
x=1:1:8;
y=[0 35 35 65 65 35 35 0];
y1=[0 33 33 63 63 33 33 0];
y2=[0 31 31 61 61 31 31 0];
y3=[0 29 29 59 59 29 29 0];
y4=[0 27 27 57 57 27 27 0];
y5=[0 25 25 55 55 25 25 0];
y6=[0 23 23 53 53 23 23 0];
plot(x,y,'r','linewidth',2);
hold on
plot(x,y1,'k','linewidth',2);
hold on
plot(x,y2,'b','linewidth',2);
hold on
plot(x,y3,'g','linewidth',2);
hold on
plot(x,y4,'--b','linewidth',2);
hold on
plot(x,y5,'g','linewidth',2);
hold on
plot(x,y6,'k','linewidth',2);
grid;
xlabel('bteween two staion speed distrbution')
ylabel('Speed of the train Km/h')
title('Sample 7 pass Speed btween two staion location')
```

2.

```
%plot the pdf
figure;
plot(x,pdf1,'r','linewidth',2);
hold on;
plot(x,pdf2,'k:','linewidth',2);
plot(x,pdf3,'b-','linewidth',2);
plot(x,pdf4,'g--','linewidth',2);
plot(x,pdf5,'b','linewidth',1);
plot(x,pdf6,'g','linewidth',2);
plot(x,pdf7,'k','linewidth',2);
plot(x,pdf8,'linewidth',2);
legend({'vmin=35,vm=40,vmax=65','vmin=33,vm=42,vmax=63','vmin=31,vm=44,
hold off;
xlabel('AALRT speed V[km/h]');
ylabel('probability density p(v)');
title('probility of the train speed for corrugtion growth of AALRT');
grid;
```

```
clear all;
close all;
pd1=makedist('Triangular');
pd2=makedist('Triangular','a',35,'b',40,'c',65);
pd3=makedist('Triangular','a',33,'b',42,'c',63);
pd4=makedist('Triangular','a',31,'b',44,'c',61);
pd5=makedist('Triangular','a',29,'b',46,'c',59);
pd6=makedist('Triangular','a',27,'b',48,'c',57);
pd7=makedist('Triangular','a',25,'b',50,'c',55);
pd8=makedist('triangular','a',23,'b',52,'c',53);
%comput the pdfs
x=0:1:70;
pdf1=pdf(pd1,x);
pdf2=pdf(pd2,x);
pdf3=pdf(pd3,x);
pdf4=pdf(pd4,x);
pdf5=pdf(pd5,x);
pdf6=pdf(pd6,x);
pdf7=pdf(pd7,x);
pdf8=pdf(pd8,x);
```

3.

```
v=0:1:70;
p=((160052.655)*(v.^-1))+4826.6;
plot(v,p);
xlabel('SPEED of the train')
ylabel('LOAD OF THE TRAIN')
title(' LOAD OFF THE TRAIN STRIGHT LINE')
```

4.

```
v=0:1:70;
R=1.5+((18*6)/(11800*9.81))+(0.03*v)+(0.006*v.^2);
plot(v,R);
xlabel('SPEED OF THE TRAIN');
ylabel('RESISTANCE TO MOVE THE TRAIN');
title('RESISTANCE OF THE TRAIN DURING TRACTION');
grid;
```

5.

```
v=0:1:70;
p=((160052.655)*(v.^-1))+4826.6;
plot(v,p,'linewidth',2);
xlabel('Speed of the train');
ylabel('Tractive effort of the train');
grid;
```

6.

```
v=0:5:75;
L=0:0.08:1.5;
[x,y]= meshgrid(v,L);
w=(x).*(y.^-1);
surf(x,y,w);
xlabel('Speed of the train (km/h)');
ylabel('wavelengeth (m)');
zlabel('Frequancey (Hz)');
title('Frequancey relation with speed and wavelengeth');
```

7.

```
v=[20  40 60];
c=[0.00000025   0.000000006 0.000000001];
plot(v,c,'linewidth',2)
grid;
xlabel('Speed (km/h)')
ylabel('Corrugation growth')
title('Corrugation and speed relation in stright line')
```

8.

```
v=1:0.1:30;
pH=107.58*v.^2+100320;
plot(v,pH,'b','linewidth',2);
hold on;
pL= -27.343*v.^2+124260;
plot(v,pL,'r','linewidth',2);
grid;
title('wheel load in curve by high rail and low rail')
xlabel('Speed of the train km/h')
ylabel('load N')
```

9.

```
v=1:0.1:30;
q=22.52*v.^2+6094.6;
plot(v,q);
grid;
title('traction effort to speed graph');
xlabel('Speed of the train(v)');
ylabel('Traction effrort(Q)');
```

10.

```
v=1:0.1:30;
z0=(4.2015e-9)*v.^2-1.1370e-6;
plot(v,z0);
grid;
title('Nominal steady state change in profile per wheelset pass')
xlabel('Speed of the train(v)');
ylabel('Steady state change in profile');
```

11.

```
v=1:0.1:30;
k=49779*((107.58*v.^2+100320).^-1);
plot(v,k,'b','linewidth',2);
hold on;
k1=49779*((-27.343*v.^2+124260).^-1);
plot(v,k1,'r','linewidth',2);
grid;
ylabel('sensetivity K');
xlabel('Speed of the train');
title ('sensetivity of the wear in high and low rail')
```

12.

Apaa

```
v=1:0.1:30;
z1=(exp(((107.58*v.^2+100320)*((145.26).^-1)).*log(abs(3235.6*((107.58*v.^2+100320).^-1)-1))+0.065*v));
plot(v,z1,'r', 'linewidth',2);
hold on;
z2=(exp(((-27.343*v.^2+124260)*((145.26).^-1)).*log(abs(3235.6*((-27.343*v.^2+124260).^-1)-1))+0.065*v));
plot(v,z2,'b', 'linewidth',2);
grid;
title('corrugation growth in curve by high rail and low rail')
xlabel('Speed of the train km/h')
ylabel('corrugation(Gr(v))(km)')
```

Appendix B

Mass of the vehicle in single wheelset is about 11000kg and mass of wheel is 350kg

$v = \frac{l}{time}$ and assuming that l is the unit length unit deformation so the time will be calculated

$$time = \frac{1}{speed\ of\ the\ train}$$

Then to obtain the modal spring constant and modal damping constant per pass of the tram car the

$$k = \frac{mass}{time^2} \text{ and } C = \frac{mass}{time}$$

Reference

[1]. Grassiest S L, Kalousek J. Rail corrugation: characteristics, causes and treatments. Journal of Rail Rapid Transit[J]. Proceeding of Institute of Mechanical Engineering, 207F, 5768(1993).

[2]. Wang A and Cox S J. Effect of rail pad stiffness on rail roughness growth and wayside noise levels on high speed track[C]. The 6th World Congress on Railway Research, Edinburgh, UK, (2003).

[3]. Lias H. The influence of rail pad stiffness on wheelset/track interaction and corrugation growth. Journal of Sound and Vibration, 227, 935-948(1999).

[4]. Collette, Christophe; Horodinca, Mihaita. Preumont, Andre: Rotational vibration absorber for the mitigation of rail rutting corrugation[J]. Vehicle System Dynamics. Volume 47, Number 6, June 2009, pp. 641-659(19).

[5]. Grassie S L and Cox S J. The dynamic response of railway track with flexible sleepers to high frequency vertical excitation[J]. Proceedings of Institute of Mechanical Engineering Vol. 198D (7), 117-124(1984).

[6]. Gomez I, Vadillo E G. An analytical approach to study a special case of booted sleeper track rail corrugation[J]. Wear, 2001(251):916.

[7]. Kalousesek J, Johnson K L. An investigation of short pitch wheel and rail corrugations on the Vancouver mass transit system[J]. Pro of the institution of mechanical engineers Rail Rapid Transit, 1992(206):127.

[8]. S.L. Grassie, Rail irregularities, corrugation and acoustic roughness: characteristics, significance and effects of reprofiling. Proceedings of the Institution of Mechanical Engineers, Part F: Journal of Rail and Rapid Transit 226 (2012) pp. 542–557

[9]. P.T. Torstensson, J.C.O. Nielsen, Monitoring of rail corrugation growth due to irregular wear on a railway metro curve. Stockholm Wear 267 (2009) pp. 556–561

[10]. Nielsen, J. C. O. and Johansson, A. Out-of-round railway wheels – a literaturesurvey. Proc. IMechE, Part F: J. Rail and Rapid Transit, 2000, 214F, 79–91.

[11]. Knothe, K. and Grassie, S. L. (Eds). Proceedings of a Workshop on Rail Corrugations and Out-of-Round Wheels. J. Sound Vibr., 1999, 227, 895–986.

[12]. Sato, Y., Matsumoto, A. and Knothe, K., 2002, "Review on rail corrugation studies", Wear 253 pp. 130-139.

[13]. WANG Anbin, WANG Zhiqiang, ZHANG Pan, ZHANG Zheyu, XU Ning"The Mechanism of rail corrugation growth and development" Luoyang Ship Material Research Institute, Luoyang, 471003, China e-mail: wangab725@163.com.

[14]. Grassie, S. L. and Kalousek, J. Rail corrugation: characteristics, causes and treatments. Proc. IMechE, Part F: J. Rail and Rapid Transit, 1993, 207F, 57–68.

[15]. Grassie, S. L. and Elkins, J. A. Corrugation on North American transit lines. Vehicle Syst. Dyn., 1998, 28(Suppl.),5–17.

[16]. Rail corrugation: characteristics, causes, and treatments S L Grassie Abbauernring 1, 30900 Wedemark, Germany. email: stuart@stuartgrassie.comThe manuscript was received on 29 November 2008 and was accepted after revision for publication on 20 May 2009. DOI: 10.1243/09544097JRRT264

[17]. E. Tassilly, N. Vincent, Rail corrugations: analytical model and field tests, Wear 144 (1991) 163–178.

[18]. Effect of passenger car curving on rail corrugation at a curved track Xuesong Jin ∗, Zefeng Wen, Kaiyun Wang, Xinbiao Xiao State Key Laboratory of Traction Power, Southwest Jiaotong University, Chengdu 610031, China Received 5 April 2004; received in revised form 3 February 2005; accepted 16 March 2005 Available online 24 May 2005

[19]. A. Igeland, H. Ilias, Rail head corrugation growth predictions based on non-linear high frequency vehicle/track interaction, Wear 213 (1997) 90–97.

[20]. Effects of wheel passing frequency on wear-type corrugations P.A. Meehan W.J.T. Daniel CRC for Railway Engineering and Technologies, Mechanical Engineering, University of Queensland, Queensland, Australia.

[21]. Effects of variable pass speed on wear-type corrugation growth P.A. Bellette, P.A. Meehan, W.J.T. Daniel CRC for Railway Engineering and Technology (Rail CRC), School of Engineering, University of Queensland, Brisbane, Qld 4072, Australia Received 20 March 2007; received in revised form 9 November 2007; accepted 31 December 2007 Handling Editor: J. LamAvailable online 4 March 2008

[22]. The effect of non-uniform train speed distribution on rail corrugation growth in curves/corners P.A. Meehan n, R.D. Batten, P.A. Bellette School of Mechanical and Mining Engineering, University of Queensland & Rail CRC, Brisbane, QLD 4072, Australia

[23]. Rail corrugation: characteristics, causes, and treatments

[24]. Johnson, K. L. Contact mechanics, 1985, ch. 9 (Cambridge University Press, Cambridge).

[25]. Grassie, S. L. Corrugation on Australian National: cause, measurement and rectification. In Proceedings of the Fourth International Conference on Heavy haul railways, Brisbane, 1989. The Institution of Engineers, Australia, NCP 89/12, pp. 188–192.

[26]. Clayton, P. and Allery, M. B. P. Metallurgical aspects of surface damage problems in rails. Can. Metall. Q., 1982, 21, 31–46.

[27]. Newcomb, S. B. and Stobbs, W. M. A transmission electron microscopy study of the white etching layer on a railhead. Mater. Sci. Engng, 1984, 66, 195–204.

[28]. Baumann, G., Fecht, H. J., and Liebelt, S. Formation of white etching layers onrail treads. Wear, 1996, 191, 131

[29]. Grassie, S. L. and Kalousek, J. Rail corrugation: characteristics, causes and treatments. Proc. IMechE, Part F: J. Rail and Rapid Transit, 1993, 207F, 57–68.

[30]. Brickle, B. J., Elkins, J. A., Grassie, S. L., and Handal, S. J. Rail corrugation mitigation in transit. Research Results Digest, Transit Cooperative Research Program, National Research Council, USA, number 26, June 1998.

[31]. N. Song, P.A. Meehan, A closed form analytical solution for a simplified wear type rail corrugation model, Proceedings of the ACOUSTICS 2004, Gold Coast, Australia, 3–5 November, 2004, pp. 227–232.

[32]. 32 Grassie, S. L. and Elkins, J. A. Traction and curving behaviour of a railway bogie. Veh. Syst. Dyn., 2006, 44 (Suppl.), 883–891.

[33]. Daniel,W. J. T., Horwood, R. J., Meehan, P. A., andWheatley, N. Analysis of rail corrugation in cornering. Wear,2008, 265, 1183–1192

[34]. N. Song, P.A. Meehan, A closed form analytical solution for a simplified wear type rail corrugation model, Proceedings of the ACOUSTICS 2004, Gold Coast, Australia, 3–5 November, 2004, pp. 227–232.

[35]. Effects of variable pass speed on wear-type corrugation growth P.A. Bellette, P.A.Meehan, W.J.T.2008.

[36]. Prediction of the growth of wear-type rail corrugation P.A. Meehan∗, W.J.T. Daniel, T. Campey CRC for Railway Engineering and Technologies (Rail CRC), Department of Mechanical l corrugation: characteristics, causes, and treatments

[37]. K.L. Johnson, Contact Mechanics, Cambridge University Press, United Kingdom, 1987, ISBN 0 521 34796 3.

[38]. K. Hempelmann, K. Knothe, An extended linear model for the prediction of short pitch corrugation, Wear 191 (1996) 161–169.

[39]. A. Matsumoto, Y. Sato, et al., Study on the formation mechanism of rail corrugation on curved track, Vehicle Syst. Dynam. 25 (1996) 450–465.

[40]. P.A. Meehan, P.A. Bellette, R.D. Batten, W.J.T. Daniel, R.J. Horwood, A case study of wear-type rail corrugation prediction and control using speed variation, J. Sound Vib. 325 (2009) 85–105.

[41]. CREC, AALRT kality depot Rolling stock department

[42]. Julia I. Real Herráiz,1 Silvia Morales-Ivorra,1 Clara Zamorano Martín,2 And Vicente Soler Basauri" Analysis of Vibrations Generated by the Presence of Corrugation in a Modeled Tram Track" Received 7 August 2014; Revised 2 January 2015; Accepted 20 January 2015, Spain.